ALLOCATION SFD/PIERRE FABRE MEDICAMENT 2017

Prévention de l'inflammation du tissu adipeux blanc par les adipocytes brites.

RAPPORT SCIENTIFIQUE DE FIN DE PROJET

Résumé du projet financé.

Le diabète de type 2 est couramment associé à une augmentation de la masse grasse et à une inflammation de bas grade du tissu adipeux blanc pouvant mener à une résistance à l'insuline. De nombreuses études ont démontré que la conversion des adipocytes blancs en adipocytes thermogéniques, dit brites, permet de réduire la masse de tissu adipeux et de normaliser la glycémie et la lipidémie quand celles-ci sont anormales. Cependant, l'impact de ces adipocytes brites sur le statut inflammatoire du tissu est encore méconnu. Notre projet visait donc à identifier le sécrétome inflammatoire (cytokines et éicosanoïdes) des adipocytes brites et de déterminer leurs capacités immunomodulatrices.

Nos résultats préliminaires montraient que le sécrétome inflammatoire des adipocytes brites était différent des adipocytes blancs. Pour compléter ces données, nous proposions des approches *in vitro* et *in vivo* chez l'Homme et la souris pour caractériser le sécrétome complet (cytokines et éicosanoïdes, pro- et anti-inflammatoire) des adipocytes brites en condition normale ou inflammatoire, et déterminer les capacités immunomodulatrices de ces adipocytes.

1. Caractérisation *in vitro* du profil de sécrétion de cytokines et d'éicosanoïdes des adipocytes brites humains en condition inflammatoire et impact sur la polarisation des macrophages.

Des cellules hMADS ont été différenciées en adipocytes blancs ou brites et ensuite stimulées par du LPS (100 ng/ml) ou un acide gras saturé (Palmitate, 50 µM complexé à de la BSA). Le traitement au Palmitate n'a jamais permis de mettre en évidence une réponse de type inflammatoire par les adipocytes, ce qui rejoignait certaines données de la littérature (Erridge and Samani 2009).

Une analyse de l'expression et de la sécrétion des cytokines pro- et anti-inflammatoires ainsi que des dérivés oxygénés des acides gras polyinsaturés a été réalisée en réponse à un traitement au LPS (Figure 1A).

Nous avons ensuite généré un milieu conditionné de ces adipocytes traités au LPS, qui a été utilisé pour stimuler des macrophages différenciés à partir de la lignée monocytaire THP-1. Les capacités pro- et anti-inflammatoire de ces macrophages ont été analysé d'un point de vue sécrétion de cytokines (Figure 1B).

Ces données non publiées (résumé dans la figure 1) n'ont pas permis de mettre en évidence un effet immunomodulateur direct des adipocytes brites sur la sécrétion de cytokines par des macrophages. Néanmoins, les sécrétions accrues d'oxylipines de la famille des HODEs, connue pour leur effet anti-inflammatoire, et de la protéine IL1RA, inhibitrice de l'IL1b et donc fortement anti-inflammatoire, mettaient en évidence une effet potentiel anti-inflammatoire de ces adipocytes brites qu'il serait nécessaire de caractériser dans un système plus complexe *in vitro* ou *in vivo*.

2. Caractérisation *in vivo* du profil de sécrétion de cytokines et d'éicosanoïdes des adipocytes brites humains.

Grâce à une collaboration avec le groupe de Pirjo Nuutila et Kirsi Virtanen (PET center, Université de Turku, Finlande), nous disposons de plasmas issus d'une cohorte (n=22 ; âge de 20-50 ans ; BMI de 20 à 25 ; normoglycémique ; sélection par FDG-PET-scan) pour laquelle nous connaissions le statut thermogénique des individus (Glucose uptake, Expression de gène…) (Figure 2) (M, Saari et al. 2018). A partir de ces échantillons, nous avons mesuré les niveaux d'éicosanoïdes (approche LC-MS, plateforme Metatoul, I2MC Toulouse) et de cytokines (ELISA multiplex MSD). Nous avons pu ainsi déterminer s'il existait une corrélation entre le statut inflammatoire et le statut thermogénique *in vivo* chez l'Homme.

Différents types d'analyses ont été réalisés (corrélation ou moyenne, selon Glucose uptake, BMI, expression d'UCP1…). La figure 2 présente une série de résultats comparant les niveaux d'éicosanoides et de cytokines circulantes dans 2 groupes de 6 individus regroupés selon l'expression d'UCP1 retrouvé dans le tissu adipeux sous-scapulaire. De manière intéressante, les niveaux de HODEs sont comme pour l'analyse in vitro plus important dans le groupe exprimant le plus UCP1. Peu de cytokines ont été détectées mais les niveaux d'IL8 et d'IFNg, et dans une moindre mesure d'IL6 et de TNFalpha, étaient plus faible dans les individus exprimant le plus UCP1.

Ces résultats semblent montrer que les individus exprimant le plus UCP1 au niveau de leur tissu adipeux ont un phénotype moins inflammatoire. Néanmoins, ces résultats sont à prendre avec précaution car le statut inflammatoire/infectieux des patients est inconnu.
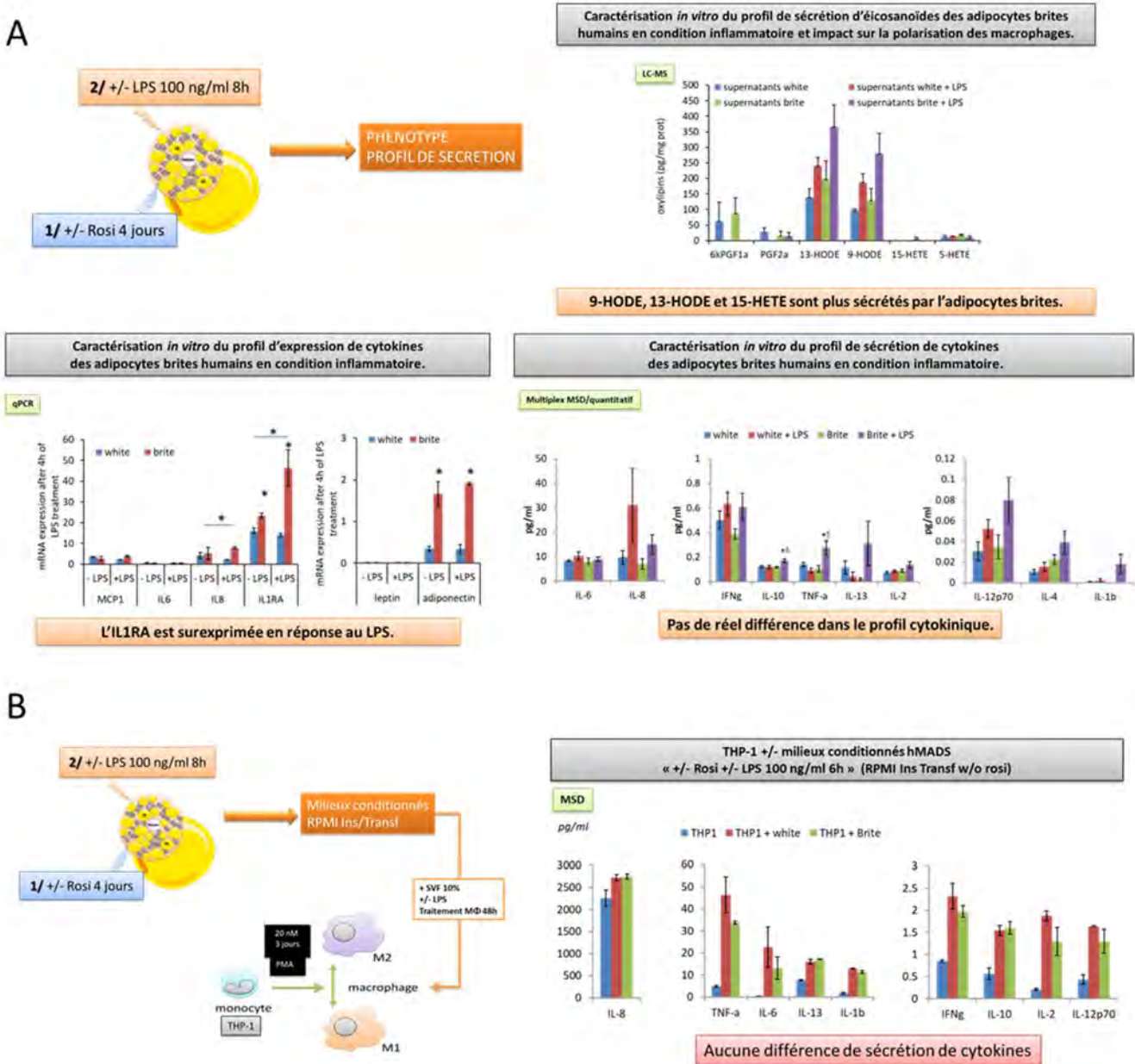
Figure 1. Résumé des résultats obtenus pour la caractérisation in vitro (A) du profil de sécrétion de cytokines et d'éicosanoïdes des adipocytes brites humains en condition inflammatoire et (B) leur impact sur la sécrétion de cytokines par le macrophage.
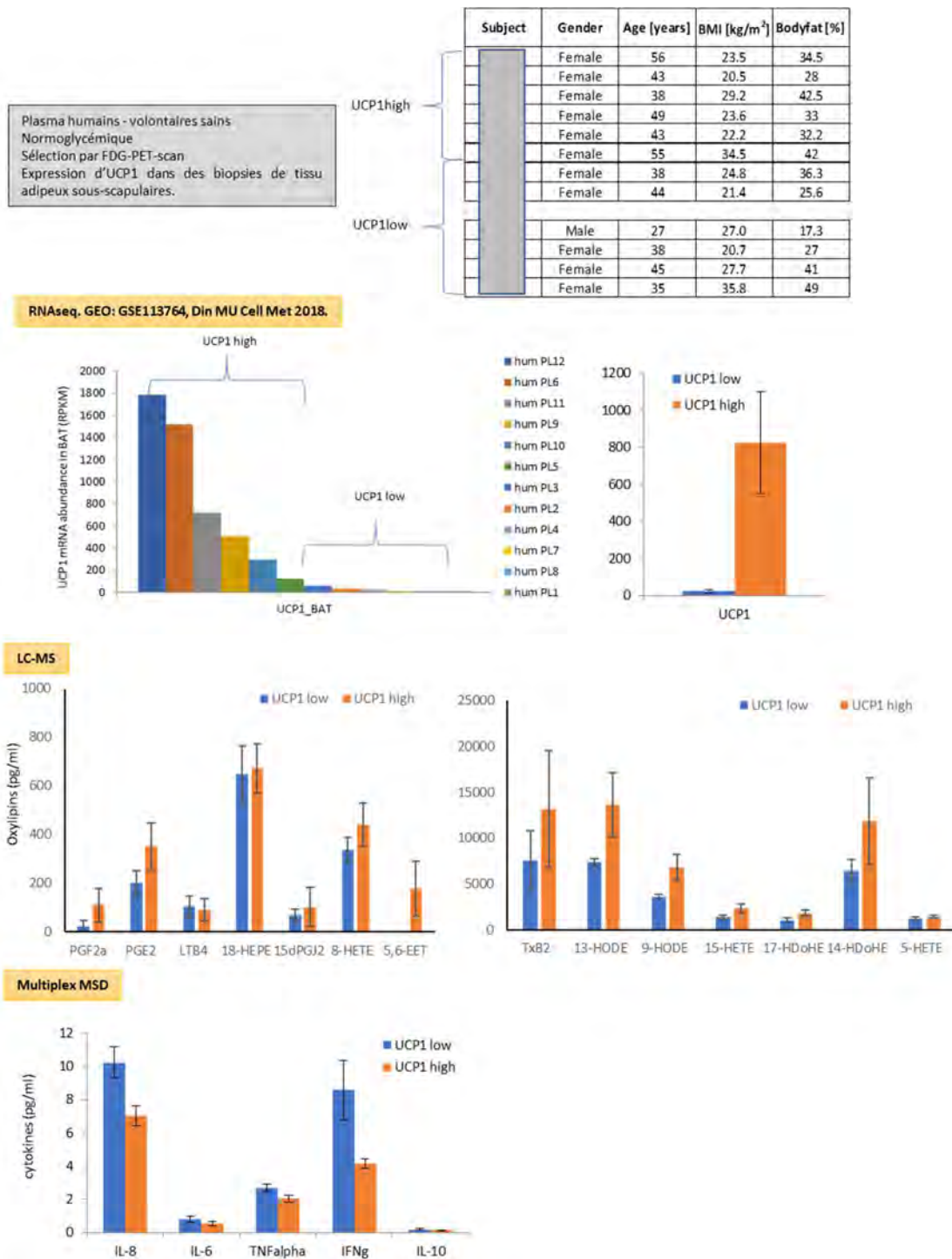
Figure 2. Analyse des profils plasmatiques d'éicosanoides (LC-MS) et de cytokines (ELISA, MSD) d'une cohorte de personnes saines (n=12). Les profils sont séparés en 2 groupes selon le niveau d'expression d'UCP1 (low ou high, RNAseq) retrouvé dans le tissu adipeux « brun » sous-scapulaire de chaque individu, correspondant à une zone positive en PET-SCAN après exposition au froid.

3.   Caractérisation *in vivo* du profil de sécrétion de cytokines et d'éicosanoïdes des adipocytes brites murins.

Les oxylipines, dérivés oxygénés des acides gras dont les éicosanoides, sont essentiellement métabolisées à partir des acides gras polyinsaturés w3 et w6 d'origine alimentaires et sont entre autres impliqués dans la réponse inflammatoire. Le statut inflammatoire du tissu adipeux est un facteur clé des troubles métaboliques et il est admis que les acides gras alimentaires, en termes de qualité et de quantité, modulent la synthèse d'oxylipines dans ce tissu. En outre, il a été montré que la supplémentation alimentaire en acides gras polyinsaturés w3 résout certaines situations inflammatoires. Il était donc intéressant d'évaluer l'influence des acides gras polyinsaturés alimentaires sur la synthèse des oxylipines et leur impact sur le statut inflammatoire du tissu adipeux. Pour cela, des souris ont été soumise à un régime alimentaire standard enrichi en w6 ou en w3 (rapport w6/w3 de 30 et 3,75, respectivement) et le contenu en oxylipines du tissu adipeux ainsi que le profils cytokiniques, local et systémique, ont été caractérisés.

Nous avons ainsi pu montrer que l'enrichissement du régime en acide gras polyinsaturés w3 induisait une augmentation des oxylipines dérivés l'acide linoléique, du DHA (acide docosahexaénoïque) et de l'EPA (acide eicosapentaénoïque) à la fois dans le tissu adipeux blanc et brun. Parmi ceux-ci, le niveau des intermédiaires des résolvines et lipoxines (pro-resolving mediators), ainsi que certains métabolites anti-inflammatoires, étaient augmentés. Parallèlement, l'expressions des marqueurs des macrophages M2 (anti-inflammatoires) étaient aussi augmentés, mais sans affecter les contenus en cytokines inflammatoires.

En conclusion, nous avons démontré qu'une alimentation enrichie en w3 induisait la synthèse d'oxylipines impliquées dans la réponse anti-inflammatoire et une signature moléculaire des macrophages M2 anti-inflammatoire, mais cela sans affecter la sécrétion de cytokines inflammatoire. Cette étude très intéressante, mais limitée car réalisé dans un contexte non-obésogène et non-inflammatoire, permettait de mettre en évidence les effets bénéfiques d'un ratio en acides gras poly-insaturés équilibrés. Ces résultats ont été publiés dans la revue Nutrients (cf Annexe 1) (Colson, Ghandour et al. 2019).

Sachant que ce type de régime favorise le recrutement et l'activation des adipocytes bruns et brites, il était intéressant de vérifier les effets bénéfiques de ces adipocytes dans un contexte inflammatoire.

4.   Détermination *in vivo* de l'impact des adipocytes bruns et brites sur la réponse inflammatoire à l'endotoxémie.

Cette partie du projet était de déterminer les capacités immunomodulatrices des adipocytes bruns et brites en réponse à une endotoxémie, retrouvée en cas d'obésité.

Des souris balb/C males de 8 semaines ont été traités pendant une semaine avec un agoniste du récepteur b3-adrénergique (CL316,243, 1mg/kg/jour) pour induire une thermogénèse chronique caractérisée par le recrutement et l'activation des adipocytes bruns et brites. Ensuite les animaux sont injectés par une solution de LPS pour générer une endotoxémie aiguë (lipopolysaccharides de E. Coli, i.p., 100 µg/souris).

Nos résultats montrent qu'en réponse au LPS, l'activité thermogénique permet de favoriser un environnement local anti-inflammatoire avec une sécrétion importante d'IL1RA et une diminution de celle de cytokines pro-inflammatoires. De manière intéressante l'activation des adipocytes beiges permet de réduire la sécrétion de leptine induite par le LPS. Ces résultats ont permis de mettre en évidence une activité immunomodulatrice des adipocytes thermogéniques en réponse à une endotoxémie, ce qui est encourageant dans le cadre d'une thérapie mettant en

jeu les adipocytes bruns et beiges pour le traitement des maladies métaboliques, présentant une endotoxémie qui participent à l'inflammation chronique de bas grade du tissu adipeux retrouvée dans ces pathologies.

Ces résultats sont en cours de publication (cf Annexe 2) et font l'objet d'une communication pour le futur congrès de la SFD 2020 (CA-190).

5. Détermination *in vivo* de l'impact des adipocytes bruns et brites sur la réponse inflammatoire à une infection bactérienne.

Des souris balb/C males de 8 semaines ont été traités pendant une semaine avec un agoniste du récepteur b3-adrénergique (CL316,243, 1mg/kg/jour) pour induire une thermogénèse chronique caractérisée par le recrutement et l'activation des adipocytes bruns et beiges. Ensuite les animaux sont infectés par des E. Coli (i.v., 1.7x107 CFU/souris). Les paramètres métaboliques et inflammatoires des souris sont alors analysés.

Nos résultats montrent qu'en réponse à une infection, l'activité thermogénique n'a d'effet ni sur la clairance bactérienne, ni sur la pyrexie et ni sur la réponse inflammatoire locale et systémique. En conclusion, l'activité immunomodulatrice des adipocytes thermogéniques décrite précédemment en réponse à une endotoxémie, n'a pas lieu en cas d'infection.

Ces résultats vont faire l'objet d'une publication en cours de rédaction (partie résultats en Annexe 3) et font l'objet d'une communication pour le futur congrès de la SFD.

6. Recherche d'un site sanctuaire d'infection par *Leishmania infantum* dans l'adipose

Récemment, certains travaux sur la bactérie *Coxiella burnetii* ont mis en évidence la persistance de cette bactéries dans le tissu adipeux (Bechah, Verneau et al. 2014), une donnée qui mettait en perspectives des résultats obtenus précédemment pour le parasite *Leishmania infantum* (Michel, Ferrua et al. 2011) où il a pu être constater la persistance du parasite au niveau abdominal dans des tissus adipeux néoformés chez la souris. Les leishmanioses sont dues à un protozoaire flagellé du genre Leishmania responsable de leishmanioses viscérales, cutanées, cutanéo-muqueuses ou encore des formes atypiques plus rares, qui sont toutes responsables d'une inflammation chronique. À ce jour, le nombre de porteurs asymptomatiques est considérablement sous-estimé et il existe des phénomènes de rechute après traitement et de développement de la maladie après la phase de portage asymptomatique, ce qui suggère la persistance de Leishmania dans les sites sanctuaires. Nous avons donc émis l'hypothèse qu'un phénomène similaire était possible pour ce parasite Leishmania et nous nous sommes posé la question de l'influence des adipocytes bruns et brites sur cette persistance et sur la réponse inflammatoire au parasite.

Nous avons étudié la présence du parasite au niveau des tissus adipeux blancs et bruns après infection par voie intraveineuse chez la souris. Nous avons ainsi pu mettre en évidence la présence de parasites au sein des tissus adipeux par qPCR et imagerie chez la souris et de manière intéressante avec une prévalence plus importante dans le tissu adipeux brun. Le même type de résultat a été obtenu in vitro dans des adipocytes bruns et brites.

Ces résultats sont très intéressants et pourrait être reliés au statut plutôt anti-inflammatoire des adipocytes bruns et brites qui permettrait une persistance du parasite en limitant la réponse anti-inflammatoire classique.

Ces données sont en cours de publication (cf Annexe 4) et ont fait l'objet d'une communication en congrès (ECCMID 2018, Madrid, O0682).

7.   Conclusion

Au cours de ce projet nous avons pu montrer que le recrutement et l'activation des adipocytes brites et bruns permettaient la mise en place d'un environnement plutôt anti-inflammatoire avec une sécrétion d'IL1RA importante. Ce phénomène semble particulièrement vrai lorsque le tissu est soumis à une endotoxémie aigue. Cela est très intéressant dans le cadre des maladies métaboliques qui présente une inflammation chronique de bas grade du tissu adipeux essentiellement en réponse à l'augmentation des niveaux de LPS circulants. Il s'agit pour nous maintenant de démontrer que le recrutement et l'activation des adipocytes bruns et brites permet de diminuer cette inflammation lors d'expérience d'exposition chronique à du LPS, différemment du traitement aigu que nous avons utilisé ici. De plus, nous avons démontré d'un côté qu'un régime équilibré en acides gras polyinsaturés w6/w3 favorisait le recrutement d'adipocytes brites (Ghandour, Colson et al. 2018), et d'un autre côté que ce même type de régime favorisait un phénotype anti-inflammatoire au niveau du tissu adipeux avec entre autres la synthèse accrue d'intermédiaires des médiateurs de résolution de l'inflammation comme les résolvines. Il serait donc intéressant de caractériser la combinaison d'effet que pourrait avoir ce type de régime avec le recrutement et l'activation des adipocytes bruns et brites dans un contexte d'endotéxémie, comme retrouvée chez les patients obèses.

Par contre, les études d'infections bactérienne et parasitaire que nous avons réalisées ont montré des résultats contrastés. Lors d'une infection bactérienne, le recrutement et l'activation des adipocytes bruns et brites ne modifient ni la réponse inflammatoire, ni l'élimination des bactéries ; et lors d'une infection parasitaire, la présence de ces adipocytes semblent même favoriser la persistance des parasites dans l'organisme.

En conclusion, stimuler l'activité thermogénique des adipocytes bruns et brites pourrait permettre de limiter l'inflammation chronique retrouvée de maladies métaboliques, mais n'offrirait aucun avantage en cas d'infection.

8.   Bibliographie

Bechah, Y., J. Verneau, A. Ben Amara, A. O. Barry, C. Lepolard, V. Achard, L. Panicot-Dubois, J. Textoris, C. Capo, E. Ghigo and J. L. Mege (2014). "Persistence of Coxiella burnetii, the agent of Q fever, in murine adipose tissue." PLoS One **9**(5): e97503.

Colson, C., R. A. Ghandour, O. Dufies, S. Rekima, A. Loubat, P. Munro, L. Boyer and D. F. Pisani (2019). "Diet Supplementation in omega3 Polyunsaturated Fatty Acid Favors an Anti-Inflammatory Basal Environment in Mouse Adipose Tissue." Nutrients **11**(2).

Erridge, C. and N. J. Samani (2009). "Saturated fatty acids do not directly stimulate Toll-like receptor signaling." Arterioscler Thromb Vasc Biol **29**(11): 1944-1949.

Ghandour, R. A., C. Colson, M. Giroud, S. Maurer, S. Rekima, G. P. Ailhaud, M. Klingenspor, E. Z. Amri and D. F. Pisani (2018). "Impact of dietary omega3 polyunsaturated fatty acid supplementation on brown and brite adipocyte function." J Lipid Res.

M, U. D., T. Saari, J. Raiko, N. Kudomi, S. F. Maurer, M. Lahesmaa, T. Fromme, E. Z. Amri, M. Klingenspor, O. Solin, P. Nuutila and K. A. Virtanen (2018). "Postprandial Oxidative Metabolism of Human Brown Fat Indicates Thermogenesis." Cell Metab **28**(2): 207-216 e203.

Michel, G., B. Ferrua, T. Lang, M. P. Maddugoda, P. Munro, C. Pomares, E. Lemichez and P. Marty (2011). "Luciferase-expressing Leishmania infantum allows the monitoring of amastigote population size, in vivo, ex vivo and in vitro." PLoS Negl Trop Dis **5**(9): e1323.

ANNEXE 1.

Colson et al. Nutrients 2019.

Diet Supplementation in ω3 Polyunsaturated Fatty Acid Favors an Anti-Inflammatory Basal Environment in Mouse Adipose Tissue

Cecilia Colson [1], Rayane A. Ghandour [1], Océane Dufies [2], Samah Rekima [1], Agnès Loubat [1], Patrick Munro [2] , Laurent Boyer [2] and Didier F. Pisani [1,3,*]

[1] Université Côte d'Azur, CNRS, Inserm, iBV, 06107 Nice, France; Ceciclia.Colson@unice.fr (C.C.); ghandourrayane@hotmail.com (R.A.G.); Samah.Rekima@unice.fr (S.R.); Agnes.Loubat@unice.fr (A.L.)
[2] Université Côte d'Azur, Inserm, C3M, 06107 Nice, France; oceane.dufies@unice.fr (O.D.); Patrick.Munro@unice.fr (P.M.); Laurent.Boyer@unice.fr (L.B.)
[3] Didier Pisani, Laboratoire de PhysioMédecine Moléculaire—LP2M, Univ. Nice Sophia Antipolis, 28 Avenue de Valombrose, 06107 Nice CEDEX 2, France
[*] Correspondence: pisani@unice.fr; Tel.:+33-0493377037

Abstract: Oxylipins are metabolized from dietary ω3 and ω6 polyunsaturated fatty acids and are involved in an inflammatory response. Adipose tissue inflammatory background is a key factor of metabolic disorders and it is accepted that dietary fatty acids, in terms of quality and quantity, modulate oxylipin synthesis in this tissue. Moreover, it has been reported that diet supplementation in ω3 polyunsaturated fatty acids resolves some inflammatory situations. Thus, it is crucial to assess the influence of dietary polyunsaturated fatty acids on oxylipin synthesis and their impact on adipose tissue inflammation. To this end, mice fed an ω6- or ω3-enriched standard diet (ω6/ω3 ratio of 30 and 3.75, respectively) were analyzed for inflammatory phenotype and adipose tissue oxylipin content. Diet enrichment with an ω3 polyunsaturated fatty acid induced an increase in the oxylipins derived from ω6 linoleic acid, ω3 eicosapentaenoic, and ω3 docosahexaenoic acids in brown and white adipose tissues. Among these, the level of pro-resolving mediator intermediates, as well as anti-inflammatory metabolites, were augmented. Concomitantly, expressions of M2 macrophage markers were increased without affecting inflammatory cytokine contents. In vitro, these metabolites did not activate macrophages but participated in macrophage polarization by inflammatory stimuli. In conclusion, we demonstrated that an ω3-enriched diet, in non-obesogenic non-inflammatory conditions, induced synthesis of oxylipins which were involved in an anti-inflammatory response as well as enhancement of the M2 macrophage molecular signature, without affecting inflammatory cytokine secretion.

Keywords: oxylipins; brown adipose tissue; white adipose tissue; macrophages; inflammation

1. Introduction

ω6 linoleic acid (LA), a precursor of dihomo-γ-linolenic acid (DGLA) and arachidonic acid (ARA), and ω3 α-linolenic acid, a precursor of eicosapentaenoic (EPA) and docosahexaenoic (DHA) acids are essential polyunsaturated fatty acids (PUFAs) only supplied by food. These PUFAs are required for healthy development from embryonic steps to adult life and are involved in a variety of biological processes, especially, in adipose tissue [1,2]. It is now well accepted that insufficient intakes of ω3 PUFAs, as well as an excess of ω6 PUFAs, correlate with various diseases; especially, metabolic diseases [3–5]. For example, ARA intake correlates positively with being overweight/obese, inflammatory diseases, and associated metabolic syndrome [6–10]. Indeed, ω6 oxylipins (oxygenated

derivatives of PUFAs) are known to favor inflammatory responses [11], as well as to promote energy storage [12] and to inhibit energy expenditure [13,14]. The dietary *ω6/ω3* PUFAs ratio is more important than the total amount of PUFA intake as it determines the level of synthesized ω6-derived oxylipins. Indeed, ω3 PUFAs modulate ω6-derived oxylipins synthesis [15]. Mechanistically this is characterized by (i) the capacity of ω6 and ω3 PUFAs to compete at the level of lipoxygenase (LOX) and cyclooxygenase (COX), their two major metabolization pathways and ii) the capacity of various ω3 PUFAs to inhibit these pathways.

The increase in the number of overweight or obese people has reached an epidemic stage in the 21st century. More than 2 billion adults are overweight (body mass index (BMI) > 25 kg/m^2) and at least 600 million are clinically obese (BMI > 30 kg/m^2). Obesity and being overweight are the consequences of a positive energy balance that leads to an increase in the mass of subcutaneous and visceral white adipose tissue. White adipocytes are storing energy under the form of triglycerides whereas brown adipocytes dissipate energy from triglycerides by producing heat (=thermogenesis). In addition, white and brown adipocytes are able to secrete molecules acting on their environment, and especially, on immune cells [16]. For example, white adipocytes secrete adipokines (e.g., adiponectin) and pro-inflammatory factors (e.g., PAI-1, MCP-1, or IL-6) which are able to recruit and activate macrophages [17]. Furthermore, it has also been shown that the white adipose tissue of obese subjects is characterized by low-grade inflammation that can lead to metabolic disorders such as insulin resistance [18]. This inflammation, characterized by an increase in inflammatory markers such as TNFα, PAI-1, or interleukins 1 and 6 (IL-1, IL-6), promotes the macrophage infiltration of adipose tissue and the polarization of macrophages of the alternative M2 type in classic pro-inflammatory M1 type [19].

The macrophages respond to environmental cues by acquiring specific functional phenotypes. Pro-inflammatory M1 macrophages are involved in the fight against many infections. They are activated by Toll-like receptor (TLR) ligands such as lipopolysaccharide and saturated fatty acids, but also by IFNγ and TNFα. They participate in the inflammatory environment by secreting many cytokines such as IL-1, IL-6, IL-12, IL-23, and TNFα, and by participating in the chemo-attraction of other immune cells [20]. M2 macrophages are more heterogeneous at functional and secretory levels. Considered as anti-inflammatory or inactive, they normally reside in tissues and are involved in tissue homeostasis by participating in the remodeling, repair, and activation of certain metabolic functions. They can be activated by cytokines such as IL-4, IL-10, and IL-13, but also by more specific signals from the tissue environment [21].

The accumulation of immune cells, especially that of macrophages, as well as their inflammatory phenotype, affect adipose tissue homeostasis and, more specifically, the recruitment and function of adipocytes in white and brown adipose tissues [16]. It has been shown that TNFα secreted by M1 macrophages inhibited adipocyte differentiation [22] and that IL-1β blocked insulin signaling [23], thus favoring insulin-resistance. Recently, it has also been shown that IL-1β and TNFα can affect the thermogenic function of brown adipocyte [24–26]. These inflammatory cytokines thus participate in the deregulation of tissue homeostasis by limiting its ability to dissipate an excessive supply of substrate in the form of heat. On the contrary, it was shown that M2 macrophages, via the secretion of factors such as IL-4 or IL-13 favored the formation of brown adipocytes and their activation [27,28]. In addition, immune cells can modulate insulin sensitivity and local secretion of catecholamines [29]. This secretion, that represents the preferential inducer of lipolysis and thermogenesis through the activation of the β-adrenergic pathway, appears to be crucial during prolonged exposure to cold or aging [28,30].

Similarly to adipokines, the oxygenated derivatives of ω6 PUFAs such as the *n*-2 series prostaglandins or the *n*-4 series leukotrienes, which are synthesized and secreted by adipocytes, participate in the inflammatory state of the tissue [31,32]. Furthermore, adipocytes are able to metabolize ω3 PUFAs, in the same way as ω6, to produce oxygenated anti-inflammatory derivatives such as *n*-3 series prostaglandins (PG), *n*-5 series leukotrienes (LT), as well as resolvins (Rv) and

protectins (PD) [32]. For example, the administration of ω3 PUFAs to obese mice as well as resolvin D1 (RvD1), an oxygenated derivative of DHA, limits macrophage infiltration, favors their polarization toward the M2 phenotype, and rescues adipocyte metabolic dysfunction [33,34]. Thus, ω6- and ω3-derived oxylipins are able to modulate the inflammatory phenotype of immune cells, especially macrophages [11,35]. As dietary ω6 and ω3 PUFAs directly affect the quality and the quantity of oxylipins synthesized and secreted by the adipocytes, it is of high interest to characterize the impact of ω3 PUFA diet supplementation on the inflammatory state of adipose tissue.

2. Materials and Methods

2.1. Reagents

Culture media and buffer solutions were purchased from Lonza (Ozyme, St-Quentin en Yvelines, France), fetal bovine serum (FBS) from Eurobio (Courtaboeuf, France), insulin and trypsin from InVitrogen (Cergy Pontoise, France). Oxylipins and inhibitors were purchased from Cayman (BertinPharma, Montigny le Bretonneux, France). Other culture reagents were from Sigma-Aldrich Chimie (Saint-Quentin Fallavier, France).

2.2. Animals and Diets

The experiments were conducted in accordance with the French and European regulations (Directive 2010/63/EU) for the care and use of research animals and were approved by national experimentation committees (MESR 01947.03). Ten-week-old C57BL/6J male mice from Janvier Laboratory (France) were maintained at thermoneutrality ($28 \pm 2\ ^\circ$C) and 12:12-h light-dark cycles, with ad libitum access to food and water to not hide any behavioral modification. Mice were fed for 12 weeks with isocaloric isoenergetic (3.2 kCal/g–13.5 kJ/g) ω6- or ω3-enriched diets (12% energy content as lipids). The diets were prepared by Harlan (WI, USA) from standard chow diets (reference number 2016) by the addition of specific fatty acid ethyl-esters from NuChekPrep (Elysian, MIN, USA). Detailed compositions are displayed in Table 1. Blood, interscapular brown adipose tissue (iBAT), epididymal (eWAT), and inguinal subcutaneous (scWAT) white adipose tissues were sampled and used for different analyses.

Table 1. Diet compositions.

	ω6-Enriched Diet	ω3-Enriched Diet
Protein [% by weight]	16	
Carbohydrate [% by weight]	52	
Fat [% by weight]	5	
Saturated fatty acids (FAs) [% of total FAs]	12	
Monounsaturated FAs [% of total FAs]	26	14
Polyunsaturated FAs [% of total FAs]	62	74
Linoleic acid [% by weight]	3	
α-linolenic acid [% by weight]	0.1	0.64
EPA [% by weight]	-	0.08
DHA [% by weight]	-	0.08
ω6/ω3 PUFA ratio	30	3.75

2.3. Cell Culture

THP-1, a human pro-monocytic cell line, was cultured in RPMI GlutaMax medium, supplemented with 10% FBS and 10 mM sodium pyruvate, at 37 $^\circ$C and 5% CO_2. Differentiation in macrophages-like cells was induced by treatment with 20 nmol/L phorbol 12-myristate 13-acetate (PMA) for 72 h. Then, media were replaced and polarization was induced for 48 h either with lipopolysaccharides (LPS, 100 ng/mL) for M1 like-phenotype or with IL-4/IL-10 (10 ng/mL each) for M2 like-phenotype acquisition. Treatments with a LOX inhibitor (=carnosic acid (CA), 10 µM), and/or with 9-HODE and 13-HODE (50 nmol/L + 50 nmol/L), were performed during the 48 h polarization step.

2.4. Oxylipin Quantification

For quantification of unesterified oxylipins, tissues were snap-frozen with liquid nitrogen immediately after retrieval and stored at -80 °C. Extraction and analysis by mass spectrometry were performed at METATOUL platform (MetaboHUB, INSERM UMR 1048, I2MC, Toulouse, France) as previously described [13,36].

2.5. Cytokine Quantification

For blood analysis, plasmas were diluted twice and analysis following manufacturer's instructions using the mouse V-PLEX Proinflammatory Panel 1 Kit (Meso Scale Discovery, # K15048D) on a QuickPlex SQ 120 apparatus (Meso Scale Discovery).

For tissue analysis, proteins were extracted from frozen organs using an ULTRA TURRAX T25 (Ika, Germany) and lysis buffer (25 mM Tris-Cl (pH 7.4), 100 mM NaCl, 1 mM EDTA, 1% Triton X-100, 0.5% Nonidet P40 and protease inhibitors (Roche Diagnostics, Meylan, France)). Protein concentration was evaluated by BCA assay (Sigma-Aldrich Chimie, Saint-Quentin Fallavier, France). 10 µg proteins were used to evaluate cytokine concentration using the same kit and apparatus as those used for blood cytokine analysis.

2.6. Histology

Freshly sampled tissues were fixed in 4% paraformaldehyde overnight at RT and then paraffin-embedded. Embedded tissues were cut into 5-µm sections and dried overnight at 37 °C. For immunohistochemistry, sections were then deparaffinized in xylene, rehydrated using alcohol, and washed in phosphate-buffered saline (PBS).

For histology analysis, sections were stained with hematoxylin-eosin and mounted in Mowiol.

For immunohistochemistry analysis, antigen unmasking was performed in boiling citrate buffer (10 mM, pH 6.0) for 6 minutes. Sections were then permeabilized in PBS with 0.2% Triton X-100 at room temperature for 20 minutes and blocked in the same buffer containing 3% BSA for 30 min. Sections were co-incubated with rat anti-F4/80 antibody (Biorad, clone Cl:A3-1, dilution 1:100) and rabbit anti-Arginase-1 (ThermoFisher Scientific, #PA5-29645, dilution 1:100) overnight at 4 °C.

Following a 30-min incubation with biotinylated anti-rat and TRITC-coupled anti-rabbit secondary antibodies, the sections were incubated for another 30 min at room temperature with avidin–biotin complex (Vector Lab, VECTASTAIN ABC Kit, PK-4000), and were then labeled with 3,3′-diaminobenzidine solution (Vector Lab, DAB, SK-4100). Nuclear staining was performed with DAPI and sections were mounted in Mowiol.

Visualization was performed with an Axiovert microscope. Pictures were captured using AxioVision software (Carl Zeiss, Jena, Germany).

2.7. Isolation and Analysis of RNA

Procedures follow MIQE recommendations [37]. Total RNA was extracted using a TRI-Reagent kit (Euromedex, Souffelweyersheim, France) according to the manufacturer's instructions. For RNA isolation from organs, tissues were homogenized in TRI-Reagent using a dispersing instrument (ULTRA TURRAX T25). A reverse transcription-polymerase chain reaction (RT-PCR) was performed using M-MLV-RT (Promega). SYBR qPCR premix Ex TaqII from Takara (Ozyme, France) was used for quantitative PCR (qPCR), and assays were run on a StepOne Plus ABI real-time PCR machine (PerkinElmer Life and Analytical Sciences, Boston). The expression of selected genes was normalized to that of the TATA-box binding protein (TBP) and 36B4 housekeeping genes and then quantified using the comparative-ΔCt method. Primer sequences are available upon request.

2.8. Statistical Analysis

Data were expressed as mean values ± standard error of the mean (SEM). Data were analyzed using InStat software (GraphPad Software) by one-way ANOVA followed by a Mann-Whitney (for in vivo experiments) or a Student-Newman-Keuls (for in vitro experiments) post-test to assess statistical differences between experimental groups. Differences were considered statistically significant with $p < 0.01$.

3. Results

3.1. Impact of ω3 PUFA Supplementation on General Parameters of Mice

3.1.1. General Metabolic Parameters

Ten-week-old male mice were fed for 12 weeks with an isocaloric isoenergetic standard diet enriched in ω6 PUFAs (ω6-enriched diet, *ω6/ω3* = 30), or supplemented with ω3 PUFAs (ω3-enriched diet, *ω6/ω3* = 3.7), see Table 1. Mice were housed at 28 °C, near thermoneutrality, in order to limit energy expenditure due to thermogenic metabolism and to avoid any effect of this activity on inflammatory response, as demonstrated previously [38].

Mice body weight, see Figure 1a, as well as food intake (ω6-enriched diet, 4.49 g/day; ω3-enriched diet, 4.46 g/day per mouse) were similar between the two groups. Epididymal white adipose tissue mean weight, see Figure 1b, and fed glycaemia, see Figure 1c, were not different after 12 weeks of the diets. Altogether, these results indicated that the *ω6/ω3* ratio of a standard diet, equilibrated in carbohydrate, protein, and fat quantities (respectively, 20.1%, 65.4%, and 14.5% of energy supply), did not modify general metabolic parameters of mice.
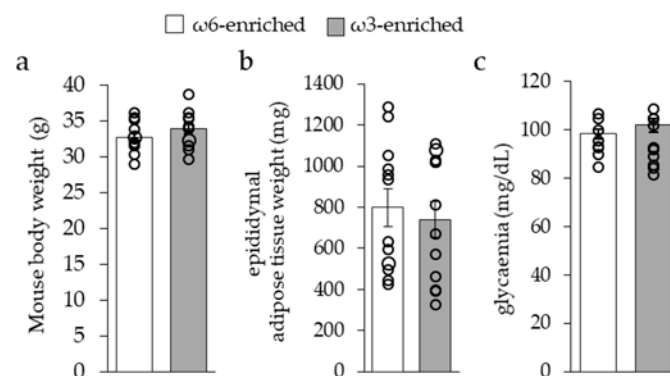

Figure 1. Mice general metabolic parameters. (**a**) Mouse body weight, (**b**) epididymal white adipose tissue weight, and (**c**) blood glycaemia evaluated after 12 weeks of ω6- or ω3-enriched diet. Results are displayed as independent mouse values (dots) and mean ± SEM (histograms). *n* = 12.

3.1.2. Plasmatic Inflammatory Phenotype

To characterize the systemic inflammatory effect of a PUFA-enriched diet, we evaluated the blood circulating level of a panel of cytokines, see Figure 2.
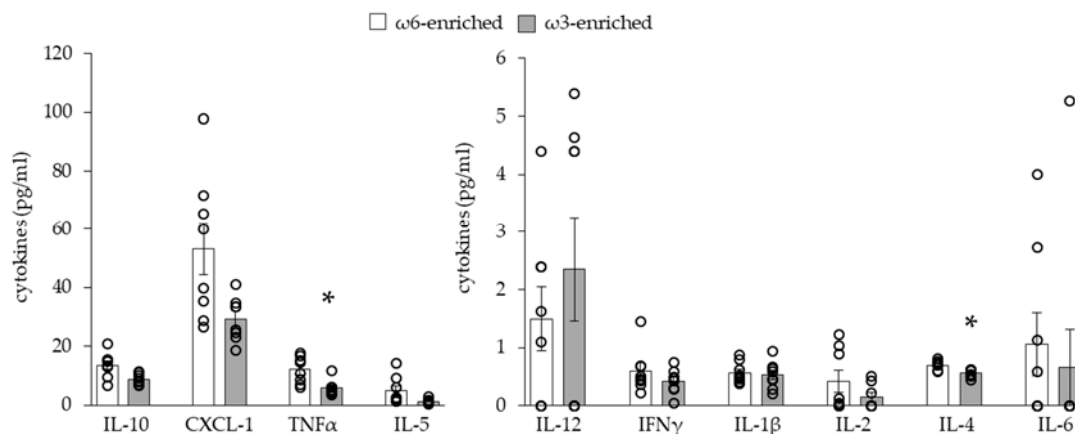
Figure 2. Analysis of blood cytokines. Results are displayed as independent mouse values (dots) and mean ± SEM (histograms). *n* = 8. *, *p* < 0.01.

As expected, the level of most of the pro-inflammatory and anti-inflammatory cytokines was unchanged between the two groups of mice. Only TNFα (pro-inflammatory cytokine) and IL-4 (anti-inflammatory cytokine) levels slightly but significantly decreased in mice fed an ω3-enriched diet.

3.1.3. Impact of ω3 PUFA Supplementation on Adipose Tissue Oxylipin Content

To investigate the modification induced by the two different diets within adipose tissues, we quantified the levels of 33 PUFA-metabolites within iBAT, see Figure 3, and scWAT, see Figure 4, of mice. These oxylipins were analyzed by groups following their PUFA origin, see Figures 3a and 4a, or separately, see Figures 3b and 4b. In the iBAT, ω3 PUFA supplementation led to a significant increase of the oxylipins deriving from ω3 PUFAs EPA (PGE3, LTB5, 18-HEPE) and DHA (RvD2, RvD1, MaR1, PDx, 17-HDoHE, 14-HDoHE), but did not affect ω6-derived metabolites (6kPGF1a, TxB2, 11B-PGF2a, PGF2a, PGE2, PGD2, 8isoPGA2, 15dPGJ2, LxB4, LxA4, LTB4, 5,6-DiHETE, 15-HETE, 8-HETE, 12-HETE, 5-HETE, 5oxoETE, 14,15-EET, 11,12-EET, 8,9-EET, 5,6-EET derived from ARA; 13-HODE, 9-HODE derived from LA), see Figure 3a.

In scWAT, while similar results were found for ω3 PUFA-derived and ARA-derived oxylipins, LA-derived metabolites were highly increased, as shown in Figure 4a.

LA and ω3-PUFA derived oxylipins are considered as anti-inflammatory and pro-resolving mediators, especially through the modulation of macrophage function. Along with these oxylipins, we have found that 14- and 17-HDoHEs and 18-HEPE levels were increased in iBAT and scWAT of mice fed the ω3-enriched diet, and 9- and 13-HODEs were increased only in scWAT, see Figures 3b and 4b. 14- and 17-HDoHE are metabolized in pro-resolving mediators as RvD1, RvD2, Mar1, PDx, and PD1, while 18-HEPE leads to RvE1 synthesis. It is interesting to note that these final metabolites were barely (PDx) or not detected within the tissue, see Figures 3b and 4b.
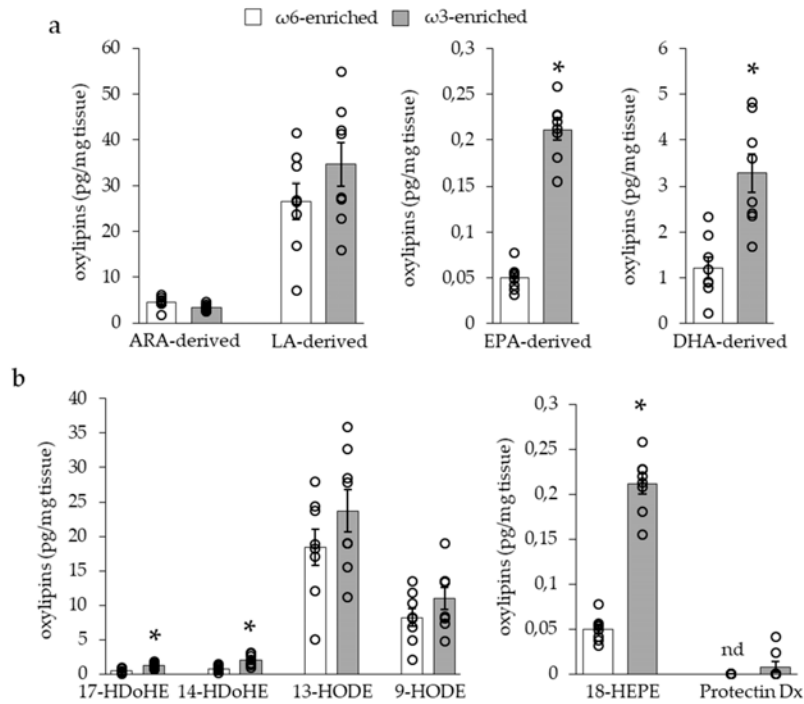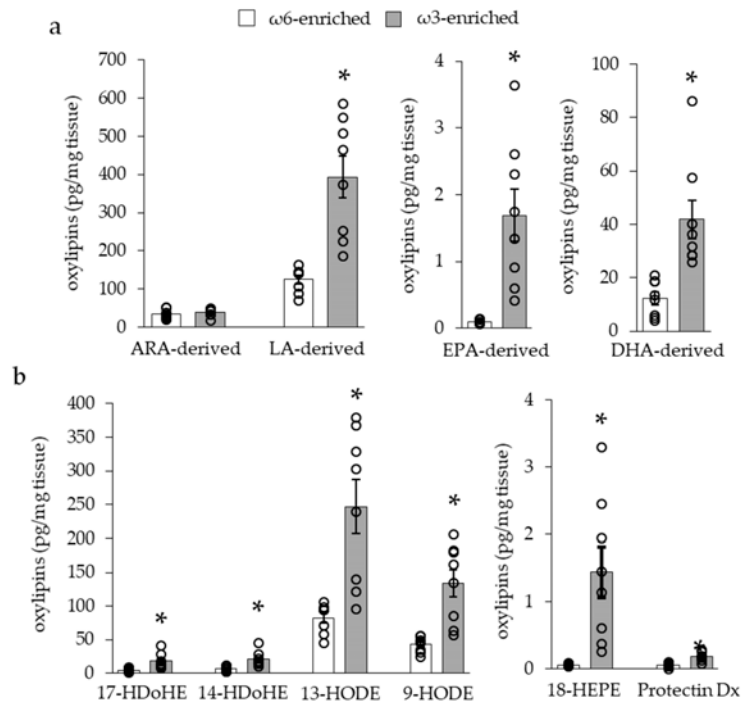
Figure 3. Quantities of oxylipins derived from dietary polyunsaturated fatty acids (PUFAs) in interscapular brown adipose tissue (iBAT). (**a**) Quantities of oxylipins derived from arachidonic acid (ARA) and linoleic acid (LA) ω6 PUFAS or eicosapentaenoic acid (EPA) and docosahexaenoic acid (DHA) ω3 PUFAs. (**b**) Quantities of oxylipins considered as anti-inflammatory or pro-resolving mediator intermediates. Results are displayed as independent mouse values (dots) and mean ± SEM (histograms). $n = 8$. *, $p < 0.01$.

Figure 4. Quantities of oxylipins derived from dietary PUFAs in inguinal subcutaneous white adipose tissues (scWAT). (**a**) Quantities of oxylipins derived from ARA and LA ω6 PUFAS or EPA and DHA ω3 PUFAs. (**b**) Quantities of oxylipins considered as anti-inflammatory or pro-resolving mediator intermediates. Results are displayed as independent mouse values (dots) and mean ± SEM (histograms). $n = 8$. *, $p < 0.01$.

3.2. Effect on Inflammatory Phenotype of Adipose Tissue

3.2.1. Histology and Cytokine Content

The histological analysis of iBAT and scWAT, see Figure 5a, revealed neither cell infiltration nor crown structure that were typical of an adipose tissue inflammatory response in both groups of mice.
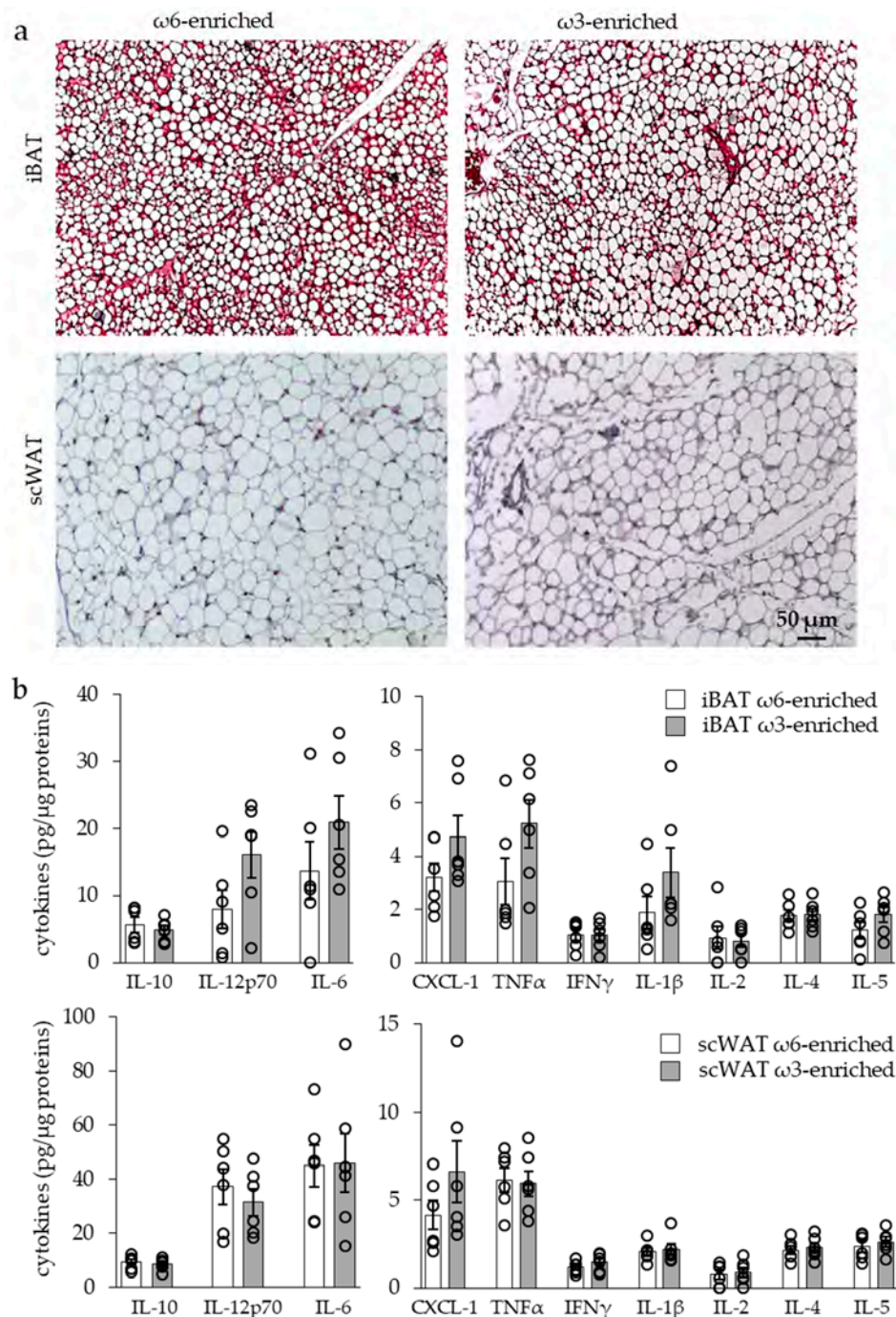

Figure 5. Inflammatory profile of iBAT and scWAT of mice submitted to ω6- or ω3-enriched diet. (**a**) Hematoxylin and eosin staining of tissue sections. (**b**) Analysis of adipose tissue cytokine levels. Results are displayed as independent mouse values (dots) and mean ± SEM (histograms). $n = 6$. *, $p < 0.01$.

In the same way, analysis of the iBAT and scWAT cytokine contents showed similar levels of both pro- and anti-inflammatory cytokines in the two groups of mice, as shown in Figure 5b.

3.2.2. Expression of Inflammatory Markers

As we did not find any modulation of cytokine levels, we analyzed marker expression of specialized macrophages to evaluate the inflammatory background of the tissue, see Figure 6.
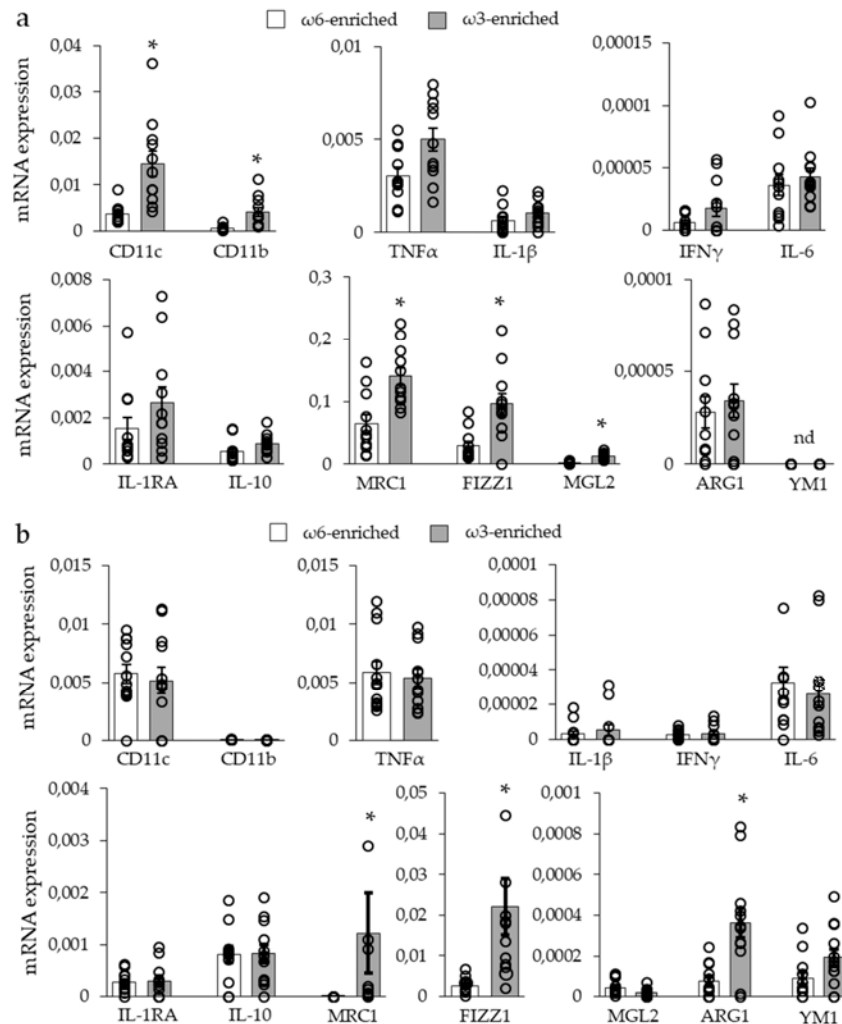

Figure 6. Macrophage marker expression in adipose tissue of mice submitted to ω6- or ω3-enriched diet. mRNA level analysis of general (CD11c, CD11b), M1 (TNFα, IL-1β, IFNγ, IL-6) and M2 (IL-1RA, IL-10, MRC1, FIZZ1, MGL2, ARG1, YM1) macrophage markers in (**a**) iBAT and (**b**) scWAT. Histograms display mean ± SEM. *n* = 12. *, *p* < 0.01.

The analysis of macrophage markers in iBAT derived from the ω3-enriched diet group, see Figure 6a, revealed an increase in CD11b (or ITGAM, integrin αM) and CD11c (or ITGAX, integrin αX) mRNA expression, concomitantly to an increase in major M2 macrophage markers, namely MRC1 (mannose receptor 1), FIZZ1 (found in inflammatory zone 1 or RELMα), and MGL2 (macrophage galactose N-acetyl-galactosamine specific lectin 2). No change was found for other M2 macrophage markers or for M1 macrophage markers. To note, ARG1 (arginase 1) and Ym1 (chitinase 3-like 3) were either barely detected or undetected in this tissue.

The analysis of the scWAT, see Figure 6b, from ω3-supplemented mice, showed an increased the expression of the M2 macrophage markers MRC1 and FIZZ1 (not MGL2), but no increase of CD11c (CD11b was undetected). In contrast to iBAT, our data revealed an increase of ARG1 mRNA expression

and the induction of YM1 mRNA expression. Finally, as for iBAT, no change was found for mRNA expression of M1 macrophage markers.

Altogether, these results demonstrated that an ω3-enriched diet led to a general increase in M2 anti-inflammatory macrophage marker expression without modification in M1 pro-inflammatory markers. This was correlated and perhaps due to the increased amount of substrates for pro-resolving mediator synthesis, as well as an increased quantity of M2 polarizing oxylipins.

3.3. Effect of Potential Anti-Inflammatory Oxylipins Modified in an ω3-Enriched Diet on THP1 Monocyte Cells

The oxylipins 9- and 13-HODEs (LA-derived oxylipins metabolized by LOX) are not known to be precursors of pro-resolving mediators but display high contents in iBAT, see Figure 3b, and scWAT, see Figure 4b, and are strongly increased in scWAT after the implementation of an ω3-enriched diet. In order to investigate the role of 9- and 13-HODEs on macrophage polarization, we used THP-1 macrophage cell lines activated in pro-inflammatory M1 (LPS 100 ng/mL, Figure 7a) or anti-inflammatory M2-like phenotype (IL4 + IL-10 10 ng/mL each, Figure 7b). THP-1 cells were treated with 9- and 13-HODEs (9/13-HODEs, 50 nmol/L each) or with carnosic acid (CA, 10 μM), a lipoxygenase inhibitor [39], or a combination of both.
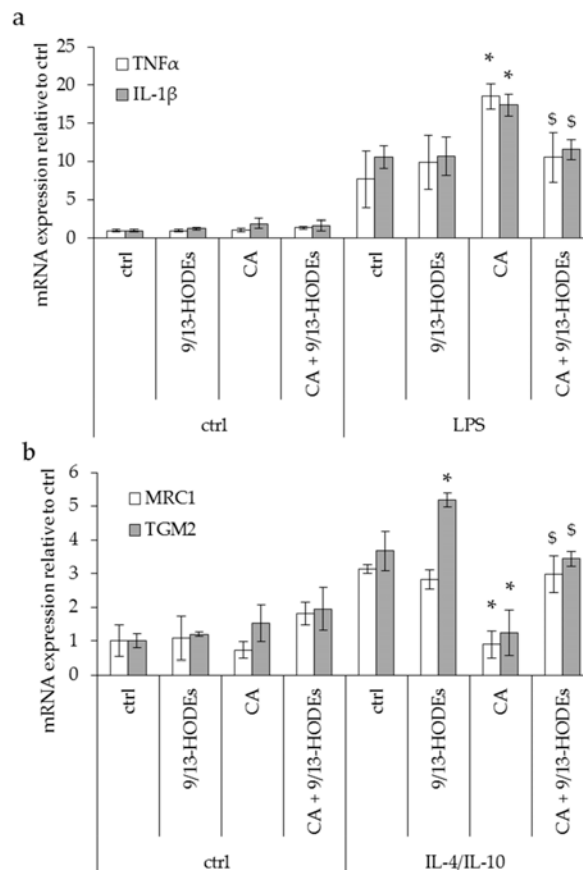

Figure 7. Macrophage marker expression in THP-1 cells under 9- and 13-HODE treatment. mRNA level analysis by RT-qPCR of M1 (TNFα, IL-1β) and M2 (MRC1, TGM2) macrophage markers in control, lipopolysaccharides (LPS) (upper panel) or IL-4/IL-10 (lower panel) treated THP-1 macrophages. Cells were co-treated for 48 h with carnosic acid (CA, 10 μM) and or 9- and 13-HODEs. (**a**) CA treatment induced opposite effects in M1- and M2-like macrophages as it increased inflammatory markers in THP-1 M1-like macrophages, and (**b**) decreased M2-like macrophages' markers. Histograms display mean ± SEM. n = 3. *, p < 0.01 vs. ctrl and $, p < 0.01 vs. CA.

None of the treatments modulated non-polarized THP-1, see Figure 7. Treatment with 9/13-HODEs alone showed no effect on macrophages' M1-like phenotype but increased TGM2 expression on M2-like macrophages. Remarkably, CA treatment induced opposite effects in M1- and M2-like macrophages as it increased inflammatory markers in THP-1 M1-like macrophages, see Figure 7a, and decreased M2-like macrophages' markers, see Figure 7b. Interestingly, 9/13-HODEs supplementation reversed CA effects, see Figure 7.

4. Discussion

Dietary fats are the source of essential PUFAs that are required for fetal and newborn development and trigger a variety of biological responses in adults, especially, in adipose tissue. New dietary recommendations warn against the insufficient intake of ω3 PUFAs and the excess of ω6 PUFAs which correlate with various disease developments [3,4]. In the first year of life, a high dietary *ω6/ω3* ratio is positively associated with adiposity of infants [40–42]. In the same way, in adults, a high *ω6/ω3* ratio can correlate to an increase of fat mass and the development of metabolic complications [6–10].

Conversely, it has been described that a low *ω6/ω3* ratio seems to be correlated with metabolic disorder protection in different populations [43]. On a metabolic point of view, diets exhibiting a high *ω6/ω3* ratio allow a higher ARA bioavailability for the synthesis of ω6-derived eicosanoids due to an insufficient compensatory effect of EPA and DHA [15]. Indeed, both ω6 and ω3 PUFAs are metabolized using the same enzymatic pathways. First, LA and LNA are modified by common Δ-desaturases and elongases [44]; then, their metabolites, i.e., ARA, DGLA, EPA, and DHA, are metabolized in oxygenated derivatives also using common pathways involving cyclooxygenases, lipoxygenases, and CYP450 enzymatic reactions. Here, we provided evidence that, compared to a high *ω6/ω3* PUFA ratio, an equilibrated ratio of four allows the synthesis of LA and EPA/DHA oxylipins instead of ARA oxylipins. As LA and LNA use a common pathway (Δ-desaturase) to be transformed, respectively, into DGLA/ARA and EPA/DHA, we hypothesize that LNA supplementation could limit LA desaturation and thus increase LA bioavailability and metabolization in oxylipins through the LOX pathways. Thus, these competitive phenomena, in addition to dietary intake, determine PUFA availability in oxylipins synthesis and, in turn, their various metabolic effects, especially for inflammatory responses [45].

It has already been described in rodents that an increase of white adipose tissue mass can be related to an ω6 PUFA-enriched high-fat diet and can be prevented by ω3 PUFA supplementation [12, 46]. It is suggested that this could only be due to a specific subset of ω3 PUFA such as EPA [47]. Moreover, eicosanoids derived from ω6 PUFA inhibit adipocyte thermogenic activity both in vitro and in vivo [11,13,48]. We and others demonstrated previously, using the same nutritional approach as in the present work, that an ω3 PUFA diet supplementation improved the thermogenic adipocyte function by promoting a more oxidative phenotype in response to β-adrenergic stimulation [14,49]. In the present study, ω3 PUFA supplementation does not induce any change in body mass, glycaemia, or white and brown adipose tissue morphologies since the mice were fed diets with normal fat content and did not receive any β-adrenergic challenge.

Most studies concerning ω3 PUFA supplementations were carried out in a context of obesity (high-fat diet) or infection (LPS treatment) and demonstrate a positive effect of ω3 PUFA supplementation on the analyzed parameters [35]. Nevertheless, other studies demonstrate the inability of ω3 PUFAs to modulate inflammation after LPS treatment [50] or in obese mice [51,52]. These discrepancies are essentially due to the differences in the experimental approaches (diet composition, mouse strain, challenge . . . .) and in the analyzed parameters (cytokine concentration, mRNA expression, histology . . .). In humans, several experimental approaches have tried to link an ω3 PUFA intake to inflammatory response, again with inconsistent conclusions. For example, a one-year dietary supplementation in ω3 PUFA does not modify the circulating cytokine levels in healthy volunteers [53]. Conversely, other studies show a decrease of blood inflammatory markers after ω3 PUFA supplementation [54,55]. It is important to note that a plasma inflammatory mediator profile seems to be less representative compared to the one of adipose tissue [56]. The same discrepancy

is found for studies analyzing adipose tissue inflammation. Although one human trial (4g ω3 PUFAs/day; 12 weeks) on insulin-resistant adults demonstrates a decrease in the crown-like structure number [57], corresponding to phagocytic activity of macrophage on adipocyte, another trial on the same type of patients (4.2g ω3 PUFAs/day; 6 months) demonstrates no effect of ω3 PUFA supplementation on the same parameter [58]. Moreover, a recent paper establishes that the oxylipin profile in rat adipose tissue after dietary ω3 PUFA supplementation (ratio *ω6/ω3* of 0.6) is dependent of (i) the kind of ω3 PUFA used, (ii) the kind of adipose tissue analyzed, and (iii) the sex [59].

In view of these heterogeneities, we decided to analyze the effect of PUFA intake in normal physiological conditions (thermoneutrality, no β-adrenergic challenge) using an isocaloric, isoenergetic standard diet supplemented with ethyl esters of fatty acids (instead of classic oil supplementation) and various technical approaches to characterize the inflammatory profile. With this strategy, we characterize fatty acid metabolism within subcutaneous and brown adipose tissues and the related inflammatory phenotype. Our results linking ω3 PUFA supplementation and M2 macrophage are in line with other studies, such as a recent one demonstrating that (i) treatment of human adipose tissue explants with ω3 PUFAs lead to an anti-inflammatory phenotype characterized by a decrease of M1 marker expression, and (ii) treatment of THP-1 cells increased expression of M2 markers [60]. In the same way, DHA supplementation in a high-fat diet context promotes mRNA expression of M2 markers within white adipose tissue without affecting the total macrophage number [61]. In this study, the authors describe the same effect for RvD1, DHA metabolites, and conclude that DHA leads to an anti-inflammatory phenotype via RvD1 synthesis. Unfortunately, they never quantify RvD1 production in vivo and thus do not link DHA supplementation to RvD1 synthesis [61]. In our study, we have not been able to detect resolvins but only their substrates. We assume that without a specific inflammatory signal, intermediates of pro-resolving mediators are synthesized but not metabolized. Indeed, these mediators are involved in the resolution of inflammation and appeared late in the process as they are not required before, differently to prostaglandins and leukotrienes which appear early [62].

In our study, we measure a defined set of oxylipins. Even if this panel includes oxylipins deriving from all pathways and PUFAs, we cannot exclude that unmeasured oxylipins triggered the anti-inflammatory effect of ω3 PUFA supplementation found in our model. In this way, epoxide and diol metabolites derived from CYP epoxygenase/soluble epoxide hydrolase activity [63], as well as endocannabinoids, are known and interesting potential mediators of the inflammatory effect of PUFA [64]. In addition, the esterification of oxylipins, especially of eicosanoids, was described as an active and major mechanism in various cell biological responses including inflammation [65]. These esterified oxylipins can represent the majority of cell oxylipins and can be hydrolyzed from the membrane under specific stimuli [66]. In this way, it could be interesting to quantify all oxylipins (unesterified and esterified) in adipose tissue under ω3 PUFA diet supplementation and to evaluate their hydrolysis under inflammatory conditions. Nevertheless, our unexhaustive analysis allowed a correlation between the synthesis of several oxylipins and the expression of M2 macrophage markers. We propose that 9- and 13-HODEs could drive this effect. In our in vitro results on the THP-1 cell line, we demonstrate that 9- and 13-HODEs are not enough to directly drive the polarization of THP-1 macrophage but are required to maintain the phenotype. Indeed, their supplementation restores control level expression of M1-like and M2-like markers after CA treatment. Moreover, 9- and 13-HODEs seem to play a role in the anti-inflammatory effects since they are able to increase M2 markers such as TGM2. These results are consistent with some studies describing 9- and 13-HODEs as known mediators of macrophage polarization [67] in a PPARγ-dependent manner [68]. Of course, other oxylipins could be involved in the anti-inflammatory environment found in our mice. For example, the study of Fat-1 mouse, which is able to synthesize ω3 PUFAs itself, displays a lowered inflammatory environment induced by obesity, correlatively to 17-HDoHE synthesis [69]. In addition to oxylipins involvement, we cannot exclude a direct action of ω3 PUFAs on the membrane receptor. Indeed, it is shown that DHA is able to directly activate, via GPR120, an anti-inflammatory response driven by macrophage within adipose tissue [33]. This activity could be linked to the recent characterization of the DHA

inhibitory effect on NLRP3 inflammasome activity, an effect triggered by GPR40/GPR120 pathways and leading to a decreased production of mature IL-1β [70]. As NLRP3 is activated essentially in response to an infectious environment, we do not correlate ω3 PUFA supplementation with a decrease in IL-1β production in our physiological context.

It is interesting to note that the ω3 PUFA intake finely drives the kind of oxylipins synthesized. A recent study analyzed the effect of an ω3 PUFA dietary supplementation of an already equilibrated diet (ratio *ω6/ω3* = 6.7) to reach an *ω6/ω3* ratio of 0.8. Thus, differently to our situation, LA and LNA are already desaturated equivalently, and the increase in ω3 PUFA intake leads to a decrease of LA-derived oxylipins (9/13-HODEs) in favor of EPA and DHA derived oxylipins in the brain. Moreover, this "over"-supplementation ameliorates against an inflammatory response [71].

5. Conclusions

Previous studies have demonstrated the positive effect of ω3 PUFA intake to counteract the adverse consequences of a high-fat diet or inflammatory situation. Herein, our study was conducted in non-obesogenic non-inflammatory conditions and also showed a beneficial influence of ω3 PUFA dietary supplementation on the adipose tissue inflammatory phenotype. Moreover, while ω3 PUFA metabolites have been involved in this effect, we additionally highlighted the unsuspected role of LA-derived metabolites. Finally, this already assumed beneficial outcome of ω3 PUFA supplementation is in line with a human situation where a high *ω6/ω3* ratio is correlated with the development of inflammatory diseases in metabolic tissue.

References

1. Simopoulos, A.P. The importance of the ratio of omega-6/omega-3 essential fatty acids. *Biomed. Pharmacother.* **2002**, *56*, 365–379. [CrossRef]
2. Simopoulos, A.P. An Increase in the Omega-6/Omega-3 Fatty Acid Ratio Increases the Risk for Obesity. *Nutrients* **2016**, *8*, 128. [CrossRef]
3. Ailhaud, G.; Massiera, F.; Weill, P.; Legrand, P.; Alessandri, J.M.; Guesnet, P. Temporal changes in dietary fats: Role of *n*-6 polyunsaturated fatty acids in excessive adipose tissue development and relationship to obesity. *Prog. Lipid Res.* **2006**, *45*, 203–236. [CrossRef] [PubMed]
4. Muhlhausler, B.S.; Ailhaud, G.P. Omega-6 polyunsaturated fatty acids and the early origins of obesity. *Curr. Opin. Endocrinol. Diabetes Obes.* **2013**, *20*, 56–61. [CrossRef] [PubMed]
5. Simopoulos, A.P.; DiNicolantonio, J.J. The importance of a balanced omega-6 to omega-3 ratio in the prevention and management of obesity. *Open Heart* **2016**, *3*, e000385. [CrossRef]
6. Inoue, K.; Kishida, K.; Hirata, A.; Funahashi, T.; Shimomura, I. Low serum eicosapentaenoic acid/arachidonic acid ratio in male subjects with visceral obesity. *Nutr. Metab. (Lond.)* **2013**, *10*, 25. [CrossRef] [PubMed]
7. Savva, S.C.; Chadjigeorgiou, C.; Hatzis, C.; Kyriakakis, M.; Tsimbinos, G.; Tornaritis, M.; Kafatos, A. Association of adipose tissue arachidonic acid content with BMI and overweight status in children from Cyprus and Crete. *Br. J. Nutr.* **2004**, *91*, 643–649. [CrossRef]

8. Williams, E.S.; Baylin, A.; Campos, H. Adipose tissue arachidonic acid and the metabolic syndrome in Costa Rican adults. *Clin. Nutr.* **2007**, *26*, 474–482. [CrossRef]

9. Claria, J.; Nguyen, B.T.; Madenci, A.L.; Ozaki, C.K.; Serhan, C.N. Diversity of lipid mediators in human adipose tissue depots. *Am. J. Physiol. Cell Physiol.* **2013**, *304*, C1141–C1149. [CrossRef]

10. Garaulet, M.; Perez-Llamas, F.; Perez-Ayala, M.; Martinez, P.; de Medina, F.S.; Tebar, F.J.; Zamora, S. Site-specific differences in the fatty acid composition of abdominal adipose tissue in an obese population from a Mediterranean area: Relation with dietary fatty acids, plasma lipid profile, serum insulin, and central obesity. *Am. J. Clin. Nutr.* **2001**, *74*, 585–591. [CrossRef]

11. Ghoshal, S.; Trivedi, D.B.; Graf, G.A.; Loftin, C.D. Cyclooxygenase-2 deficiency attenuates adipose tissue differentiation and inflammation in mice. *J. Biol. Chem.* **2011**, *286*, 889–898. [CrossRef] [PubMed]

12. Massiera, F.; Saint-Marc, P.; Seydoux, J.; Murata, T.; Kobayashi, T.; Narumiya, S.; Guesnet, P.; Amri, E.Z.; Negrel, R.; Ailhaud, G. Arachidonic acid and prostacyclin signaling promote adipose tissue development: A human health concern? *J. Lipid Res.* **2003**, *44*, 271–279. [CrossRef] [PubMed]

13. Pisani, D.F.; Ghandour, R.A.; Beranger, G.E.; Le Faouder, P.; Chambard, J.C.; Giroud, M.; Vegiopoulos, A.; Djedaini, M.; Bertrand-Michel, J.; Tauc, M.; et al. The omega6-fatty acid, arachidonic acid, regulates the conversion of white to brite adipocyte through a prostaglandin/calcium mediated pathway. *Mol. Metab.* **2014**, *3*, 834–847. [CrossRef] [PubMed]

14. Ghandour, R.A.; Colson, C.; Giroud, M.; Maurer, S.; Rekima, S.; Ailhaud, G.P.; Klingenspor, M.; Amri, E.Z.; Pisani, D.F. Impact of dietary omega3 polyunsaturated fatty acid supplementation on brown and brite adipocyte function. *J. Lipid Res.* **2018**. [CrossRef] [PubMed]

15. Fischer, R.; Konkel, A.; Mehling, H.; Blossey, K.; Gapelyuk, A.; Wessel, N.; von Schacky, C.; Dechend, R.; Muller, D.N.; Rothe, M.; et al. Dietary omega-3 fatty acids modulate the eicosanoid profile in man primarily via the CYP-epoxygenase pathway. *J. Lipid Res.* **2014**, *55*, 1150–1164. [CrossRef] [PubMed]

16. Odegaard, J.I.; Chawla, A. The immune system as a sensor of the metabolic state. *Immunity* **2013**, *38*, 644–654. [CrossRef] [PubMed]

17. Tilg, H.; Moschen, A.R. Adipocytokines: Mediators linking adipose tissue, inflammation and immunity. *Nat. Rev. Immunol.* **2006**, *6*, 772–783. [CrossRef] [PubMed]

18. Hotamisligil, G.S. Inflammation and metabolic disorders. *Nature* **2006**, *444*, 860–867. [CrossRef]

19. Lumeng, C.N.; Bodzin, J.L.; Saltiel, A.R. Obesity induces a phenotypic switch in adipose tissue macrophage polarization. *J. Clin. Investig.* **2007**, *117*, 175–184. [CrossRef]

20. Sica, A.; Mantovani, A. Macrophage plasticity and polarization: In vivo veritas. *J. Clin. Investig.* **2012**, *122*, 787–795. [CrossRef]

21. Roszer, T. Understanding the Mysterious M2 Macrophage through Activation Markers and Effector Mechanisms. *Mediat. Inflamm.* **2015**, *2015*, 816460. [CrossRef] [PubMed]

22. Hotamisligil, G.S.; Shargill, N.S.; Spiegelman, B.M. Adipose expression of tumor necrosis factor-alpha: Direct role in obesity-linked insulin resistance. *Science* **1993**, *259*, 87–91. [CrossRef] [PubMed]

23. Jager, J.; Gremeaux, T.; Cormont, M.; Le Marchand-Brustel, Y.; Tanti, J.F. Interleukin-1beta-induced insulin resistance in adipocytes through down-regulation of insulin receptor substrate-1 expression. *Endocrinology* **2007**, *148*, 241–251. [CrossRef] [PubMed]

24. Okla, M.; Zaher, W.; Alfayez, M.; Chung, S. Inhibitory Effects of Toll-Like Receptor 4, NLRP3 Inflammasome, and Interleukin-1beta on White Adipocyte Browning. *Inflammation* **2018**, *41*, 626–642. [CrossRef] [PubMed]

25. Goto, T.; Naknukool, S.; Yoshitake, R.; Hanafusa, Y.; Tokiwa, S.; Li, Y.; Sakamoto, T.; Nitta, T.; Kim, M.; Takahashi, N.; et al. Proinflammatory cytokine interleukin-1beta suppresses cold-induced thermogenesis in adipocytes. *Cytokine* **2016**, *77*, 107–114. [CrossRef] [PubMed]

26. Sakamoto, T.; Takahashi, N.; Sawaragi, Y.; Naknukool, S.; Yu, R.; Goto, T.; Kawada, T. Inflammation induced by RAW macrophages suppresses UCP1 mRNA induction via ERK activation in 10T1/2 adipocytes. *Am. J. Physiol. Cell Physiol.* **2013**, *304*, C729–C738. [CrossRef]

27. Lee, Y.H.; Kim, S.N.; Kwon, H.J.; Maddipati, K.R.; Granneman, J.G. Adipogenic role of alternatively activated macrophages in beta-adrenergic remodeling of white adipose tissue. *Am. J. Physiol. Regul. Integr. Comp. Physiol.* **2016**, *310*, R55–R65. [CrossRef]

28. Qiu, Y.; Nguyen, K.D.; Odegaard, J.I.; Cui, X.; Tian, X.; Locksley, R.M.; Palmiter, R.D.; Chawla, A. Eosinophils and type 2 cytokine signaling in macrophages orchestrate development of functional beige fat. *Cell* **2014**, *157*, 1292–1308. [CrossRef]

29. Bolus, W.R.; Hasty, A.H. Contributions of Innate Type 2 Inflammation to Adipose Function. *J. Lipid Res.* **2018**. [CrossRef]

30. Camell, C.D.; Sander, J.; Spadaro, O.; Lee, A.; Nguyen, K.Y.; Wing, A.; Goldberg, E.L.; Youm, Y.H.; Brown, C.W.; Elsworth, J.; et al. Inflammasome-driven catecholamine catabolism in macrophages blunts lipolysis during ageing. *Nature* **2017**, *550*, 119–123. [CrossRef]

31. Hardwick, J.P.; Eckman, K.; Lee, Y.K.; Abdelmegeed, M.A.; Esterle, A.; Chilian, W.M.; Chiang, J.Y.; Song, B.J. Eicosanoids in metabolic syndrome. *Adv. Pharmacol.* **2013**, *66*, 157–266. [CrossRef] [PubMed]

32. Masoodi, M.; Kuda, O.; Rossmeisl, M.; Flachs, P.; Kopecky, J. Lipid signaling in adipose tissue: Connecting inflammation & metabolism. *Biochim. Biophys. Acta* **2015**, *1851*, 503–518. [CrossRef] [PubMed]

33. Oh, D.Y.; Talukdar, S.; Bae, E.J.; Imamura, T.; Morinaga, H.; Fan, W.; Li, P.; Lu, W.J.; Watkins, S.M.; Olefsky, J.M. GPR120 is an omega-3 fatty acid receptor mediating potent anti-inflammatory and insulin-sensitizing effects. *Cell* **2010**, *142*, 687–698. [CrossRef] [PubMed]

34. Titos, E.; Claria, J. Omega-3-derived mediators counteract obesity-induced adipose tissue inflammation. *Prostaglandins Other Lipid Mediat.* **2013**, *107*, 77–84. [CrossRef] [PubMed]

35. Liddle, D.M.; Hutchinson, A.L.; Wellings, H.R.; Power, K.A.; Robinson, L.E.; Monk, J.M. Integrated Immunomodulatory Mechanisms through which Long-Chain *n*-3 Polyunsaturated Fatty Acids Attenuate Obese Adipose Tissue Dysfunction. *Nutrients* **2017**, *9*, 1289. [CrossRef] [PubMed]

36. Le Faouder, P.; Baillif, V.; Spreadbury, I.; Motta, J.P.; Rousset, P.; Chene, G.; Guigne, C.; Terce, F.; Vanner, S.; Vergnolle, N.; et al. LC-MS/MS method for rapid and concomitant quantification of pro-inflammatory and pro-resolving polyunsaturated fatty acid metabolites. *J. Chromatogr. B Analyt. Technol. Biomed. Life Sci.* **2013**, *932*, 123–133. [CrossRef] [PubMed]

37. Bustin, S.A.; Benes, V.; Garson, J.A.; Hellemans, J.; Huggett, J.; Kubista, M.; Mueller, R.; Nolan, T.; Pfaffl, M.W.; Shipley, G.L.; et al. The MIQE guidelines: Minimum information for publication of quantitative real-time PCR experiments. *Clin. Chem.* **2009**, *55*, 611–622. [CrossRef]

38. Tian, X.Y.; Ganeshan, K.; Hong, C.; Nguyen, K.D.; Qiu, Y.; Kim, J.; Tangirala, R.K.; Tontonoz, P.; Chawla, A. Thermoneutral Housing Accelerates Metabolic Inflammation to Potentiate Atherosclerosis but Not Insulin Resistance. *Cell Metab.* **2016**, *23*, 165–178. [CrossRef]

39. Poeckel, D.; Greiner, C.; Verhoff, M.; Rau, O.; Tausch, L.; Hornig, C.; Steinhilber, D.; Schubert-Zsilavecz, M.; Werz, O. Carnosic acid and carnosol potently inhibit human 5-lipoxygenase and suppress pro-inflammatory responses of stimulated human polymorphonuclear leukocytes. *Biochem. Pharmacol.* **2008**, *76*, 91–97. [CrossRef]

40. Donahue, S.M.; Rifas-Shiman, S.L.; Gold, D.R.; Jouni, Z.E.; Gillman, M.W.; Oken, E. Prenatal fatty acid status and child adiposity at age 3 y: Results from a US pregnancy cohort. *Am. J. Clin. Nutr.* **2011**, *93*, 780–788. [CrossRef]

41. Moon, R.J.; Harvey, N.C.; Robinson, S.M.; Ntani, G.; Davies, J.H.; Inskip, H.M.; Godfrey, K.M.; Dennison, E.M.; Calder, P.C.; Cooper, C.; et al. Maternal plasma polyunsaturated fatty acid status in late pregnancy is associated with offspring body composition in childhood. *J. Clin. Endocrinol. Metab.* **2013**, *98*, 299–307. [CrossRef]

42. Rudolph, M.C.; Young, B.E.; Lemas, D.J.; Palmer, C.E.; Hernandez, T.L.; Barbour, L.A.; Friedman, J.E.; Krebs, N.F.; MacLean, P.S. Early infant adipose deposition is positively associated with the *n*-6 to *n*-3 fatty acid ratio in human milk independent of maternal BMI. *Int. J. Obes. (Lond.)* **2017**, *41*, 510–517. [CrossRef] [PubMed]

43. Muley, A.; Muley, P.; Shah, M. ALA, fatty fish or marine *n*-3 fatty acids for preventing DM? A systematic review and meta-analysis. *Curr. Diabetes Rev.* **2014**, *10*, 158–165. [CrossRef] [PubMed]

44. D'Andrea, S.; Guillou, H.; Jan, S.; Catheline, D.; Thibault, J.N.; Bouriel, M.; Rioux, V.; Legrand, P. The same rat Delta6-desaturase not only acts on 18- but also on 24-carbon fatty acids in very-long-chain polyunsaturated fatty acid biosynthesis. *Biochem. J.* **2002**, *364*, 49–55. [CrossRef] [PubMed]

45. Monk, J.M.; Liddle, D.M.; Cohen, D.J.; Tsang, D.H.; Hillyer, L.M.; Abdelmagid, S.A.; Nakamura, M.T.; Power, K.A.; Ma, D.W.; Robinson, L.E. The delta 6 desaturase knock out mouse reveals that immunomodulatory effects of essential *n*-6 and *n*-3 polyunsaturated fatty acids are both independent of and dependent upon conversion. *J. Nutr. Biochem.* **2016**, *32*, 29–38. [CrossRef] [PubMed]

46. Muhlhausler, B.S.; Cook-Johnson, R.; James, M.; Miljkovic, D.; Duthoit, E.; Gibson, R. Opposing effects of omega-3 and omega-6 long chain polyunsaturated Fatty acids on the expression of lipogenic genes in omental and retroperitoneal adipose depots in the rat. *J. Nutr. Metab.* **2010**, *2010*. [CrossRef] [PubMed]

47. Pinel, A.; Pitois, E.; Rigaudiere, J.P.; Jouve, C.; De Saint-Vincent, S.; Laillet, B.; Montaurier, C.; Huertas, A.; Morio, B.; Capel, F. EPA prevents fat mass expansion and metabolic disturbances in mice fed with a Western diet. *J. Lipid Res.* **2016**, *57*, 1382–1397. [CrossRef] [PubMed]

48. Fjaere, E.; Aune, U.L.; Roen, K.; Keenan, A.H.; Ma, T.; Borkowski, K.; Kristensen, D.M.; Novotny, G.W.; Mandrup-Poulsen, T.; Hudson, B.D.; et al. Indomethacin Treatment Prevents High Fat Diet-induced Obesity and Insulin Resistance but Not Glucose Intolerance in C57BL/6J Mice. *J. Biol. Chem.* **2014**, *289*, 16032–16045. [CrossRef] [PubMed]

49. Zhao, M.; Chen, X. Eicosapentaenoic acid promotes thermogenic and fatty acid storage capacity in mouse subcutaneous adipocytes. *Biochem. Biophys. Res. Commun.* **2014**, *450*, 1446–1451. [CrossRef]

50. Shin, S.; Ajuwon, K.M. Lipopolysaccharide Alters Thermogenic and Inflammatory Genes in White Adipose Tissue in Mice Fed Diets with Distinct 18-Carbon Fatty-Acid Composition. *Lipids* **2018**, *53*, 885–896. [CrossRef]

51. Sundaram, S.; Bukowski, M.R.; Lie, W.R.; Picklo, M.J.; Yan, L. High-Fat Diets Containing Different Amounts of n3 and n6 Polyunsaturated Fatty Acids Modulate Inflammatory Cytokine Production in Mice. *Lipids* **2016**, *51*, 571–582. [CrossRef] [PubMed]

52. Todoric, J.; Loffler, M.; Huber, J.; Bilban, M.; Reimers, M.; Kadl, A.; Zeyda, M.; Waldhausl, W.; Stulnig, T.M. Adipose tissue inflammation induced by high-fat diet in obese diabetic mice is prevented by *n*-3 polyunsaturated fatty acids. *Diabetologia* **2006**, *49*, 2109–2119. [CrossRef] [PubMed]

53. Blok, W.L.; Deslypere, J.P.; Demacker, P.N.; van der Ven-Jongekrijg, J.; Hectors, M.P.; van der Meer, J.W.; Katan, M.B. Pro- and anti-inflammatory cytokines in healthy volunteers fed various doses of fish oil for 1 year. *Eur. J. Clin. Investig.* **1997**, *27*, 1003–1008. [CrossRef]

54. Cooper, A.L.; Gibbons, L.; Horan, M.A.; Little, R.A.; Rothwell, N.J. Effect of dietary fish oil supplementation on fever and cytokine production in human volunteers. *Clin. Nutr.* **1993**, *12*, 321–328. [CrossRef]

55. James, M.J.; Gibson, R.A.; Cleland, L.G. Dietary polyunsaturated fatty acids and inflammatory mediator production. *Am. J. Clin. Nutr.* **2000**, *71*, 343S–348S. [CrossRef] [PubMed]

56. Balvers, M.G.; Verhoeckx, K.C.; Meijerink, J.; Bijlsma, S.; Rubingh, C.M.; Wortelboer, H.M.; Witkamp, R.F. Time-dependent effect of in vivo inflammation on eicosanoid and endocannabinoid levels in plasma, liver, ileum and adipose tissue in C57BL/6 mice fed a fish-oil diet. *Int. Immunopharmacol.* **2012**, *13*, 204–214. [CrossRef]

57. Spencer, M.; Finlin, B.S.; Unal, R.; Zhu, B.; Morris, A.J.; Shipp, L.R.; Lee, J.; Walton, R.G.; Adu, A.; Erfani, R.; et al. Omega-3 fatty acids reduce adipose tissue macrophages in human subjects with insulin resistance. *Diabetes* **2013**, *62*, 1709–1717. [CrossRef]

58. Hames, K.C.; Morgan-Bathke, M.; Harteneck, D.A.; Zhou, L.; Port, J.D.; Lanza, I.R.; Jensen, M.D. Very-long-chain omega-3 fatty acid supplements and adipose tissue functions: A randomized controlled trial. *Am. J. Clin. Nutr.* **2017**, *105*, 1552–1558. [CrossRef]

59. Mendonca, A.M.; Cayer, L.G.J.; Pauls, S.D.; Winter, T.; Leng, S.; Taylor, C.G.; Zahradka, P.; Aukema, H.M. Distinct effects of dietary ALA, EPA and DHA on rat adipose oxylipins vary by depot location and sex. *Prostaglandins Leukot. Essent. Fatty Acids* **2018**, *129*, 13–24. [CrossRef]

60. Ferguson, J.F.; Roberts-Lee, K.; Borcea, C.; Smith, H.M.; Midgette, Y.; Shah, R. Omega-3 polyunsaturated fatty acids attenuate inflammatory activation and alter differentiation in human adipocytes. *J. Nutr. Biochem.* **2018**, *64*, 45–49. [CrossRef]

61. Titos, E.; Rius, B.; Gonzalez-Periz, A.; Lopez-Vicario, C.; Moran-Salvador, E.; Martinez-Clemente, M.; Arroyo, V.; Claria, J. Resolvin D1 and its precursor docosahexaenoic acid promote resolution of adipose tissue inflammation by eliciting macrophage polarization toward an M2-like phenotype. *J. Immunol.* **2011**, *187*, 5408–5418. [CrossRef] [PubMed]

62. Fredman, G.; Serhan, C.N. Specialized proresolving mediator targets for RvE1 and RvD1 in peripheral blood and mechanisms of resolution. *Biochem. J.* **2011**, *437*, 185–197. [CrossRef] [PubMed]

63. Fleming, I. The pharmacology of the cytochrome P450 epoxygenase/soluble epoxide hydrolase axis in the vasculature and cardiovascular disease. *Pharmacol. Rev.* **2014**, *66*, 1106–1140. [CrossRef] [PubMed]

64. Balvers, M.G.; Verhoeckx, K.C.; Bijlsma, S.; Rubingh, C.M.; Meijerink, J.; Wortelboer, H.M.; Witkamp, R.F. Fish oil and inflammatory status alter the *n*-3 to *n*-6 balance of the endocannabinoid and oxylipin metabolomes in mouse plasma and tissues. *Metabolomics* **2012**, *8*, 1130–1147. [CrossRef] [PubMed]

65. Hammond, V.J.; O'Donnell, V.B. Esterified eicosanoids: Generation, characterization and function. *Biochim. Biophys. Acta* **2012**, *1818*, 2403–2412. [CrossRef] [PubMed]

66. Quehenberger, O.; Dahlberg-Wright, S.; Jiang, J.; Armando, A.M.; Dennis, E.A. Quantitative determination of esterified eicosanoids and related oxygenated metabolites after base hydrolysis. *J. Lipid Res.* **2018**, *59*, 2436–2445. [CrossRef] [PubMed]

67. Vangaveti, V.N.; Jansen, H.; Kennedy, R.L.; Malabu, U.H. Hydroxyoctadecadienoic acids: Oxidised derivatives of linoleic acid and their role in inflammation associated with metabolic syndrome and cancer. *Eur. J. Pharmacol.* **2016**, *785*, 70–76. [CrossRef]

68. Nagy, L.; Tontonoz, P.; Alvarez, J.G.; Chen, H.; Evans, R.M. Oxidized LDL regulates macrophage gene expression through ligand activation of PPARgamma. *Cell* **1998**, *93*, 229–240. [CrossRef]

69. White, P.J.; Arita, M.; Taguchi, R.; Kang, J.X.; Marette, A. Transgenic restoration of long-chain *n*-3 fatty acids in insulin target tissues improves resolution capacity and alleviates obesity-linked inflammation and insulin resistance in high-fat-fed mice. *Diabetes* **2010**, *59*, 3066–3073. [CrossRef]

70. Yan, Y.; Jiang, W.; Spinetti, T.; Tardivel, A.; Castillo, R.; Bourquin, C.; Guarda, G.; Tian, Z.; Tschopp, J.; Zhou, R. Omega-3 fatty acids prevent inflammation and metabolic disorder through inhibition of NLRP3 inflammasome activation. *Immunity* **2013**, *38*, 1154–1163. [CrossRef]

71. Rey, C.; Delpech, J.C.; Madore, C.; Nadjar, A.; Greenhalgh, A.D.; Amadieu, C.; Aubert, A.; Pallet, V.; Vaysse, C.; Laye, S.; et al. Dietary *n*-3 long chain PUFA supplementation promotes a pro-resolving oxylipin profile in the brain. *Brain Behav. Immun.* **2019**, *76*, 17–27. [CrossRef] [PubMed]
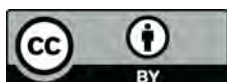
ANNEXE 2.

Munro et al. Submitted.

Modulation of the inflammatory response to LPS by the recruitment and activation of brown and brite adipocytes in mice

Patrick Munro[1], Océane Dufies[1], Samah Rekima[2], Agnès Loubat[2], Christophe Duranton[3], Laurent Boyer[1*] and Didier F. Pisani[3*$].

[1] Université Côte d'Azur, Inserm, C3M, Nice, France.

[2] Université Côte d'Azur, CNRS, Inserm, iBV, Nice, France.

[3] Université Côte d'Azur, CNRS, LP2M, Nice, France.

[*] Co-last authors

[$] Correspondence: Didier Pisani, Laboratoire de PhysioMédecine Moléculaire, CNRS UMR7370, Faculté de Médecine – Tour Pasteur, 28 Avenue de Valombrose, 06107 Nice Cedex 2, France. Phone: +33493377036. e-mail: didier.pisani@univ-cotedazur.fr.

Highlights.

- Brown and brite adipocyte functions were unaffected by acute LPS treatment.
- Brown and brite adipocyte recruitment did not prevent the inflammatory response.
- Brite adipocytes highly secreted IL-1RA in response to LPS.
- Brite adipocytes limited leptin secretion in response to LPS.

Abstract.

Objectives. Numerous studies have shown that the recruitment and activation of thermogenic adipocytes, which are brown and beige/brite, reduces the mass of adipose tissue and normalizes abnormal glycaemia and lipidaemia. However, the impact of these adipocytes on the inflammatory state of adipose tissue is still not well understood, especially in response to endotoxaemia, which is a major aspect of obesity and metabolic diseases.

Methods. First, we analysed the phenotype and metabolic function of white and brite primary adipocytes in response to lipopolysaccharide (LPS) treatment *in vitro*. Then, 8-week-old male BALB/c mice were treated for one week with a β3-adrenergic receptor agonist (CL316,243, 1 mg/kg/day) to induce recruitment and activation of brown and brite adipocytes and were subsequently injected with LPS (*E. coli* lipopolysaccharide, i.p., 100 µg/mouse) to generate acute endotoxaemia. The metabolic and inflammatory parameters of the mice were analysed 6 hours later.

Results. Our results showed that in response to LPS, thermogenic activity promoted a local anti-inflammatory environment with high secretion of IL-1RA without affecting other anti- or pro-inflammatory cytokines. Interestingly, activation of brite adipocytes reduced the LPS-induced secretion of leptin. However, thermogenic activity and adipocyte function were not altered by LPS treatment *in vitro* or by acute endotoxaemia *in vivo*.

Conclusion. In conclusion, these results suggest an IL-1RA-mediated immunomodulatory activity of thermogenic adipocytes specifically in response to endotoxaemia. This encourages potential therapy involving brown and brite adipocytes for the treatment of obesity and associated metabolic diseases.

Keywords. brown adipose tissue; white adipose tissue; cytokines; inflammation; catecholamines.

1. Introduction

White adipocytes are specialized for the storage and release of energy (carbohydrates and lipids), while brown adipocytes dissipate this energy in the form of heat (thermogenesis) through the activity of uncoupling protein-1 (UCP1) [1]. Brown adipocytes constitute brown adipose tissue (BAT) but can also be found within white adipose tissue (WAT). They are then called beige or brite adipocytes ("brown in white") and have a high thermogenesis capacity in response to conditions such as prolonged cold exposure [2].

Overweight (body mass index, BMI > 25 kg/m^2) and obesity (BMI > 30 kg/m^2) are the consequences of a positive energy balance (energetic substrate storage > expenditure) that leads to an increase in the mass of subcutaneous and visceral white adipose tissue. Obesity is a major risk factor for type 2 diabetes development, as 90% of patients suffering from type 2 diabetes are overweight or obese. It has also been shown that metabolic organs of obese subjects, especially WAT, are characterized by low-grade inflammation that can lead to metabolic disorders such as insulin resistance [3]. Inflammation is characterized in WAT by an increase in inflammatory cytokines such as tumour necrosis factor α (TNFα), plasminogen activator inhibitor-1 (PAI-1) or interleukin-1β and -6 (IL-1β and IL-6). This promotes immune cell infiltration of adipose tissue, particularly infiltration of macrophages and their polarization to an inflammatory M1 phenotype [4]. Immune cell accumulation and secretion of inflammatory cytokines affect adipose tissue homeostasis and, more specifically, the recruitment and function of adipocytes in WAT and BAT [5]. Previous studies have shown that TNFα inhibits adipocyte differentiation [6] and that IL-1β blocks insulin signalling, thus favouring insulin resistance [7]. Recently, it has also been shown that IL-1β and TNFα affect the thermogenic function of brown adipocytes [8-10]. Altogether, these studies showed that inflammatory cytokines participate in the development of an inflammatory environment, leading to the deregulation of adipose tissue homeostasis. However, the origin of low-grade metabolic inflammation is still under debate. Growing evidence indicates that the gut microbiota is a major player in metabolic inflammation. The gut of obese patients is characterized by an alteration in the microbiota (dysbiosis) and a disruption of the intestinal barrier, increasing its permeability to microbiota metabolites and degradation products. Consequently, systemic endotoxin levels increase (endotoxaemia), including the levels of lipopolysaccharide (LPS) [11]. It has been demonstrated using germ-free rodent models that this endotoxaemia is directly linked to adipose tissue inflammation [12-14]. In this pathophysiological condition, LPS directly activates Toll-like receptor 4 (TLR-4), which is displayed by tissue macrophages and adipocytes [15]. In response, white and brown/beige adipocytes exhibit an altered function [8; 16] and secrete inflammatory cytokines (TNFα and IL-1β), which alter tissue homeostasis. Recently, it has been

shown that brown and white adipocytes respond differently to *in vitro* LPS stimulation and mediate different inflammatory responses [17].

One of the strategies for treating type 2 diabetes associated with obesity is to increase energy expenditure by stimulating the formation and activity of brown and/or beige adipocytes [18]. While little is known about the impact of this strategy on the balance and functionality of the immune system, it is a key element in the pathology of metabolic syndrome, especially in low-grade inflammation and inherent insulin resistance. In this work, we investigated the response of white and brown/brite adipocytes to LPS treatment with regard to their impact on the inflammatory environment induced by LPS. Using *ex vivo* and *in vivo* approaches in mice, we demonstrated that recruitment/activation of brown/brite adipocytes by β-adrenergic receptor agonists was not affected by LPS treatment and led to a reduced inflammatory response to LPS, especially by the overexpression of an IL-1 receptor antagonist (IL-1RA) that is known to inhibit the action of IL-1β.

2.   Materials and Methods

2.1.   Reagents

Culture media and buffer solutions were purchased from Lonza (Ozyme, St-Quentin en Yvelines, France), foetal bovine serum (FBS) was purchased from Eurobio (Courtaboeuf, France), and insulin was purchased from Invitrogen (Cergy Pontoise, France). LPS (LPS-EK Ultrapure isolated from *E. coli* K12 strain) was obtained from InvivoGen (Toulouse, France). Other reagents were obtained from Sigma-Aldrich (Saint-Quentin Fallavier, France).

2.2.   Animals

The experiments were conducted in accordance with the French and European regulations (2010/63/EU directive) for the care and use of research animals and were approved by national experimentation committees (MESR No.: APAFIS#18322-2018121809427035 v2). Eight-week-old male BALB/c mice from Janvier Laboratory (France) were maintained at housing temperature (22°C) on a 12:12-hour light-dark cycle, with *ad libitum* access to food and water.

The mice were treated daily with the β3-adrenergic receptor agonist CL316,243 (1 mg/kg in saline solution, intraperitoneal injection, n=12) (Sigma-Aldrich) or with vehicle only (saline solution, n=12). To induce endotoxaemia, 6 mice from each group were injected at day 7 with LPS (100 μg/mouse in PBS, intraperitoneal) or vehicle only and were sacrificed 6 hours later. At the end of the experiment, blood, interscapular brown adipose tissue (iBAT), epididymal white adipose tissue (eWAT) and inguinal subcutaneous white adipose tissue (scWAT) were sampled and used for different analyses.

2.3.   Cytokine and metabolic parameter quantification

For blood analysis, freshly prepared plasma was diluted twice before analysis. For tissue analysis, freshly sampled WAT and BAT were washed in PBS, weighed and incubated in free Dulbecco's modified Eagle's medium for 2 hours at 37°C. The media were preserved for analysis of various secreted proteins.

Leptin was assayed using a mouse leptin kit (Meso Scale Discovery, # K152BYC), and cytokines were measured using a mouse V-PLEX pro-inflammatory panel 1 kit (# K15048D) according to the manufacturer's instructions using a QuickPlex SQ 120 apparatus (Meso Scale Discovery, Rockville, Maryland, USA). IL-1RA levels were assayed using a mouse IL-1RA ELISA kit (#EMIL1RN) from Thermo Fisher Scientific (Courtaboeuf, France). Glycerol and triglyceride

determinations were performed using a dedicated kit (free glycerol reagent and triglyceride reagent, Sigma Aldrich).

2.4. Histology

Freshly sampled tissues were fixed in 4% paraformaldehyde overnight at RT and then paraffin-embedded. Embedded tissues were cut into 5 µm sections and dried overnight at 37°C.

For histological analysis, the sections were stained with haematoxylin-eosin and mounted in vectamount (Vecto laboratories).

For immunohistochemical analysis, antigen retrieval was performed in buffer low pH in a de-cloaking chamber (Dako, S2367). The sections were then permeabilized in PBS with 0.2% Triton X-100 at room temperature for 10 min and blocked in the same buffer containing 3% BSA for 1 hour. The sections were incubated with rat anti-F4/80 antibody (Biorad, clone CI:A3-1, dilution 1:100) overnight at 4°C. Following a 1 hour incubation with A568-coupled anti-rabbit secondary antibodies, nuclear staining was performed with DAPI, and the sections were mounted in PermaFluor mounting Media (Thermofisher).

Visualization was performed with an Axiovert microscope. Images were captured using AxioVision software (Carl Zeiss, Jena, Germany).

2.5. Stromal vascular fraction cell isolation and culture

Subcutaneous WAT (scWAT, inguinal) deposits were sampled from 8-week-old BALB/c male mice, washed in PBS, and minced. Adipose tissue samples were digested for 45 min at 37°C in DMEM containing 2 mg/ml collagenase A (Roche Diagnostics, Meylan, France) and 20 mg/ml bovine serum albumin (Sigma-Aldrich Chimie, Saint-Quentin Fallavier, France). The sample was successively filtered through 250, 100 and 27 µm nylon sheets and centrifuged for 5 min at 500 g. The pellet containing stromal vascular fraction (SVF) cells was subjected to red blood cell lysis.

SVF cells were plated and maintained in DMEM containing 10% FCS until confluence. Differentiation was induced in the same medium supplemented with 1 µM dexamethasone, 0.5 mM isobutylmethylxanthine and 860 nM insulin for two days. Then, the cells were maintained for 7 days in the presence of 860 nM insulin for white adipogenesis and 860 nM insulin, 1 µM rosiglitazone and 2 nM triiodothyronine for brite adipogenesis. Media were changed every other day. On the final day, the adipocytes were stimulated with or without 1 µM isoproterenol for 6 hours.

2.6. Isolation and analysis of RNA

Procedures were performed according to MIQE recommendations [19]. Total RNA was extracted using a TRI-Reagent kit (Euromedex, Souffelweyersheim, France) according to the manufacturer's instructions. For RNA isolation from organs, tissues were homogenized in TRI-Reagent using a dispersing instrument (ULTRA TURRAX T25). Reverse transcription-polymerase chain reaction (RT-PCR) was performed using M-MLV-RT (Promega). SYBR qPCR premix Ex Taq II from Takara (Ozyme, France) was used for quantitative PCR (qPCR), and assays were run on a StepOne Plus ABI real-time PCR instrument (PerkinElmer Life and Analytical Sciences, Boston). The expression of selected genes was normalized to that of the TATA-box binding protein (TBP) and 36B4 housekeeping genes and then quantified using the comparative-ΔCt method. Primer sequences are available upon request.

2.7. Oxygen consumption analysis

The oxygen consumption rate (OCR) of 17-day-old differentiated hMADS cells was determined using an XF24 Extracellular Flux Analyser (Seahorse Bioscience, Agilent Technologies France, Courtaboeuf, France). Uncoupled and maximal OCR were determined using oligomycin (1.2 μM) and FCCP (1 μM). Rotenone and antimycin-A (2 μM each) were used to inhibit mitochondrial respiration. All parameters were calculated as described previously [20].

2.8. Statistical analysis

Animal cohort size was determined using G*Power [21], and animals were allocated to experimental groups by randomization. The data were analysed using GraphPad Prism 6 software and evaluated by ordinary one-way ANOVA followed by Tukey's multiple comparisons post-test to assess significant differences between experimental groups. Differences were considered statistically significant with $p<0.05$. The data are displayed as scatter plots of independent values and group mean values ± SD.

3. Results

3.1. In vitro phenotypic and functional metabolic response of white and brite adipocytes to LPS treatment

White and brite adipocytes were obtained after differentiation of preadipocytes that were isolated from the stromal vascular fraction of mouse subcutaneous white adipose tissue. On the last day of differentiation, the adipocytes were treated for 6 hours with 1 µM isoproterenol (a nonspecific β-adrenergic receptor agonist that activates lipolysis and/or UCP1 activity) and/or 100 ng/ml LPS and were then used for mRNA expression and functional metabolism modification analysis (Figure 1).

Acute LPS treatment did not alter perilipin 1 mRNA expression but strongly inhibited leptin mRNA expression in white adipocytes (Figure 1A). Isoproterenol treatment induced a similar inhibition but had no synergistic effect with LPS. White adipocytes barely expressed Ucp1 and perilipin 5 mRNA, and LPS and isoproterenol did not alter these expression levels. The same result was found for leptin mRNA in brite adipocytes. In addition, in brite adipocytes, perilipin 1 mRNA expression was unaffected by the treatments, unlike that of perilipin 5, which was slightly inhibited by LPS treatment independent of isoproterenol. Interestingly, LPS alone did not alter Ucp1 expression in brite adipocytes but blunted the increase in Ucp1 mRNA expression due to acute isoproterenol treatment (Figure 1A).

Analysis of Tnfα and Il-6 mRNA levels showed that they were overexpressed after acute LPS treatment. Interestingly, isoproterenol completely inhibited Tnfα overexpression in the two kinds of adipocytes. A more complex situation was found for Il-6 mRNA, which was positively affected by the combination of isoproterenol and LPS treatment in white adipocytes but inhibited by the same cotreatment in brite adipocytes (Figure 1A). Analysis of Il-1β mRNA expression showed an increase after LPS treatment of adipocytes. Isoproterenol did not alter this expression except when white adipocytes were treated with both isoproterenol and LPS. As Il-1β mRNA encodes the pro-form of the protein before its maturation and secretion, these results need to be analysed with caution. mRNA expression of Il-1rn, which codes for the IL-1RA protein that counteracts the effect of IL-1β, was increased after LPS treatment, similar to that of Il-1β mRNA. Interestingly, brite adipocytes expressed more Il-1rn than white adipocytes. This expression in brite adipocytes was increased by LPS treatment and, more importantly, by isoproterenol with or without LPS.

At the metabolic level, isoproterenol treatment induced glycerol release (a reflection of lipolysis) in both types of adipocytes, but cotreatment with LPS had no effect (Figure 1B-D).

Interestingly, LPS slightly but significantly increased glycerol release in white and brite adipocytes. The extracellular acidification rate (ECAR) (Figure 1C) and oxygen consumption rate (OCR) (Figure 1D) were analysed concomitantly and were increased by acute isoproterenol treatment in brite adipocytes, while only the OCR was increased in white adipocytes. Uncoupling mitochondrial oxygen consumption (the OCR due to proton leakage) was increased in brite adipocytes after isoproterenol stimulation, which is a reflection of Ucp1 activity (Figure 1D). Neither ECAR nor OCR was affected by LPS treatment (Figure 1C-D).

Taken together, these *in vitro* adipocyte experiments suggest that activation of adipocyte β-adrenergic receptors decreased the inflammatory phenotype and that LPS treatment did not clearly affect the thermogenic phenotype.

3.2. In vivo effects of acute LPS treatment on browning and BAT activation induced by the β3-adrenergic receptor agonist (CL316,243)

Eight-week-old male BALB/c mice were treated daily with a β3-adrenergic receptor agonist (CL316,243, 1 mg/kg) that activates brown and brite adipocyte thermogenesis and adipocyte lipolysis and were finally treated with 100 µg of LPS for 6 hours. Body weight was unaffected by treatment with CL316,243 or LPS (Figure 2A). Different weights of epididymal WAT showed that fat mass was decreased after CL316,243 treatment but was unaffected by LPS treatment (Figure 2A). While the plasma glycerol level did not change, we found a decrease in plasma triglyceride levels, probably due to the high use of this substrate by activated brown and brite adipocytes (Figure 2B). Interestingly, LPS treatment also decreased triglyceride levels, but no additive effect was found in the cotreated mouse group (Figure 2B). Leptin plasma levels increased in LPS-treated mice, and the effect was blunted when the mice were pre-treated with CL316,243 (Figure 2C). To assess the secretory capacity of adipose tissue, we freshly sampled and washed scWAT and iBAT from the 4 groups of mice and analysed secreted cytokines and adipokines two hours later. With this approach, we found a decrease in secreted leptin from scWAT explants. Thus, in our experiment, leptin levels did not follow the fat mass of the animals and corresponded to an adipose tissue inflammatory response to LPS (Figure 2C).

To assess the effects of acute LPS treatment on brown and brite adipocyte recruitment and activation, we performed histological and molecular analyses of WAT and BAT from mice in each group. As shown in Figure 2D, CL316,243 decreased quantity of lipid droplets in brown adipose tissue and slightly increased Ucp1 and Cpt1m mRNA expression, which is characteristic of activated BAT, without affecting Perilipin 1 and 5 expressions (Supplementary Figure 1A). scWAT histological sections from CL316,243-treated groups displayed massive recruitment of

multiloculated adipocytes (Figure 2D), which is a characteristic morphology of brite adipocytes. This was confirmed by the overexpression of Ucp1 and Perilipin 5 mRNA (Supplementary Figure 1B).

Perilipin 1 and Leptin mRNA expression in scWAT did not change with LPS and/or CL316,243 treatment. This discrepancy between leptin secretory levels and mRNA expression supports an acute response independent of fat mass change (Supplementary Figure 1B). Interestingly, we did not detect inflammatory cell infiltration after acute LPS treatment by histological analysis (Figure 2D), which was confirmed by negative staining for the macrophagic marker F4/80 (data not shown).

3.3.   Acute LPS treatment induces an inflammatory response and secretion of anti-inflammatory cytokines.

Inflammation is mainly triggered by inflammatory cytokine secretion, followed by a resolution step that is characterized by secretion of anti-inflammatory cytokines. This effect was observed in mice that were treated with LPS. Terminal LPS treatment induced an increase in the plasma level of IL-1β, as well as IL-1β secretion in BAT and scWAT explants, and CL316,243 did not alter this effect (Figure 3A). IL-1RA plasma levels equivalently increased after administration of LPS to untreated and CL316,243-treated mice (Figure 3B). In contrast, in scWAT and BAT, while LPS treatment increased IL-1RA secretion, CL316,243 also increased IL-1RA secretion, and this effect was additive in the presence of LPS (Figure 3B).

In addition to IL-1β/IL-1RA, other cytokine levels were affected. TNFα and IL-12 plasma levels were increased after LPS treatment independent of CL316,243 treatment, and the same trend was found for IL-6 (Supplementary Figure 2). KC/GRO (CXCL-1) was detected in the plasma of mice but was not affected by the different treatments. Interestingly, LPS-induced IFNγ and IL-2 plasma levels increases were abrogated when the mice were treated with CL316,243 (Supplementary Figure 2).

A different profile of secreted cytokines was found in the adipose tissue explant media. IFNγ was undetected, and IL-2 and IL-12 were barely detected (Figure 4), with a slight increase only in the iBAT of LPS-treated mice (Figure 4A). Secreted IL-6 increased in the iBAT of LPS-treated mice independent of CL316,243 treatment and only in LPS plus CL316,243 in scWAT (Figure 4). In contrast, KC/GRO and TNFα increased in all groups of LPS-treated mice independent of CL316,243 treatment and had the same trend (Figure 4).

Although the anti-inflammatory cytokine IL-4 was barely detected in plasma and undetected in explants of adipose tissues, the plasma level of IL-10 was increased in response to

LPS (Supplementary Figure 3). None of these were altered by CL316,243. In contrast, local secretion of IL-10 by adipose tissue was not stimulated by LPS alone, but an increasing trend was observed after CL316,243 treatment, especially in BAT that was cotreated with LPS (Supplementary Figure 3).

4. Discussion

Obesity disturbs the gut epithelium, which allows LPS from gram-negative gut bacteria to enter the systemic circulation [13]. This metabolic endotoxaemia leads to systemic and local inflammation, which is a central feature of metabolic syndrome development. Several studies have shown the action of LPS on white and brown adipocyte differentiation and function. LPS modulates adipocyte functions directly via TLR-4 activation or indirectly, especially through macrophage activation which in turn secrete cytokines that modulate adipocyte functions. In WAT, LPS directly induces lipolysis and cytokine secretion by adipocytes and indirectly (mainly by macrophage-derived cytokines) inhibits differentiation and insulin resistance [22; 23]. In BAT, LPS has been suspected to be an activator of brown adipocyte thermogenesis [24], but recent studies demonstrated that acute (*in vitro*) and chronic (*in vivo*) exposure to LPS inhibits UCP1 expression and function in these adipocytes [16; 25]. However, little is known about the influence of white and brite or brown adipocytes on local and systemic inflammation due to LPS exposure, especially the secretion of inflammatory mediators such as cytokines and adipokines. Herein, we analysed the impact of brown and brite adipocyte recruitment and activation on systemic and local (adipose tissue) responses to acute LPS treatment, which mimics endotoxaemia.

Leptin is a well-known modulator of pyrexia in response to LPS [26-28]. We found an expected increase in leptin secretion in plasma that correlated with scWAT leptin level, which is the primary origin of this adipokine, in mice that were stimulated with acute LPS treatment. This positive effect was not found at the mRNA level in the scWAT of these mice or in primary white adipocytes that were exposed to LPS. These results suggest that LPS is unable to directly stimulate adipocyte leptin expression, suggesting the involvement of additional cell populations that respond to the LPS signal. Interestingly, these increased leptin levels were completely abolished when the mice were pre-treated with CL316,243, which induces brown/brite adipocyte recruitment and activation and thus thermogenesis. As leptin induces fever independently of thermogenesis [27], we suspect negative feedback that prevents hyperthermia due to the addition of thermogenesis and pyrexia. Unfortunately, leptin levels cannot be related to fever, as body temperature was not available in our work. Inconsistently, numerous studies have shown an

inhibitory effect of chronic LPS treatment on Ucp1 expression and function *in vivo* and thus on thermogenesis [16]. In our work, we showed that LPS did not modify Ucp1 expression or the histology of BAT and scWAT after CL316,243 treatment, strongly suggesting that LPS does not affect thermogenesis. The difference between our results and those of Okla and colleagues is probably due to the duration of LPS treatment (6 hours vs. 2 weeks) [16]. This was confirmed by an *in vitro* experiment on brite adipocytes showing that LPS slightly inhibited Ucp1 mRNA expression due to isoproterenol treatment but did not modify Ucp1 function, as demonstrated by oxygen consumption analysis. It is possible that a difference exists between brite and brown adipocytes, as LPS inhibits Ucp1 function in brown adipocytes *in vitro* [25].

Dowal and colleagues used coculture of human adipocytes and macrophage cell lines to show that brown adipocytes reduced macrophage IL-6 secretion in response to LPS compared to that of white adipocytes [17]. Under similar conditions, mRNA expression of other inflammatory markers, including Il-10, in macrophages was inhibited by brown adipocytes. These results suggest that brown adipocytes and perhaps brite adipocytes display general immunomodulatory properties of interest. Our *ex vivo* analysis showed the same results, with decreased mRNA expression of Il-6 in brite adipocytes compared to that in white adipocytes and to a lesser extent for Tnfα. We hypothesised that the inhibition of inflammatory cytokine expression in brown adipocytes participates in its immunomodulatory activity on macrophages. Unfortunately, this inhibition of pro-inflammatory and anti-inflammatory cytokine levels was not confirmed *in vivo*. Control mice and mice that were pre-treated with CL316,243 displayed an equivalent increase in the secretion of TNFα and IL-6 after LPS treatment. The same results were obtained for other pro- and anti-inflammatory cytokines in plasma and adipose tissue, except for IFNγ and IL-2 plasma levels, which were strongly decreased in the CL316,243 group after LPS treatment. As no IFNγ and very low quantities of IL-2 were found in BAT and scWAT, we can exclude the involvement of these tissues in this immunomodulatory effect.

Along pro-inflammatory cytokines, IL-1β has a central role in the immune response to LPS and in adipose tissue homeostasis [29]. More specifically, IL-1β secretion induced by LPS treatment disrupts insulin signalling in WAT [7; 30; 31] and inhibits UCP1 function in BAT both *in vitro* and *in vivo* [9; 24]. As expected, we found that LPS treatment induced IL-1β production in all conditions assayed, as shown by mRNA expression in white and brite adipocytes *in vitro* and secretion of the mature form of IL-1β in BAT and scWAT *in vivo*. In addition, we showed that recruitment and activation of brown and brite adipocytes did not modulate IL-1β levels and thus did not seem to prevent inflammatory action of this cytokine. IL-1β is mainly regulated at the expression, maturation and secretion levels, especially by modulation of the NF-kB transcription

factor and activation of inflammasomes. Another pathway exists to modulate IL-1 activity, which is the production and secretion of IL-1RA. This cytokine antagonizes the biological effects of IL-1β by competing for binding to the IL-1 receptor without inducing a cellular response [32]. Moreover, IL-1RA is highly produced by adipose tissue [33]. Interestingly, we demonstrated that Il-1rn mRNA was more highly expressed in brite adipocytes *in vitro* than in white adipocytes and that this difference was amplified when the cells were treated with a β-adrenergic receptor agonist. Importantly, these observations were confirmed *in vivo,* where CL316,243 treatment increased IL-1RA levels in WAT and BAT, with or without LPS treatment. In contrast, plasma levels of IL-1RA increased only in the presence of LPS and independently of CL316,243 treatment. Taken together, these results clearly demonstrate that brite and brown adipocytes express and/or secrete more IL-1RA than white adipocytes, especially in response to acute LPS treatment. In addition to a potential anti-inflammatory role of IL-1RA, we hypothesise that the simultaneous secretion of IL-1RA and IL-1β corresponds to a protective mechanism to preserve adipocyte function in an inflammatory context.

Increased IL-1β or decreased IL-1RA levels are linked to the development of obesity and diabetes, and among therapeutic strategies developed to normalize these levels, some studies have focused on the use of exogenous IL-1RA [29; 34]. In rodents, chronic IL-1RA treatment of mice that were fed a high-fat/high-sucrose diet prevented glucose metabolism alteration and normalized the metabolic parameters linked to obesity without affecting fat mass [35]. In addition, using IL-1RA-overexpressing mice, we detected a normalization of inflammatory marker mRNA in the WAT of mice fed a high-fat diet [35]. In humans, several clinical trials using anakinra (recombinant human IL-1RA) have been developed with obese and diabetic patients and have shown, among others, better pancreatic function and decreased systemic inflammation after treatment [36; 37]. As we demonstrated that IL-1RA adipose levels are increased after β-adrenergic receptor agonist treatment, we suggest that increasing brown/brite adipocyte recruitment and activity in humans, in addition to decreasing fat mass, protects adipose tissue from the adverse effects of IL-1β.

Finally, we have demonstrated that recruitment and activation of brown and brite adipocytes in the adipose tissue of mice led to a local anti-inflammatory phenotype characterized by an increased IL-1RA level and decreased leptin secretion in response to endotoxaemia without modulation of systemic inflammation.

Legends.

Figure 1. Effect of LPS on white and brite adipocytes *in vitro*. White and brite adipocytes were obtained after differentiation of stromal vascular fraction cells isolated from mouse scWAT. (A) mRNA expression analysis by qPCR of white (leptin and perilipin 1), brite (Ucp1 and perilipin 5) and inflammatory markers (Tnfα, Il-6, Il-1β, and Il1rn) after 6 hours of treatment with isoproterenol (1 µM) and/or LPS (100 ng/ml). (B) Glycerol levels were assayed in the supernatants of white and brite adipocytes that were treated for 2 hours with LPS and/or isoproterenol. (C-D) White and brite adipocytes were analysed for oxygen consumption and extracellular acidification following sequential injection of isoproterenol and/or LPS, oligomycin A (1.2 µM) and rotenone/antimycin A (2+2 µM). (C) ECAR in response to LPS and/or isoproterenol is displayed as % of basal ECAR. (D) Plots show mitochondrial OCR and the indicated injections. Histograms display OCR in response to LPS and/or isoproterenol and uncoupling mitochondrial respiration. The results are displayed as the mean ± SEM. n = 3. * $p<0.05$ vs. control; $ $p<0.05$ vs. LPS; § $p<0.05$ vs. isoproterenol; £ $p<0.05$ vs. white adipocytes.

Figure 2. Effect of CL316,243 and LPS on general mouse metabolic parameters. Mice were analysed after 1 week of treatment with CL316,243 daily (1 mg/kg/day) or vehicle only (NaCl), and with or without LPS treatment (1 mg/kg) during the final 6 hours. (A) Mouse body weights, epididymal white adipose tissue (eWAT) weights, (B) triglycerides and glycerol plasma levels and secreted leptin levels in (C) plasma and (E) subcutaneous white adipose tissue (scWAT). (D) Haematoxylin-eosin staining of interscapular BAT (iBAT), scWAT and eWAT sections. The results are displayed as independent mouse values (dots) and the mean ± SE. n = 8. * $p<0.05$.

Figure 3. Effect of CL316,243 and LPS on IL-1β/IL-1RA. IL-1β (A) and IL-1RA (B) protein levels were assessed in plasma (upper panel) and in the media of iBAT (middle panel) and scWAT (lower panel) explants from mice that were treated for 1 week with CL316,243 daily (1 mg/kg/day) or vehicle only (NaCl), and with or without LPS treatment (1 mg/kg) for the final 6 hours. The results are displayed as independent mouse values (dots) and the mean ± SE. n = 6 (plasma) or 8 (explant). * $p<0.05$.

Figure 4. Local inflammatory response to LPS. IFNγ, TNFα, IL-6, IL-12-p70, KC/GRO (CXCL-1) and IL-2 levels were assessed in the media of iBAT (A) and scWAT (B) explants from mice that were treated for 1 week with CL316,243 daily (1 mg/kg/day) or vehicle only (NaCl), and with or

without LPS treatment (1 mg/kg) for the final 6 hours. The results are displayed as independent mouse values (dots) and the mean ± SE. n = 8. * $p<0.05$.

Supplementary Figure 1. Effect of CL316,243 and LPS on mRNA adipocyte markers. mRNA expression of brown/brite (Ucp1, Cpt1m, and perilipin 5) and white adipocyte (leptin and perilipin 1) markers was analysed by qPCR in iBAT and scWAT from mice that were treated for 1 week with CL316,243 daily (1 mg/kg/day) or vehicle only (NaCl), and with or without LPS treatment (1 mg/kg) for the final 6 hours. The results are displayed as independent mouse values (dots) and the mean ± SE. n = 8. * $p<0.05$.

Supplementary Figure 2. Systemic inflammatory response to LPS. IFNγ, TNFα, IL-6, IL-12-p70, KC/GRO (CXCL-1) and IL-2 levels were assessed in the plasma from mice that were treated for 1 week with CL316,243 daily (1 mg/kg/day) or vehicle only (NaCl), and with or without LPS treatment (1 mg/kg) for the final 6 hours. The results are displayed as independent mouse values (dots) and the mean ± SE. n = 8. * $p<0.05$.

Supplementary Figure 3. Systemic and local anti-inflammatory responses to LPS. IL-4 and IL-10 levels were assessed in plasma (A) and in the media of iBAT (B) and scWAT (C) explants from mice that were treated for 1 week with CL316,243 daily (1 mg/kg/day) or vehicle only (NaCl), and with or without LPS treatment (1 mg/kg) for the final 6 hours. The results are displayed as independent mouse values (dots) and the mean ± SE. n = 8. * $p<0.05$.

Bibliography.

[1]   Cannon, B., Nedergaard, J., 2004. Brown adipose tissue: function and physiological significance. Physiological Reviews 84(1):277-359.

[2]   Cinti, S., 2009. Transdifferentiation properties of adipocytes in the adipose organ. American Journal of Physiology: Endocrinology and Metabolism 297(5):E977-986.

[3]   Hotamisligil, G.S., 2006. Inflammation and metabolic disorders. Nature 444(7121):860-867.

[4]   Lumeng, C.N., Bodzin, J.L., Saltiel, A.R., 2007. Obesity induces a phenotypic switch in adipose tissue macrophage polarization. Journal of Clinical Investigation 117(1):175-184.

[5]   Odegaard, J.I., Chawla, A., 2013. The immune system as a sensor of the metabolic state. Immunity 38(4):644-654.

[6]   Hotamisligil, G.S., Shargill, N.S., Spiegelman, B.M., 1993. Adipose expression of tumor necrosis factor-alpha: direct role in obesity-linked insulin resistance. Science 259(5091):87-91.

[7]   Jager, J., Gremeaux, T., Cormont, M., Le Marchand-Brustel, Y., Tanti, J.F., 2007. Interleukin-1beta-induced insulin resistance in adipocytes through down-regulation of insulin receptor substrate-1 expression. Endocrinology 148(1):241-251.

[8]   Okla, M., Zaher, W., Alfayez, M., Chung, S., 2018. Inhibitory Effects of Toll-Like Receptor 4, NLRP3 Inflammasome, and Interleukin-1beta on White Adipocyte Browning. Inflammation 41(2):626-642.

[9]   Goto, T., Naknukool, S., Yoshitake, R., Hanafusa, Y., Tokiwa, S., Li, Y., et al., 2016. Proinflammatory cytokine interleukin-1beta suppresses cold-induced thermogenesis in adipocytes. Cytokine 77:107-114.

[10]   Sakamoto, T., Takahashi, N., Sawaragi, Y., Naknukool, S., Yu, R., Goto, T., et al., 2013. Inflammation induced by RAW macrophages suppresses UCP1 mRNA induction via ERK activation in 10T1/2 adipocytes. American Journal of Physiology: Cell Physiology 304(8):C729-738.

[11]   Tilg, H., Zmora, N., Adolph, T.E., Elinav, E., 2019. The intestinal microbiota fuelling metabolic inflammation. Nature Reviews: Immunology.

[12]   Cani, P.D., Delzenne, N.M., 2010. Involvement of the gut microbiota in the development of low grade inflammation associated with obesity: focus on this neglected partner. Acta Gastroenterologica Belgica 73(2):267-269.

[13]   Cani, P.D., Bibiloni, R., Knauf, C., Waget, A., Neyrinck, A.M., Delzenne, N.M., et al., 2008. Changes in gut microbiota control metabolic endotoxemia-induced inflammation in high-fat diet-induced obesity and diabetes in mice. Diabetes 57(6):1470-1481.

[14]   Vijay-Kumar, M., Aitken, J.D., Carvalho, F.A., Cullender, T.C., Mwangi, S., Srinivasan, S., et al., 2010. Metabolic syndrome and altered gut microbiota in mice lacking Toll-like receptor 5. Science 328(5975):228-231.

[15]   Schaffler, A., Scholmerich, J., Salzberger, B., 2007. Adipose tissue as an immunological organ: Toll-like receptors, C1q/TNFs and CTRPs. Trends in Immunology 28(9):393-399.

[16]   Okla, M., Wang, W., Kang, I., Pashaj, A., Carr, T., Chung, S., 2015. Activation of Toll-like receptor 4 (TLR4) attenuates adaptive thermogenesis via endoplasmic reticulum stress. Journal of Biological Chemistry 290(44):26476-26490.

[17]   Dowal, L., Parameswaran, P., Phat, S., Akella, S., Majumdar, I.D., Ranjan, J., et al., 2017. Intrinsic Properties of Brown and White Adipocytes Have Differential Effects on Macrophage Inflammatory Responses. Mediators of Inflammation 2017:9067049.

[18]   Langin, D., 2010. Recruitment of brown fat and conversion of white into brown adipocytes: strategies to fight the metabolic complications of obesity? Biochimica et Biophysica Acta 1801(3):372-376.

[19]   Bustin, S.A., Benes, V., Garson, J.A., Hellemans, J., Huggett, J., Kubista, M., et al., 2009. The MIQE guidelines: minimum information for publication of quantitative real-time PCR experiments. Clinical Chemistry 55(4):611-622.

[20]   Brand, M.D., Nicholls, D.G., 2011. Assessing mitochondrial dysfunction in cells. Biochemical Journal 435(2):297-312.

[21]   Faul, F., Erdfelder, E., Lang, A.G., Buchner, A., 2007. G*Power 3: a flexible statistical power analysis program for the social, behavioral, and biomedical sciences. Behavior Research Methods 39(2):175-191.

[22]   Schaffler, A., Scholmerich, J., 2010. Innate immunity and adipose tissue biology. Trends in Immunology 31(6):228-235.

[23]   Wellen, K.E., Hotamisligil, G.S., 2003. Obesity-induced inflammatory changes in adipose tissue. Journal of Clinical Investigation 112(12):1785-1788.

[24]   Cannon, B., Houstek, J., Nedergaard, J., 1998. Brown adipose tissue. More than an effector of thermogenesis? Annals of the New York Academy of Sciences 856:171-187.

[25]   Bae, J., Ricciardi, C.J., Esposito, D., Komarnytsky, S., Hu, P., Curry, B.J., et al., 2014. Activation of pattern recognition receptors in brown adipocytes induces inflammation and suppresses uncoupling protein 1 expression and mitochondrial respiration. American Journal of Physiology: Cell Physiology 306(10):C918-930.

[26]   Pohl, J., Woodside, B., Luheshi, G.N., 2014. Leptin modulates the late fever response to LPS in diet-induced obese animals. Brain, Behavior, and Immunity 42:41-47.

[27]   Fischer, A.W., Hoefig, C.S., Abreu-Vieira, G., de Jong, J.M., Petrovic, N., Mittag, J., et al., 2016. Leptin Raises Defended Body Temperature without Activating Thermogenesis. Cell Rep 14(7):1621-1631.

[28]   Sachot, C., Poole, S., Luheshi, G.N., 2004. Circulating leptin mediates lipopolysaccharide-induced anorexia and fever in rats. Journal of Physiology 561(Pt 1):263-272.

[29]   Tack, C.J., Stienstra, R., Joosten, L.A., Netea, M.G., 2012. Inflammation links excess fat to insulin resistance: the role of the interleukin-1 family. Immunological Reviews 249(1):239-252.

[30]   Ballak, D.B., Stienstra, R., Tack, C.J., Dinarello, C.A., van Diepen, J.A., 2015. IL-1 family members in the pathogenesis and treatment of metabolic disease: Focus on adipose tissue inflammation and insulin resistance. Cytokine 75(2):280-290.

[31]   Lagathu, C., Yvan-Charvet, L., Bastard, J.P., Maachi, M., Quignard-Boulange, A., Capeau, J., et al., 2006. Long-term treatment with interleukin-1beta induces insulin resistance in murine and human adipocytes. Diabetologia 49(9):2162-2173.

[32]   Seckinger, P., Lowenthal, J.W., Williamson, K., Dayer, J.M., MacDonald, H.R., 1987. A urine inhibitor of interleukin 1 activity that blocks ligand binding. Journal of Immunology 139(5):1546-1549.

[33]   Juge-Aubry, C.E., Somm, E., Giusti, V., Pernin, A., Chicheportiche, R., Verdumo, C., et al., 2003. Adipose tissue is a major source of interleukin-1 receptor antagonist: upregulation in obesity and inflammation. Diabetes 52(5):1104-1110.

[34]   Stienstra, R., Tack, C.J., Kanneganti, T.D., Joosten, L.A., Netea, M.G., 2012. The inflammasome puts obesity in the danger zone. Cell Metab 15(1):10-18.

[35]   Sauter, N.S., Schulthess, F.T., Galasso, R., Castellani, L.W., Maedler, K., 2008. The antiinflammatory cytokine interleukin-1 receptor antagonist protects from high-fat diet-induced hyperglycemia. Endocrinology 149(5):2208-2218.

[36]   Larsen, C.M., Faulenbach, M., Vaag, A., Volund, A., Ehses, J.A., Seifert, B., et al., 2007. Interleukin-1-receptor antagonist in type 2 diabetes mellitus. New England Journal of Medicine 356(15):1517-1526.

[37]   van Asseldonk, E.J., Stienstra, R., Koenen, T.B., Joosten, L.A., Netea, M.G., Tack, C.J., 2011. Treatment with Anakinra improves disposition index but not insulin sensitivity in nondiabetic subjects with the metabolic syndrome: a randomized, double-blind, placebo-controlled study. Journal of Clinical Endocrinology and Metabolism 96(7):2119-2126.
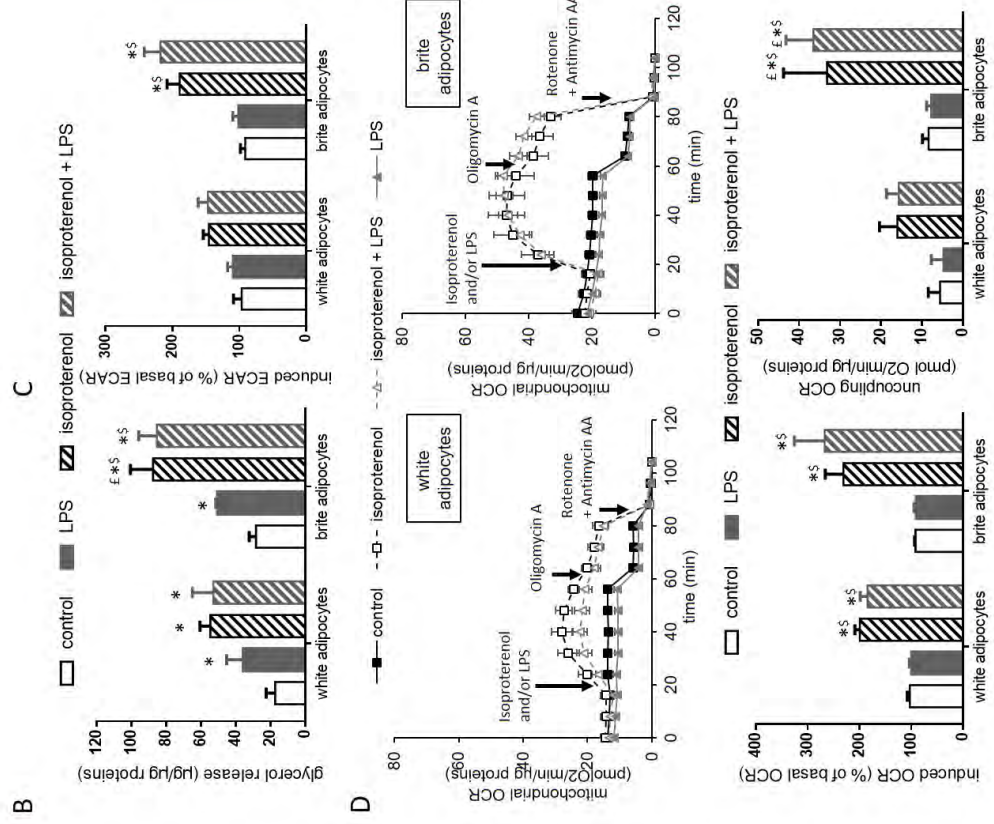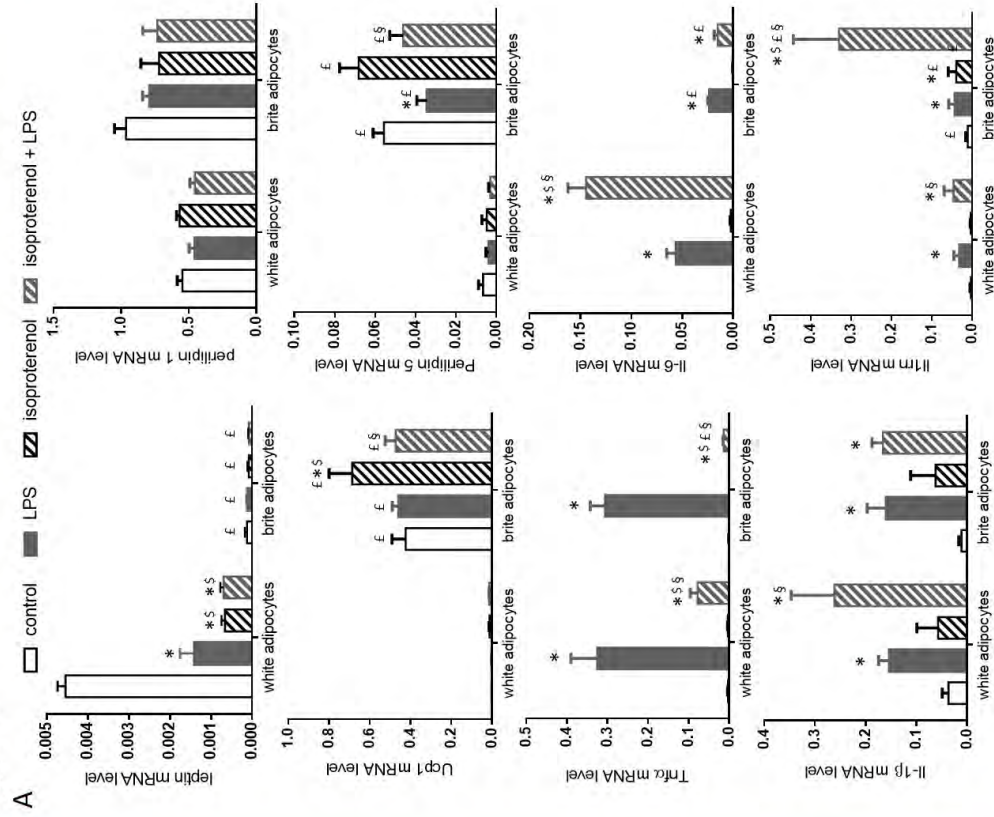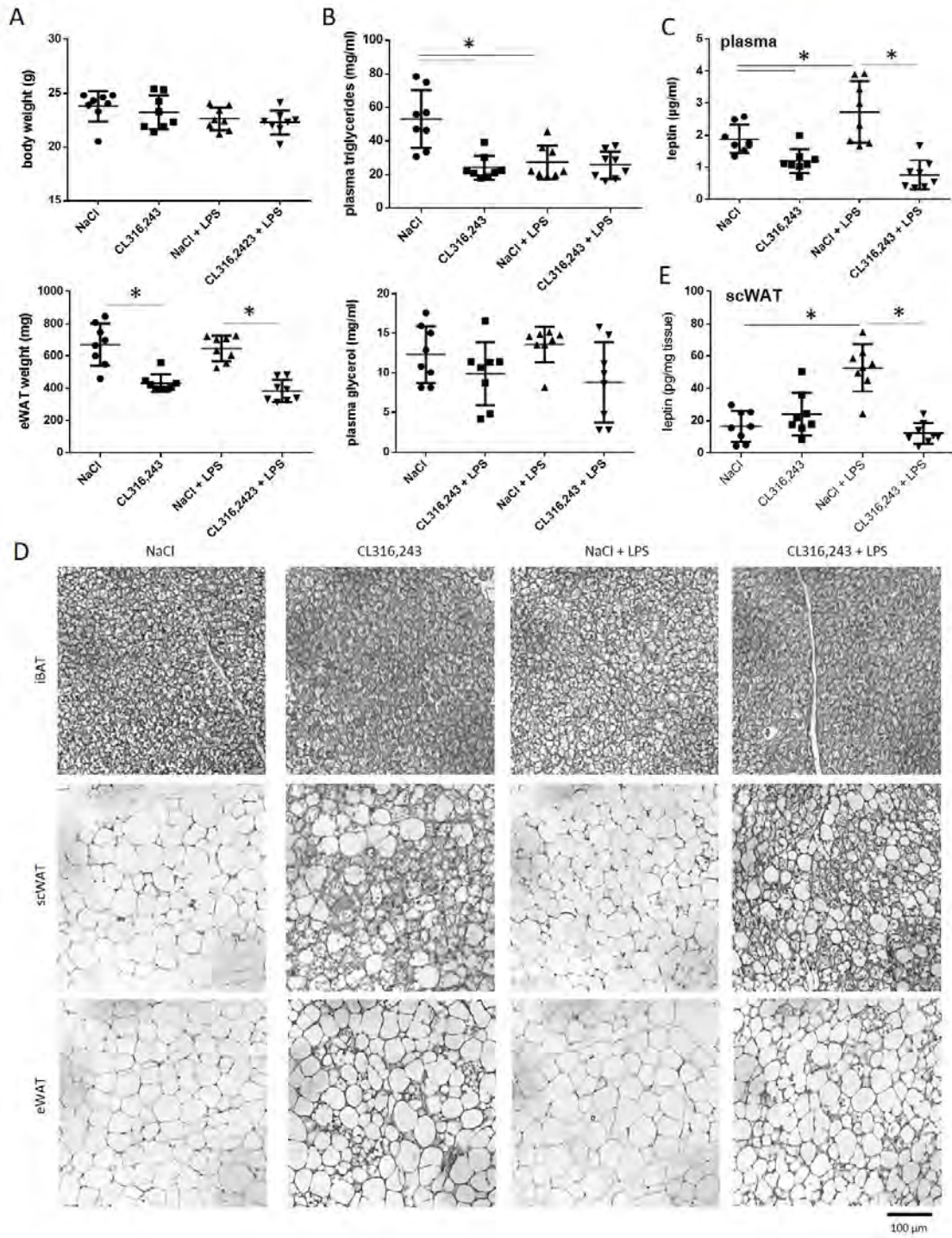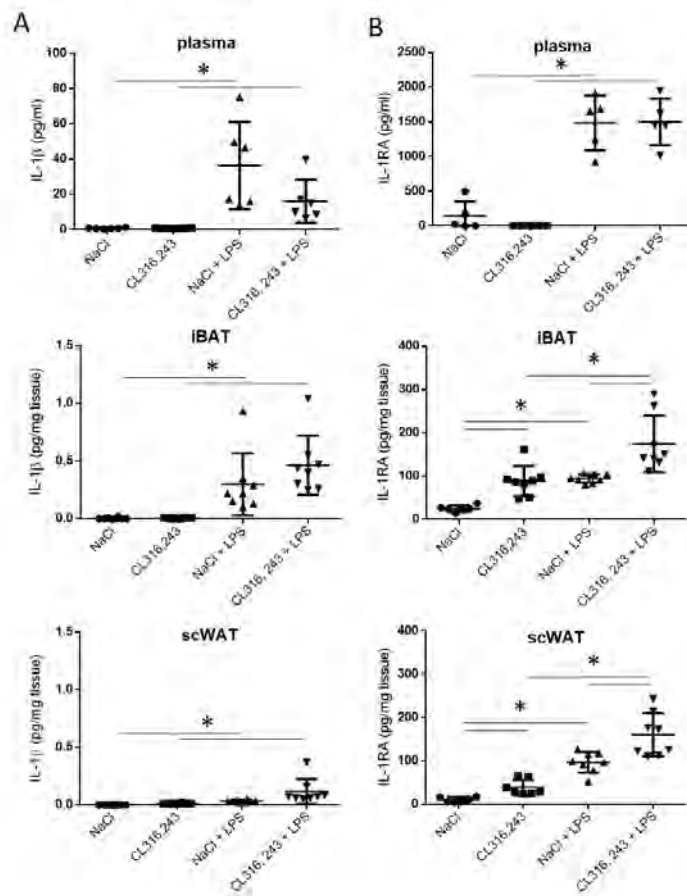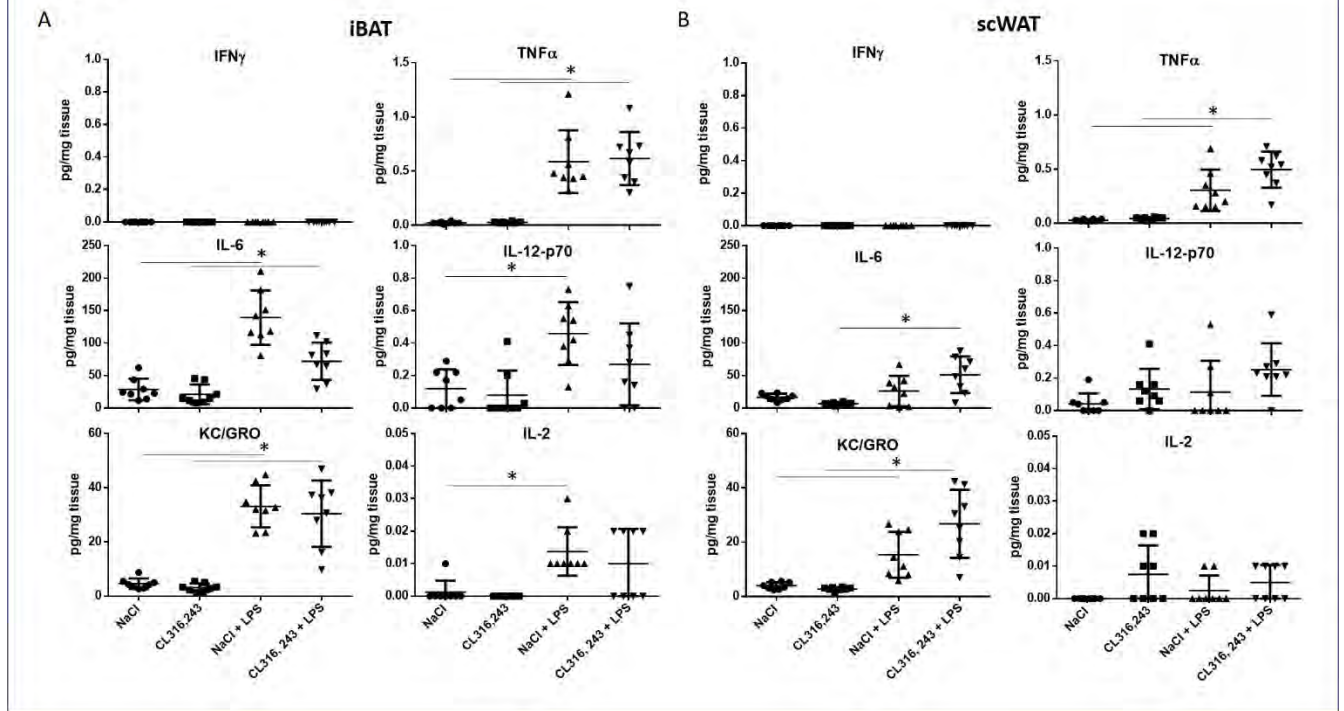
Figure 1.

Figure 2.

Figure 3.

Figure 4.

Supplemental Figure 1.

A

iBAT

B

scWAT

Supplementary figure 2.

plasma

IFNγ, TNFα, IL-6, IL-12-p70, KC/GRO, IL-2 dot plots with groups: NaCl, CL316,243, NaCl + LPS, CL316, 243 + LPS
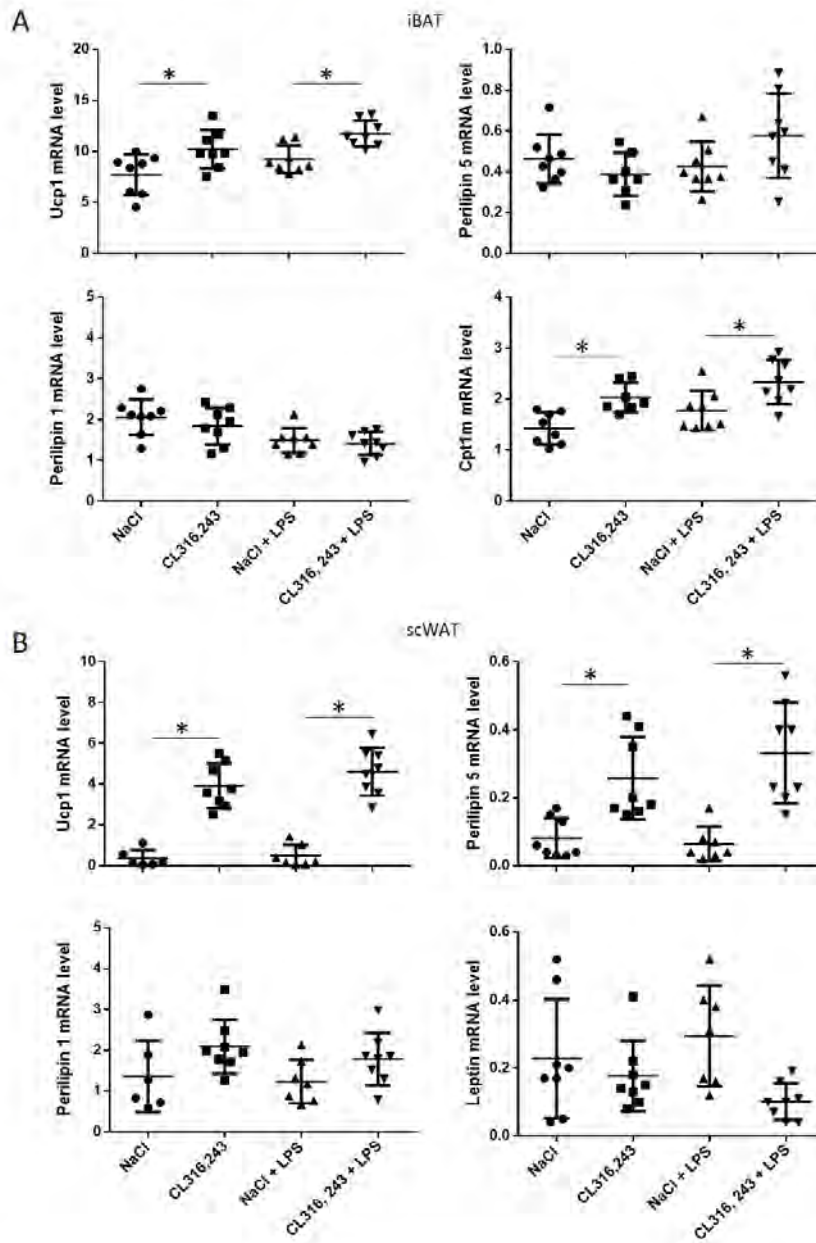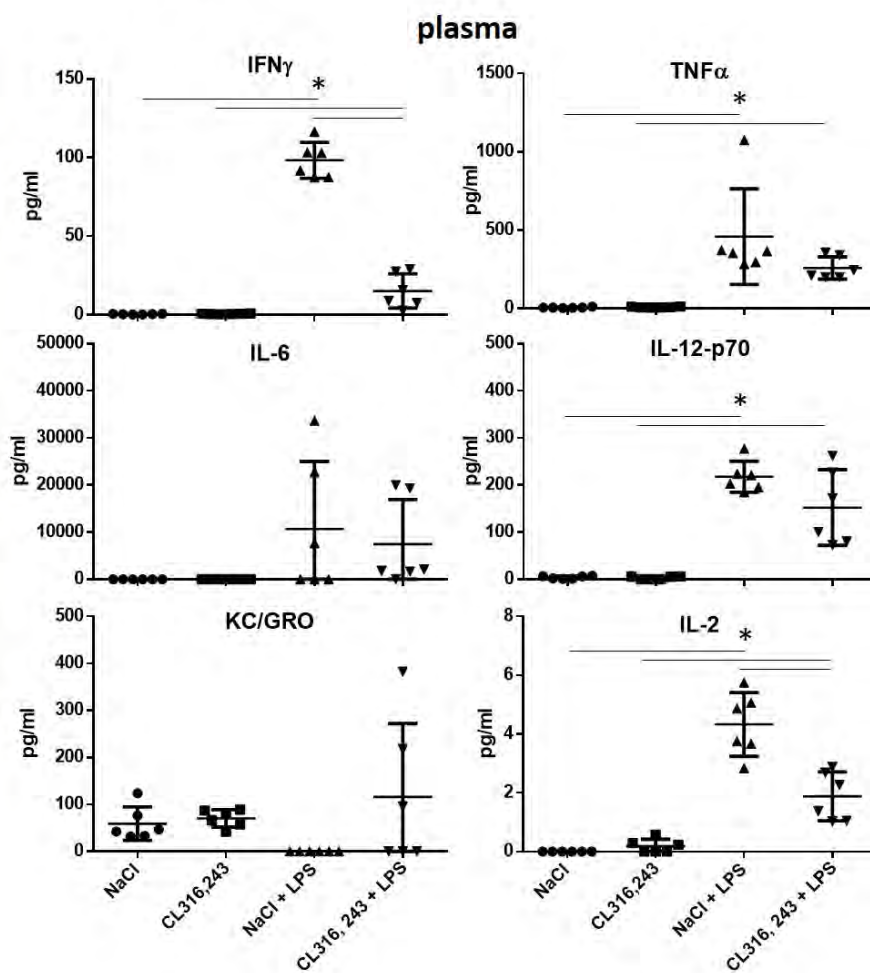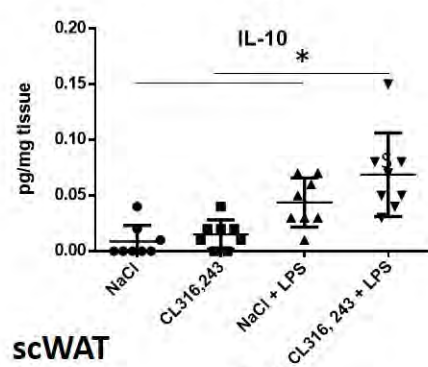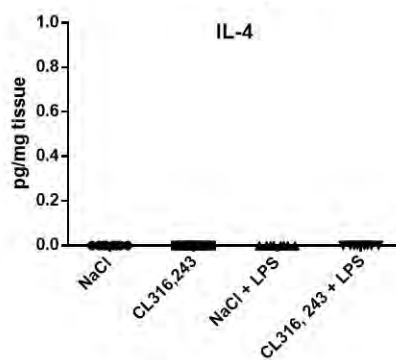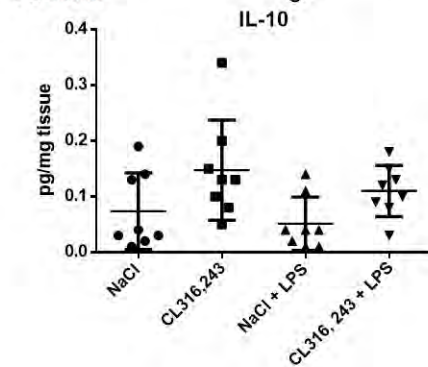
Supplementary figure 3.

plasma
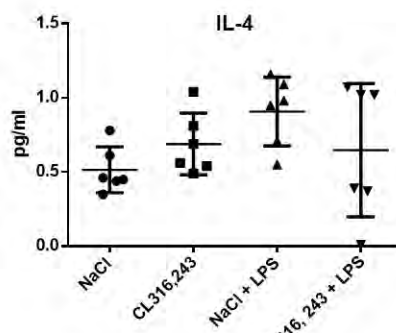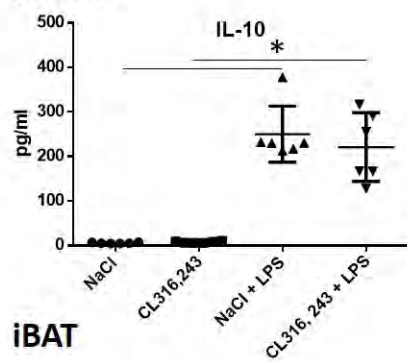
iBAT
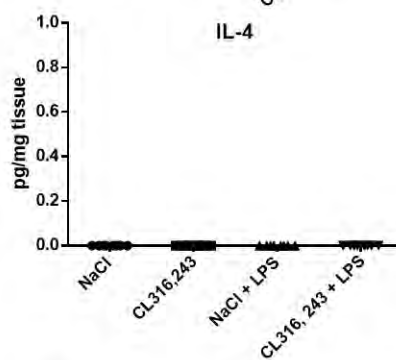
scWAT

ANNEXE 3.

Munro et al. In progress. Results part.

Modulation of infectious response by brown and brite adipocytes activation

Patrick Munro[1], Samah Rekima[2], Agnès Loubat[2], Christophe Duranton[3], Didier F. Pisani[3$] and Laurent Boyer[1$*].

[1] Université Côte d'Azur, Inserm, C3M, Nice, France.

[2] Université Côte d'Azur, CNRS, Inserm, iBV, Nice, France.

[3] Université Côte d'Azur, CNRS, LP2M, Nice, France.

[$] Equal contribution.

[*] correspondance: Laurent Boyer, Centre Méditerranéen de Médecine Moléculaire, INSERM U1065, Bâtiment ARCHIMED, Hôpital l'Archet, 06204 Nice Cedex 3, France. e-mail: laurent.boyer@univ-cotedazur.fr.

1. Results

1.1. **Bacteria injection does not modify response of mice to CL316,243.**

Mice were treated daily for 1 week with the β3-adrenergic receptor agonist CL316,243 (1 mg/kg, intraperitoneal), or vehicle only (NaCl), to induce brown adipose tissue (BAT) activation as well as recruitment and activation of brite thermogenic adipocytes within white adipose tissue (WAT). As expected, at the end of the treatment mice body weight was decreased and rectal temperature was increased in CL316,243 group compare to NaCl group (Figure 1A) due to the thermogenic activity of brown and brite adipocyte. At the end of this treatment, half of the mice of each group were infected with *E. Coli* and followed 48 hours. While bacteria induced a decrease in body weight in NaCl treated mice, no additive effect was found in CL316,243 treated mice (Figure 1B). Differently, CL316,243 treatment decreased epididymal WAT (eWAT) mass while bacteria did not modify significantly it. Plasma analysis revealed that CL316,243 treated mice displayed higher glycerol level (Figure 1C) and lower triglycerides level (Figure 1D) compared to NaCl group and independently of bacteria treatment, demonstrating increase in fatty acid oxidation in link with thermogenesis. Interestingly, an additive effect was found for triglycerides plasma level in mice treated with CL316,243 and infected with bacteria.

As they have been performed 48 hours after the end of CL316,243 treatment, histological analysis of inter-scapular BAT (iBAT) did not shown major difference between groups (Figure 1E). Nevertheless, sub-cutaneous WAT (scWAT), and for a lower extend eWAT, shown numerous multilocular adipocytes in CL316,243 treated mice, characteristic of brite adipocytes (Figure 1E). Bacteria did not modify frequency of brite adipocytes as well as iBAT morphology (Figure 1E).

1.2. **Bacteria clearance and pyrexia are independent to leptin and BAT activation.**

Intraperitoneal injection of bacteria in mice induces in the first 4 hours a pyretic response which is maintained all along the two days of analysis (Figure 2A). Interestingly, even if rectal temperature was different before infection (Figure 1A), the fever in response to bacteria is equivalent between NaCl- and CL316,243-treated mice. As expected, the bacteriemia is decreased at 24 hours and completely resolved after 48 hours, demonstrating bacteria clearance by mice (Figure 2B). Activation of brown and brite adipocytes have not modified this response to infection (Figure 2B).

Leptin is considered as a key mediator of pyrexia especially in mice by limiting body heat loss. Here it is interesting to note that leptinemia as well as leptin secretion by scWAT is decreased in mice infected with bacteria as well as in mice treated with CL316,243 (Figure 2C), demonstrating that pyrexia in response to bacteria and thermogenesis are independent to leptin action.

1.3. **Systemic and local inflammatory response to bacteria.**

CL316,243 preconditioning did not modify fever and bacteria clearance by mice. Thus, we analyzed cytokine profiling to determine if brown and brite adipocyte activity can modulate inflammatory response to bacteria. As expected, bacterial infection induces a systemic inflammatory response characterized by increased plasmatic levels of IFNγ, TNFα, IL-6 and KC/GRO (CXCL-1) compared to PBS-treated mice (Figure 3A). IL-12 does not vary between groups of mice and IL-2 is undetected (Figure 3A). CL316,243 treatment does not modulate by itself plasma cytokine levels and do not modify cytokines increased in response to bacteria, even if a slight decrease was found (Figure 3A). To note, the high variability in plasma quantity for each cytokine (Figure 3A) in response to bacteria can be relied to the high variability in bacteriemia evolution found in the mice (Figure 2B).

Adipose tissues seem less affected by bacterial infection. Indeed, in iBAT only IFNγ secretion increases in response to bacteria injection (Figure 3B), other cytokines are either unaffected (TNFα, IL-2) or decreased (IL-6, IL-12, KC/GRO) (Figure 3B). In scWAT, all cytokine secretions are unaffected except for IL-12 which is decreased (Figure 3C). In all case, CL316,243 does not modulate local cytokine secretions in response to infection (Figure 3B-C).

In search to an impact of CL316,243 pretreatment on inflammatory resolving, we analyzed IL-4 and IL-10 levels in plasma and in secretory media of adipose tissue explant. Unfortunately, IL-4 is never detected and even if IL-10 level increases in plasma of infected mice it is not modulated by CL316,243 treatment (Figure 4). Like to pro-inflammatory cytokines, IL-10 secretion is unaffected by bacteria as well as CL316,243 treatment in iBAT and scWAT (Figure 4).

Due to the basal response of scWAT to bacteria in term of cytokine secretion, we search for immune cells infiltration in this tissue. As expected, we found classic figures of inflammation in scWAT of mice infected by bacteria, pretreated or not with CL316,243, including crown structure and small cell infiltration characteristic of macrophage and lymphocyte presence

respectively (Figure 5A). This is confirmed using F4/80 immunostaining showing clearly macrophage occurrence in adipose tissue (Figure 5B).

1.4. **Systemic and local inflammatory response to bacteria.**

Along inflammatory cytokines, IL-1β is a main actor of pyrexia and anti-bacterial response and is highly secreted by adipose tissue. Thus, in response to bacteria injection, IL-1β plasma level increases in the same time to IL-1RA (IL-1 receptor antagonist) which is involved in inflammatory resolving (Figure 6A). Pre-treatment of mice with CL316,243 did not modify this response (Figure 6A). Analysis of IL-1β and IL-1RA secretion in iBAT shows that both increase in infected mice and, interestingly, IL-1β secretion is decrease in iBAT activated by CL316,243 treatment (Figure 6B). Differently, IL-1RA secretion is equivalent between iBAT of infected mice treated or not with CL316,243 (Figure 6B). scWAT situation is different as IL-1β secretion is not significantly induced by bacteria injection which increased IL-1RA secretion, CL316,243 increased it to and this effect is additive to infection (Figure 6C).

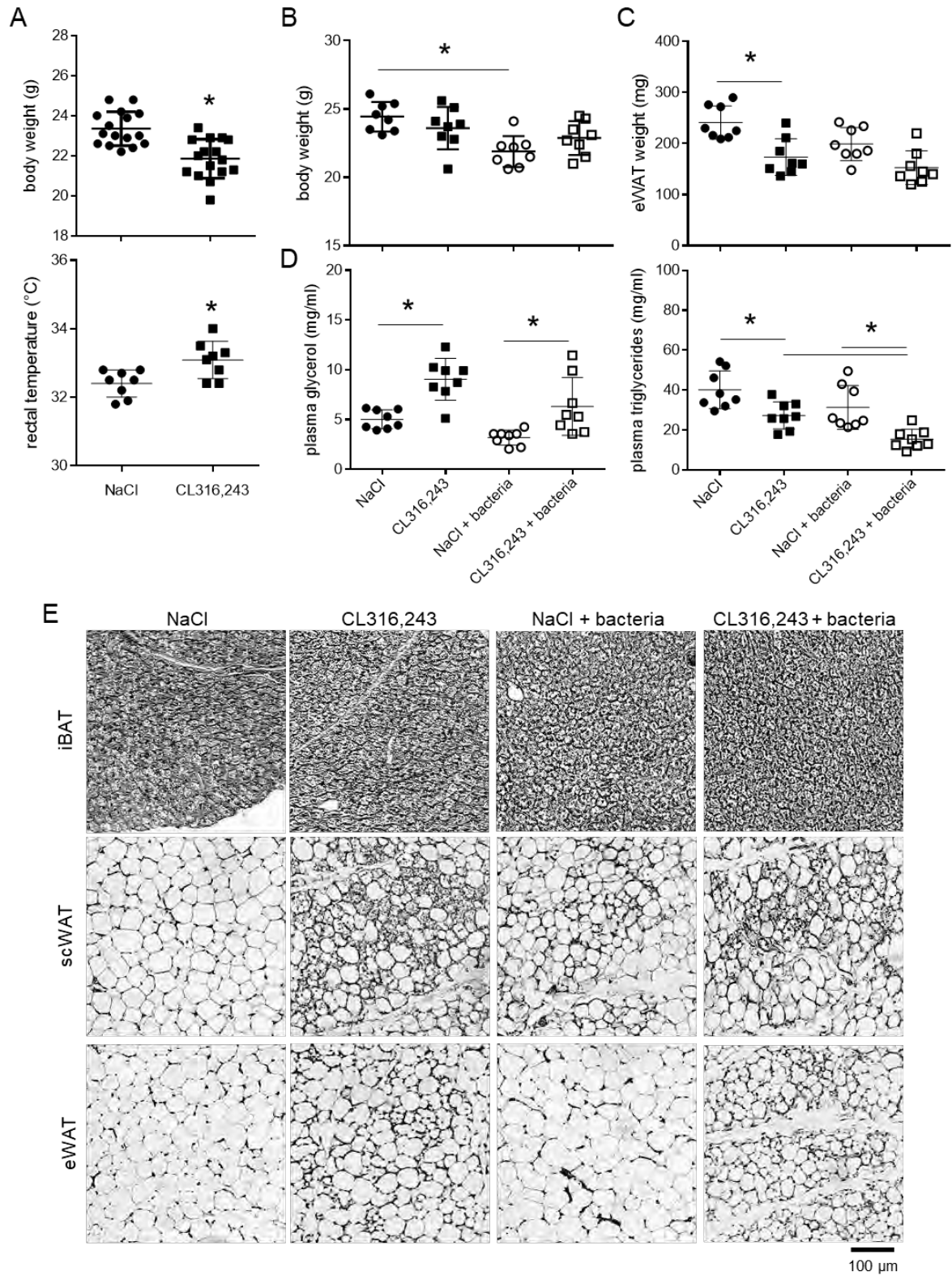Figure 1. Bacteria infection does not modify metabolic paremeters and adipose tissue morphology.

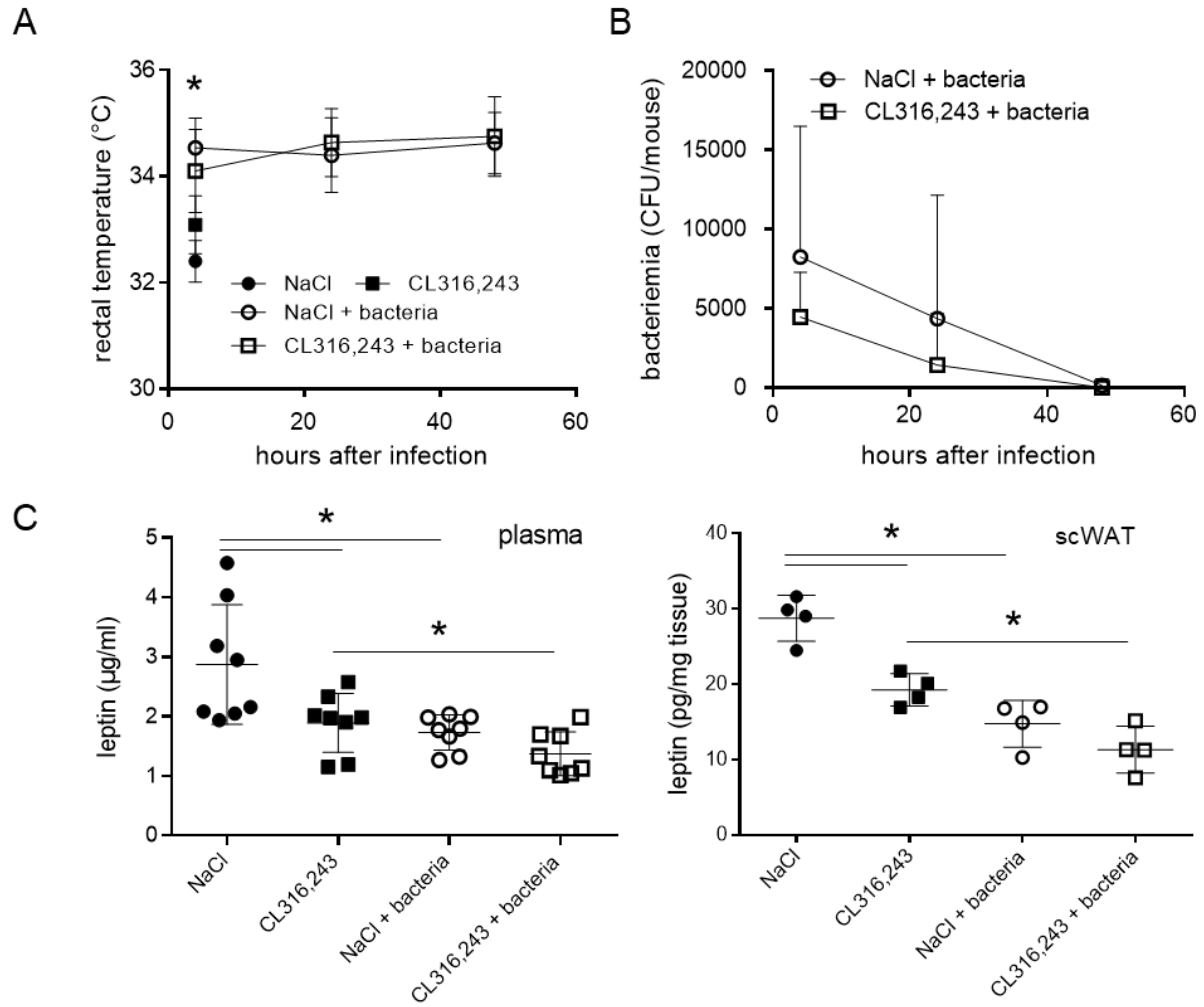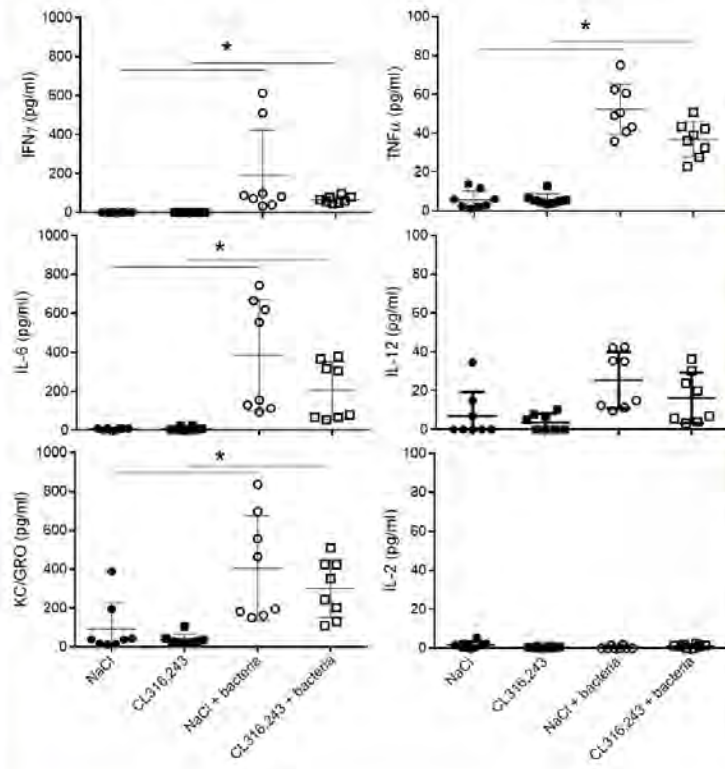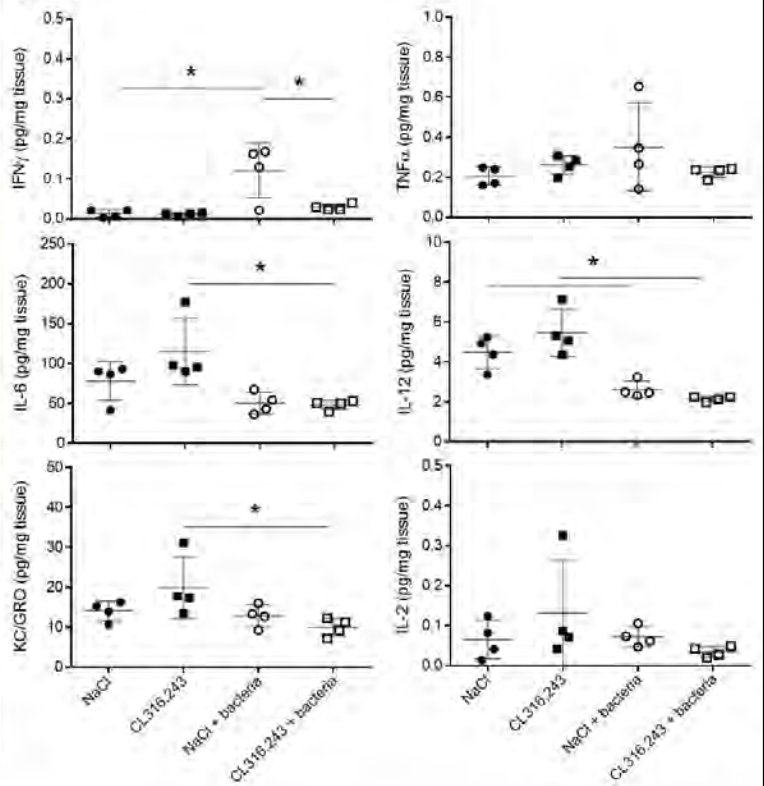Figure 2. Pyrexia, bacteriemia and leptin secretion.

Figure 3. Systemic and local inflammatory responses to infection.
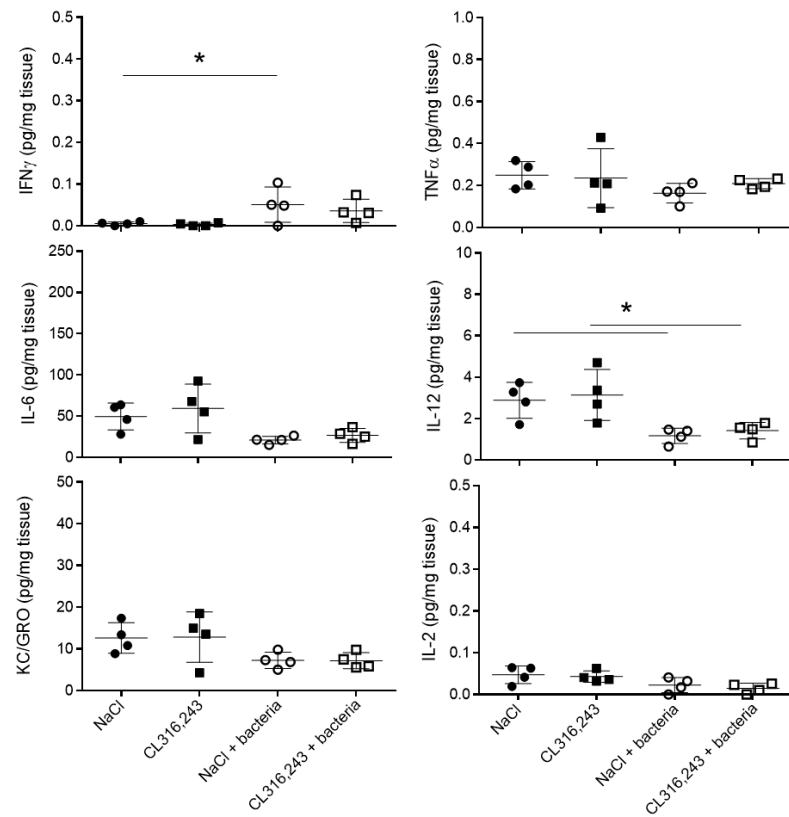
A. plasma

B. iBAT

C. scWAT

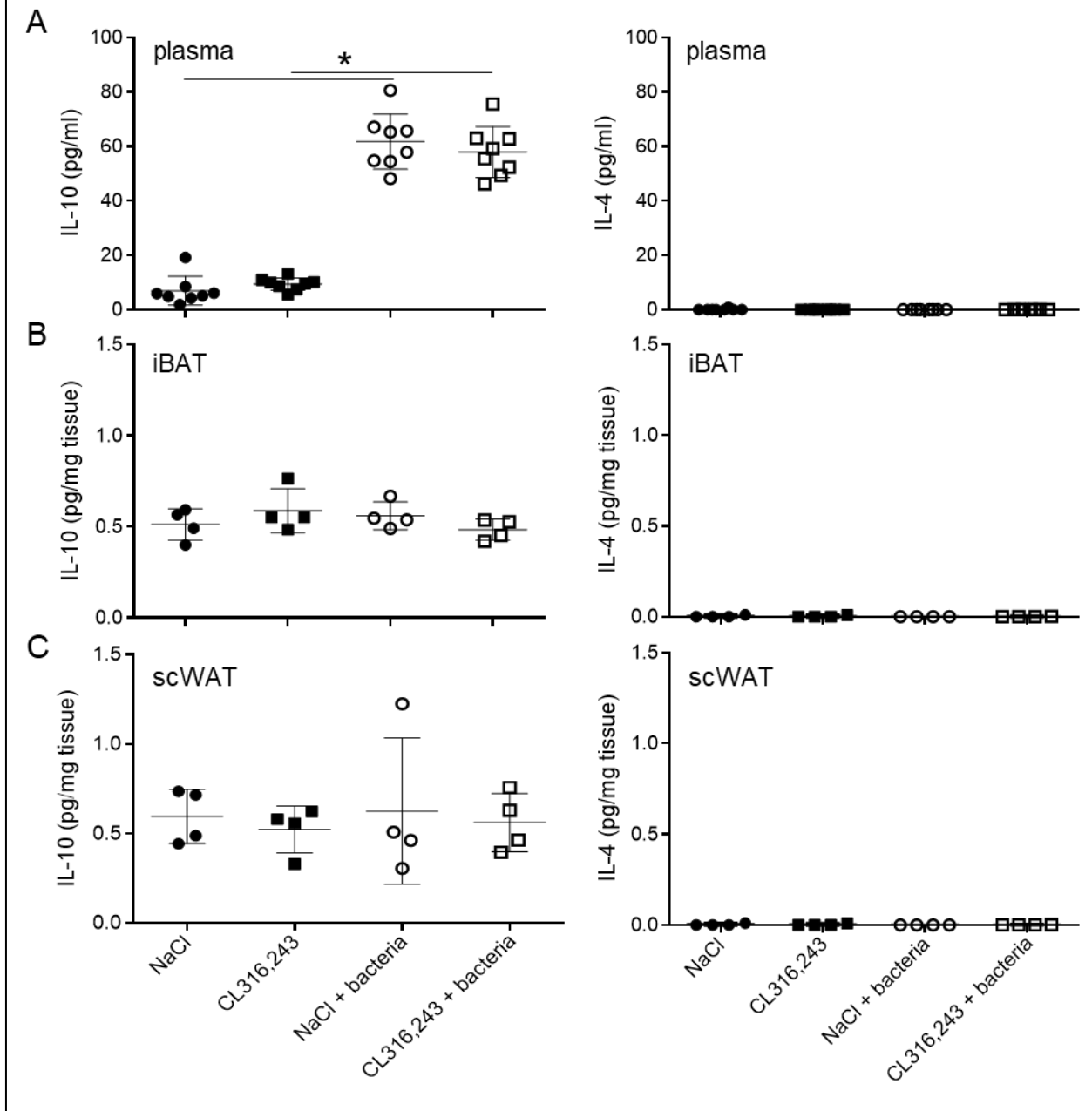Figure 4. Systemic and local anti-inflammatory response to bacteria.

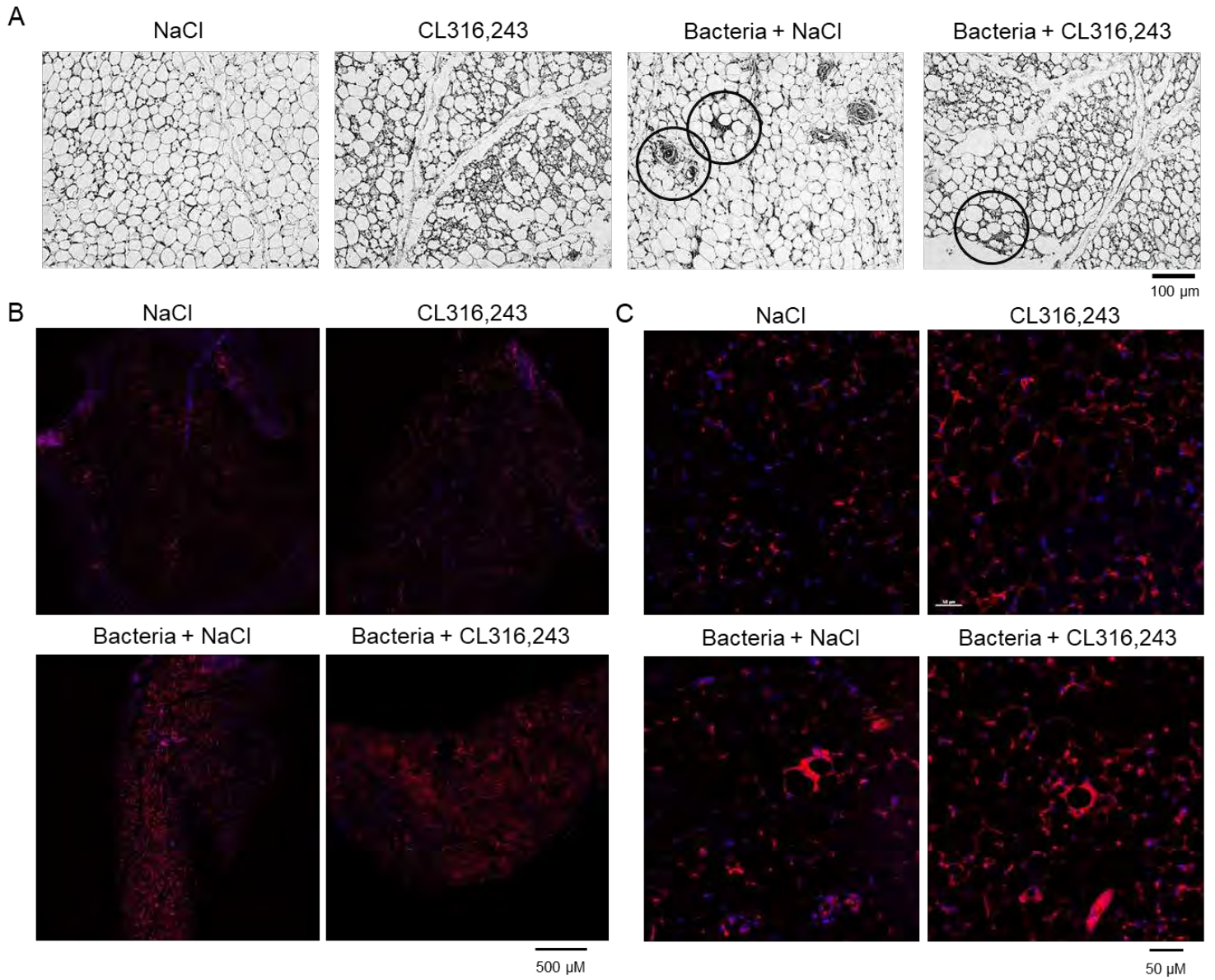Figure 5. Macrophage infiltration.

A

NaCl | CL316,243 | Bacteria + NaCl | Bacteria + CL316,243

100 µm

B

NaCl | CL316,243

Bacteria + NaCl | Bacteria + CL316,243

500 µM

C

NaCl | CL316,243

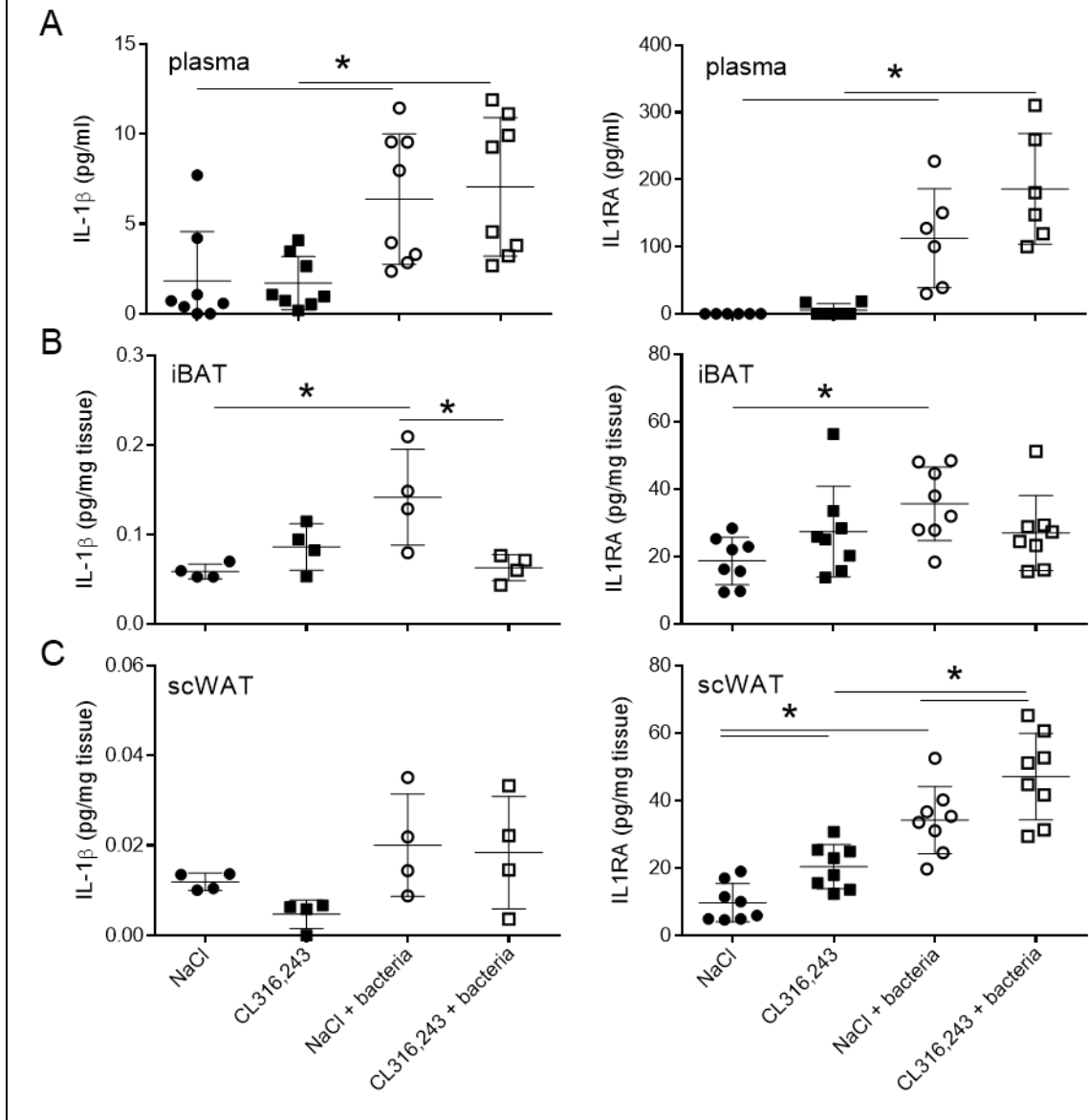Bacteria + NaCl | Bacteria + CL316,243

50 µM

Figure 6. IL-1 pathway response to bacteria infection.

ANNEXE 4.

Schwing et al. Submitted.

1 **Title**

2 Adipocytes, a potential sanctuary of persistence for *Leishmania infantum* parasites

3 **Authors list**

4 Aurélie Schwing[1,2,3], Didier F. Pisani[4], Christelle Pomares[1, 2], Alissa Majoor[2], Emmanuel

5 Lemichez[5], Pierre Marty[1,2], Laurent Boyer[2] and Grégory Michel[2]

6 **Affiliation**

7 1 Parasitologie-Mycologie, Centre Hospitalier Universitaire l'Archet, Nice, France

8 2 Université Nice Côte d'Azur, Inserm, U1065, C3M, Nice, France

9 3 Université Aix-Marseille, Marseille, France

10 4 UCA, IBV, CNRS UMR 7277, Inserm, U 1091, Nice, France

11 5 Institut Pasteur, Unité des toxines bactériennes, Paris, France

12

Introduction

Leishmania infantum (*L. infantum*) is the causative agent of visceral leishmaniasis transmitted by the bite of female sand flies. According to the WHO, the estimated annual incidence of leishmaniasis is one million new cases, resulting in 30 000 deaths per year [1]. The outcome of infection can be variable ranging from an asymptomatic form to obvious disease. Commonly, *Leishmania* infection remains asymptomatic in immunocompetent individuals [2]. Clinical features of leishmaniasis depend on the species and the immune response of the host [3]. Symptomatic leishmaniasis is characterized by 3 main forms: cutaneous leishmaniasis (CL), mucocutaneous leishmaniasis (MCL) and visceral leishmaniasis (VL). CL is a chronic infection with ulcerative skin lesion occurring at the site of innoculation. MCL is generally the result of the parasite dissemination from the skin to the naso-oropharyngeal mucosa. VL is the most serious form of leishmaniasis leading to death in a few months without treatment. It is characterized by irregular fever, weight loss, hepatosplenomegaly, lymphadenopathies and pancytopenia. Currently, there is no human vaccine and treatments are expensive. WHO guidelines recommend the use of few drugs, including Amphotericin B [4]. Over the course of the years, several cases of relapses have been documented[5,6]. These relapses call into question the efficiency of actual treatments [5] [7] and raises the question of potential persistence sites. Indeed, *Leishmania* has the ability to persist in humans for long periods of time and even after successful treatment [8]. Several potential persistence sites have already been identified and named 'safe targets'. These include immature myeloid precursor cells, monocytes, sialoadhesin-positive stromal macrophages of the bone marrow, hepatocytes and fibroblasts [8]. Previously, *L. infantum* persistence and development has been shown in intra-abdominal adipose tissue in intraperitoneally infected mice [9]. Moreover, adipose tissue has been proposed as a sanctuary of persistence for bacteria such as *Mycobacterium tuberculosis* [10], *Coxiella burnetii* [11], *Mycobacterium canettii* [12] or viruses such as Human Immunodeficiency Virus (HIV) [13], Simian Immunodeficiency Virus

39   [14] and parasites such as *Trypanosoma cruzi* , *Trypanosoma brucei* and *Plasmodium spp.*

40   [15,16]. In this paper, we addressed the question of the persistence of *L. infantum* in adipose

41   tissue and whether or not *L. infantum* could infect adipocytes.

42

Results

L. infantum is found in the adipose tissue of infected mice.

In this study, we investigated wether or not _L. infantum_ could be present in the two different adipose tissues (brown and white adipose tissue) of infected mice. For this purpose, BALB/c mice were intravenously inoculated by LUC-_L. infantum_. Mice were sacrificed after 6, 10 and 31 weeks post-infection (_p.i_). Tissues samples were analyzed for the presence of _L. infantum_ by qPCR. Verification of infection confirmed chronic infection in spleen and liver (Fig S1). 6 weeks post infection, white (subcutaneous and periovarian) and brown tissues presented a parasite burden (Fig 1). After 10 weeks post infection periovarian adipose tissue and brown adipose tissue levels of parasite burden is high. In subcutaneous tissue, between 6 and 10 weeks post infection, parasite burden decreased and totally disappeared 31 weeks post infection. Of note, the number of mice with positive parasite burden in brown adipose tissue remains higher than 70% until 31 weeks post infection. These results show the presence of _L. infantum_ in adipose tissue after an infection by intravenous route preferentially in brown adipose tissue. Furthermore, we performed histological sections on different tissues from the same infected mice in order to visualize parasites by immunolabelling. 40 weeks post infection, presence of intact _leishmania_ parasites in all adipose tissues can be observed (Fig 2). This raised the question whether parasites contained in adipose tissue from infected mice where alive and infectious. We thus performed an adoptive transfer experiment by intravenously injecting naïve mice with brown adipose tissue from previously infected mice. 34 weeks post transfer we could detect parasite DNA by qPCR in the liver, spleen and brown adipose tissue of naïve mice (Supplemental Table 1). To conclude, our results show that _L. infantum_ persists in the adipose tissue of mice, and suggests its implication as a potential reservoir for _L. infantum_ persistence.

L. infantum is contained in adipocytes enriched fraction

68 To assess whether *L. infantum* is contained in adipocytes or other cell types, we separated an

69 adipocyte enriched fraction from the stromal vascular fraction (SVF). White and brown

70 adipose tissue from 4 IV infected mice were separated into floating fraction (adipocytes

71 enriched fraction) and a pellet containing the SVF. The samples were pooled in order to

72 increase the number of parasites and improve the detection by qPCR. Separation between

73 adipocytes and stromal cells was checked by amplification of adipocyte markers mRNA (Fig

74 3A). As expected, expressions of perilipin 1, a protein coating the lipid droplet and

75 abundantly expressed only in white and brown adipocytes [17], and adiponectin, a

76 glycoprotein adipocyte-specific factor which is implicated in increasing insulin sensitivity

77 [18], were restricted to adipocyte fraction (Fig 3A). As no parasite DNA was detected in SVF

78 (Fig 3B) of each kind of adipose tissue, these results suggest the presence of *Leishmania*

79 predominantly in adipocytes.

80 ***L. infantum* can infect murine and human adipocytes *in vitro***

81 We next evaluated the ability of *L.infantum* to infect white, brown and brite adipocytes

82 derived from mouse primary pre-adipocytes. Brite adipocytes are similar to classical brown

83 adipocytes but come from white adipose tissue derived pre-adipocytes. Primary pre-

84 adipocytes from BALB/c mice were collected in subcutaneous (SC) white adipose tissue and

85 differentiated into white and brite adipocytes (Fig 4). Moreover, the pre-adipocytes from

86 brown adipose tissue were differentiated into brown adipocytes. Given that *L. infantum*

87 targets macrophages, bone marrow derived macrophages (BMDM) were taken as a positive

88 control for infection. 24 and 48 hours post infection, observation of the cells suggested the

89 presence of intracellular parasites. This infection is observed in all types of adipocytes (Fig 4).

90 This observation shows the ability of *L. infantum* to infect and survive in murine adipocytes *in*

91 *vitro*. We next investigated the ability of *L. infantum* to parasite human adipocytes. Adult SC

92 white adipose tissue progenitors were differentiated into white and brite human adipocytes

93 [19] and were infected by *L. infantum*. 24 and 48 hours post infection, we observed the

94 presence of parasites in human adipocytes (Fig 5). To confirm the intracellular localization of

95 *L. infantum* parasites in brown adipocytes, we performed an electronic microscopy

96 experiment. Finally, *L. infantum* parasites were indeed found inside a vacuole in lipid droplets

97 containing cells. In conclusion, epifluorescence and electronic microscopy combined

98 confirmed the ability of *L. infantum* to parasite adipocytes. This reinforced the hypothesis that

99 adipose tissue and more precisely adipocytes could be a 'safe target' for the persistence of *L.*

100 *infantum*.

101

Discussion

To understand *Leishmania* persistence in humans despite treatment, we searched for a tissue reservoir for this organism. Because adipose tissue has been demonstrated to be targeted and/or be a reservoir for several intracellular pathogens able to induce relapses [10–15], we hypothesized that adipose tissue could also be a reservoir for *Leishmani*a parasites. Indeed, sanctuaries of persistence of *L. infantum* parasites in humans are still undetermined. A previous study highlighted the presence of *L. infantum* in intra-abdominal fat in BALB/c mice [9]. Thus, we hypothesized that adipose tissue could be a sanctuary of persistence for *L. infantum*.

Our results have shown the presence of *L. infantum* in murine subcutaneous, periovarian, dorsal and predominantly in brown adipose tissue. Moreover, transfer of brown adipose tissue from previously infected BALB/c mice to naïve led to development of infection. This indicates that *Leishmania* present in brown adipose tissue are alive and able to infect the liver, spleen and brown adipose tissue of naïve mice. We have shown that *in vitro, L. infantum* can infect mouse and human adipocytes. It is known that adipocytes are very long-lived cells and do not significantly turn over in 6-12 months [20]. Interestingly, in HIV-positive patients, 60% of the patients relapse within 12 months after treatment [21] and in HIV-negative patients, relapses occur with a median time of 10,1 months[22]. Finally, adipocytes could act as safe targets for *Leishmania* parasites as they do not *per se* exert antimicrobial activities, have a long turnover and thus allow parasite persistence. Relapses could be explained by a failing of treatment to target intracellular *Leishmania* in adipose tissue. In this context, it is possible that relapses occur because of poor penetration into adipose tissue. Structural changes in drug design may improve the penetration of molecules active against *L. infantum* in adipose tissue.

Materials and Methods

Mice and Ethics statement: Female BALB/c and C57BL mice were purchased from Charles River (France). Mice were maintained and handled according to the regulations of the European Union, the French Ministry of Agriculture and to FELASA (the Federation of Laboratory Animal Science Associations) recommendations. Experiments were approved by ethics committee of the Nice School of Medicine, France (Protocol number: 2017-56)

Leishmania culture: L. infantum MON-1 (MHOM/FR/94/LPN101), was isolated from a patient with Mediterranean visceral leishmaniasis contracted in the Nice area (south of France). We used the generation of recombinant *L. infantum* -expressing reporter Luc genes (LUC-*L. infantum*) and a generation of recombinant *L. infantum* -expressing reporter Green Fluorescence Protein (GFP-*L. infantum*). *L. infantum* promastigotes were routinely grown at 26°C in Schneider's Insect Medium (Sigma®) supplemented with NaHCO3 0.4g/L (Janssen chimica®), CaCl 0.6g/L (Fluka Chemika®), Fetal Bovine Serum 10% (Gibco®), 10 mL urine pool for 500 mL of medium, Phenol Red 0,1%, Hepes 1M pH 7.3, penicillin/streptomycin 1% (Gibco®), L-Glutamine 1% (Gibco®).

Parasite preparation and inoculation in mice: LUC-*L. infantum* promastigotes were prepared from promastigote cultures. Briefly the promastigote forms were washed three times in PBS, and 2.10^8 parasites are injected by intravenous route in 200µL of PBS. We injected 200µL of PBS in Mice control.

Minced BAT tissue from infected BALB/c: BAT from infected BALB/c were sampled and freshly minced with potter. The minced BAT infected was injected by intraperitoneal route in naïve BALB/c.

Separation adipocytes enriched fraction and stromal vascular fraction (SVF)

149   Briefly BAT and WAT were minced and then digested for 45 min at 37°C in collagenase type

150   2. The tissue digest is passed through a 250 µm nylon sheets. Floating adipocytes are

151   separated from the SVF after decantation. The floating fraction is carefully removed

152   corresponding to the adipocytes enriched fraction.

153   *Quantification of parasites by PCR quantitative:* Each sample of AT, liver and spleen was put

154   in a sterile tube of Lysing Kits (Precellys®), and then homogenized by Precellys® (2 x 30

155   sec, with a break of 15sec) in lyse buffer of Quiagen Kit QIAmp DNA Mini Kit®. The DNA

156   extraction is realized in according to the recommendations of Quiagen®. The extracts were

157   kept at -20°C for conservation.

158   Quantitative PCR was implemented for detection and quantification of *L. infantum* targeting

159   minicircle kinetoplast DNA (kDNA). Primers and probes previously described by Mary *et al.*

160   [5]   containing 20 pmol of each forward (5'-CTTTTCTGGTCCTCCGGGTAGG-3') and

161   reverse (5'-CCACCCGGCCCTATTTTACACCAA-3') primers and 3.33 pmol of TaqMan

162   probe (FAM-TTTTCGCAGAACGCCCCTACCCGC-TAMRA) were used for *Leishmania*

163   screening and quantification [5] . The assays were performed with a final volume of 10µL

164   including 2.5µL DNA sample.

165   The standard curve was obtained from the primary DNA extraction source of $2.5.10^7$ parasites

166   and diluted serially with 1/10 rate which corresponding to the 50 000 to 0.05 parasites in

167   2,5µL. PCR program was implemented in two steps temperature of 95°C and 60°C for 40

168   cycles. The standard curve and a pair of negative controls was used for each assay.

169   *Histology and microscopic observation:* Organs fixed in PFA (ParaFormAldehyde) 4%.

170   Samples are included in paraffine automatically with the spin tissue processor STP120

171   (ThermoFisher®). The tissue processor STP120 uses alcohol to remove water from tissues

172   and replace it with a medium that allows sectioning of tissue. Thin sections (2.5 µm) were

173   realized with Microtome Microme HM340E (Leica BIOSYSTEMS®). Sections were

174 deparaffinized by 3 immersing in xylene, rehydrated by successive immersing in ethanol

175 solution with different percentages of ethanol (100%, 95%, 70%, 50%) and in water.

176 Unmasking was realized by heat in boiled 10 mM Sodium Citrate buffer (pH 6.0) .

177 Endogenous peroxidase activity, is blocked by a solution of 3.0% hydrogen peroxide. The

178 immunostaining is an antibody succession: the primary antibody is a human antibody directed

179 against *Leishmania*. This antibody is recognized by an anti-human goat antibody, which is

180 recognized by biotinylated anti-goat, the signal is amplified and revealed by Streptavidin-

181 HRP.

182 The brightfield microscope was an Eclipse Ci upright stand (Nikon, Japan), using objectives

183 20X dry NA 0.40. Acquisitions were done with a DS – Ri 1 camera (Nikon, Japan).

184 *Mouse primary pre-adipocytes purification and differenciation*

185 The method for generating white, brite and brown adipocytes from stromal vascularization

186 fraction (SVF) cells was adapted from a previous publication [23]. Briefly, fat depots were

187 sampled, minced and then digested for 45 min at 37°C in DMEM (Lonza, BE12–707F)

188 containing 2 mg/ml collagenase A (Roche Diagnostics, 11088793011) and 20 mg/ml BSA

189 (Sigma-Aldrich Chemie Gmbh, A7030). Digesta was successively filtrated through 250, 100

190 and 27 μm nylon sheets, and finally centrifuged at 500 g for 5 min. The pellet containing

191 stromal-vascular fraction (SVF) was cleaned from red blood cells using specific buffer

192 (Sigma) before to be plated and maintained in DMEM containing 10% (v/v) fetal calf serum

193 (FCS) until confluence. Differentiation was induced by supplementation with 1 μM

194 dexamethasone (Sigma-Aldrich Chemie Gmbh, D4902), 0.5 mM isobutylmethylxanthine

195 (Sigma-Aldrich Chemie Gmbh, I5879) and 860 nM insulin (Invitrogen, 12585014) for 2 d.

196 Cells were then maintained for 7–10 d in presence of 100 nM insulin for white adipogenesis

197 or a mixture containing 100 nM insulin, 1 μM rosiglitazone (BertinPharma, 71740) and

198   0.2 nM triiodothyronine (Sigma-Aldrich Chemie Gmbh, T6397) for brown or brite

199   adipogenesis.

200   *Differentiation and generation of BMDM (Bone Marrow Derived Murine):*

201   Femurs are removed and purified from the surrounding muscles and connective tissue. Under

202   sterile condition the bone marrow was flushed by pression after needle penetration in

203   epiphyses with RPMI medium BMDM with decomplemented FBS 10% and gentamycin

204   0,001%. The cells were centrifuged (400G, 5min) and resuspended in RPMI medium BMDM

205   supplemented with M-CSF 10 ng/mL. We placed 5.10^5 cells /well.

206   *Human adipocytes differentiation.*

207   Human adipose tissue primary progenitor cells are from a previous study [19] and

208   differentiated as follow. Cells were cultivated in DMEM containing 10% FCS until

209   confluence. When cells reached confluence, they were induced to differentiate for 3 days in

210   DMEM/Ham's F12 (1:1) media supplemented with 10 μg/ml transferrin, 10 nM insulin,

211   0.2 nM triiodothyronine, 1 μM dexamethasone and 500 μM isobutyl-methylxanthine. The

212   cells were next differentiated in white adipocytes using a media supplemented with 10 μg/ml

213   transferrin, 10 nM insulin, 0.2 nM triiodothyronine or in brite adipocytes in the same media

214   supplemented with 100 nM rosiglitazone.

215   *Amastigotes generation*: The BMDM and adipocytes of pre-adipocytes murine origin are

216   infected after 7 days of differentiation with 10 leishmania/cells. Human adipocytes are

217   infected after 14 days of differentiation with 10 leishmania/cells.

218   The EVOS FL microscope (AMF-4302-EU) (Labtech, France), using objectives 10X dry Ph

219   and 20X dry FL. The cubes used were LED Light cube included: GFP. Acquisitions were

220   done with Sony ICK285AL monochrome CCD, 2/3'' 1360x1024, 1,4 Megapixels camera

221   (Labtech, France).

Acknowledgments

Bibliography

1. WHO (2018) The Who leishmaniasis Fact Sheet. World Health Organization Available: https://www.ncbi.nlm.nih.gov/pubmed/21485694 via the Internet. Accessed x.

2. Michel G, Pomares C, Ferrua B, Marty P (2011) Importance of worldwide asymptomatic carriers of *Leishmania infantum* (*L. chagasi*) in human. Acta Trop 119: 69-75.

3. Marty P, Izri A, Ozon C, Haas P, Rosenthal E, Del Giudice P et al. (2007) A century of leishmaniasis in Alpes-Maritimes, France. Ann Trop Med Parasitol 101: 563-574.

4. WHO (2010) Control of the leishmaniases. Who Technical Report Series 949: 1-185.

5. Mary C, Faraut F, Lascombe L, Dumon H (2004) Quantification of *Leishmania infantum* DNA by a real-time PCR assay with high sensitivity. J Clin Microbiol 42: 5249-5255.

6. Haque L, Villanueva M, Russo A, Yuan Y, Lee EJ, Topal J et al. (2018) A rare case of visceral leishmaniasis in an immunocompetent traveler returning to the United States from Europe. PLoS Negl Trop Dis 12: e0006727.

246   7.   Tatarelli P, Fornaro G, Del Bono V, Nicolini LA, Raiola AM, Gualandi F et al. (2018)

247   Visceral leishmaniasis in hematopoietic cell transplantation: Case report and review of

248   the literature. J Infect Chemother 24: 990-994.

249   8.   Bogdan C (2008) Mechanisms and consequences of persistence of intracellular

250   pathogens: leishmaniasis as an example. Cell Microbiol 10: 1221-1234.

251   9.   Michel G, Ferrua B, Lang T, Maddugoda MP, Munro P, Pomares C et al. (2011)

252   Luciferase-expressing *Leishmania infantum* allows the monitoring of amastigote

253   population size, *in vivo*, *ex vivo* and *in vitro*. PLoS Negl Trop Dis 5: e1323.

254   10.   Neyrolles O, Hernández-Pando R, Pietri-Rouxel F, Fornès P, Tailleux L, Barrios Payán

255   JA et al. (2006) Is adipose tissue a place for *Mycobacterium tuberculosis* persistence.

256   PLoS One 1: e43.

257   11.   Bechah Y, Verneau J, Ben Amara A, Barry AO, Lépolard C, Achard V et al. (2014)

258   Persistence of *Coxiella burnetii*, the agent of Q fever, in murine adipose tissue. PLoS

259   One 9: e97503.

260   12.   Bouzid F, Brégeon F, Poncin I, Weber P, Drancourt M, Canaan S (2017)

261   *Mycobacterium canettii* Infection of Adipose Tissues. Front Cell Infect Microbiol 7:

262   189.

263   13.   Erlandson KM, Lake JE (2016) Fat Matters: Understanding the Role of Adipose Tissue

264   in Health in HIV Infection. Curr HIV/AIDS Rep 13: 20-30.

265   14.   Damouche A, Lazure T, Avettand-Fènoël V, Huot N, Dejucq-Rainsford N, Satie AP et

266   al. (2015) Adipose Tissue Is a Neglected Viral Reservoir and an Inflammatory Site

267   during Chronic HIV and SIV Infection. PLoS Pathog 11: e1005153.

268   15.   Tanowitz HB, Scherer PE, Mota MM, Figueiredo LM (2017) Adipose Tissue: A Safe

269   Haven for Parasites. Trends Parasitol 33: 276-284.

270 16. Ferreira AV, Segatto M, Menezes Z, Macedo AM, Gelape C, de Oliveira Andrade L et
271   al. (2011) Evidence for *Trypanosoma cruzi* in adipose tissue in human chronic Chagas
272   disease. Microbes Infect 13: 1002-1005.

273 17. Sztalryd C, Brasaemle DL (2017) The perilipin family of lipid droplet proteins:
274   Gatekeepers of intracellular lipolysis. Biochim Biophys Acta Mol Cell Biol Lipids
275   1862: 1221-1232.

276 18. Fang H, Judd RL (2018) Adiponectin Regulation and Function. Compr Physiol 8: 1031-
277   1063.

278 19. Giroud M, Pisani DF, Karbiener M, Barquissau V, Ghandour RA, Tews D et al. (2016)
279   miR-125b affects mitochondrial biogenesis and impairs brite adipocyte formation and
280   function. Mol Metab 5: 615-625.

281 20. Combs TP, Nagajyothi, Mukherjee S, de Almeida CJ, Jelicks LA, Schubert W et al.
282   (2005) The adipocyte as an important target cell for *Trypanosoma cruzi* infection. J Biol
283   Chem 280: 24085-24094.

284 21. Morales MA, Cruz I, Rubio JM, Chicharro C, Cañavate C, Laguna F et al. (2002)
285   Relapses versus reinfections in patients coinfected with *Leishmania infantum* and
286   human immunodeficiency virus type 1. J Infect Dis 185: 1533-1537.

287 22. Burza S, Sinha PK, Mahajan R, Lima MA, Mitra G, Verma N et al. (2014) Risk factors
288   for visceral leishmaniasis relapse in immunocompetent patients following treatment
289   with 20 mg/kg liposomal amphotericin B (Ambisome) in Bihar, India. PLoS Negl Trop
290   Dis 8: e2536.

291 23. Pisani DF, Dumortier O, Beranger GE, Casamento V, Ghandour RA, Giroud M et al.
292   (2016) Visfatin expression analysis in association with recruitment and activation of
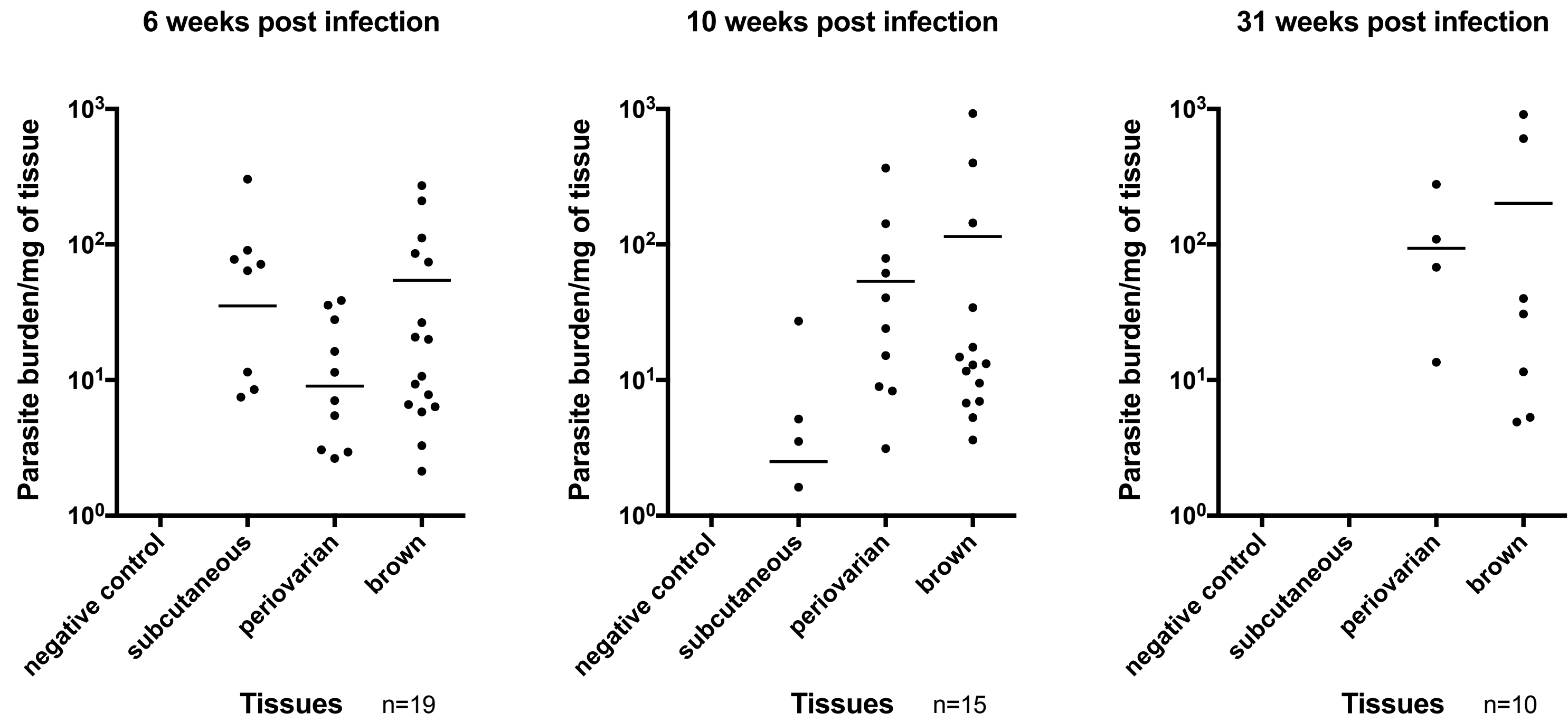293   human and rodent brown and brite adipocytes. Adipocyte 5: 186-195.

294

295

Figure 1. qPCR evaluation of parasite burden per milligram of tissue at 6, 10 and 31 weeks post infection.
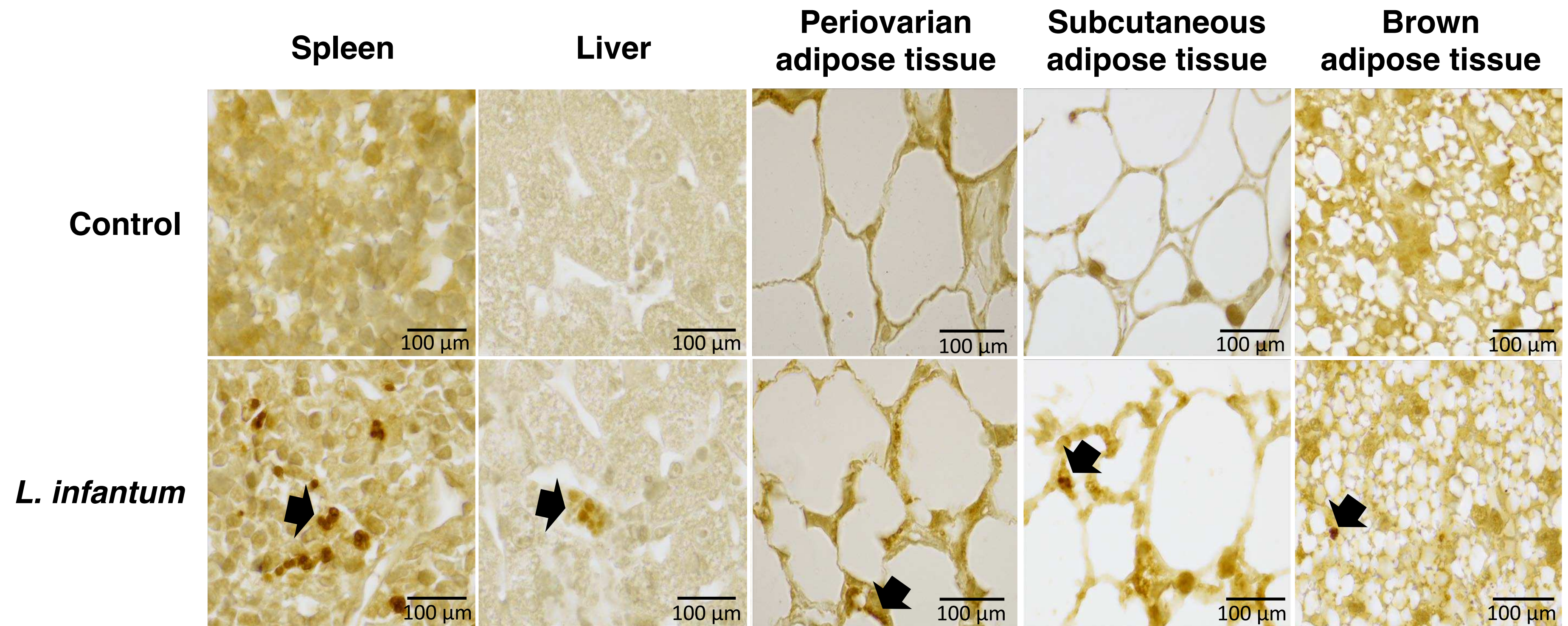
Figure 2. Immunolabelled histological sections of tissues from BALB/c mice infected with *Leishmania infantum,* 40 weeks post infection*.*
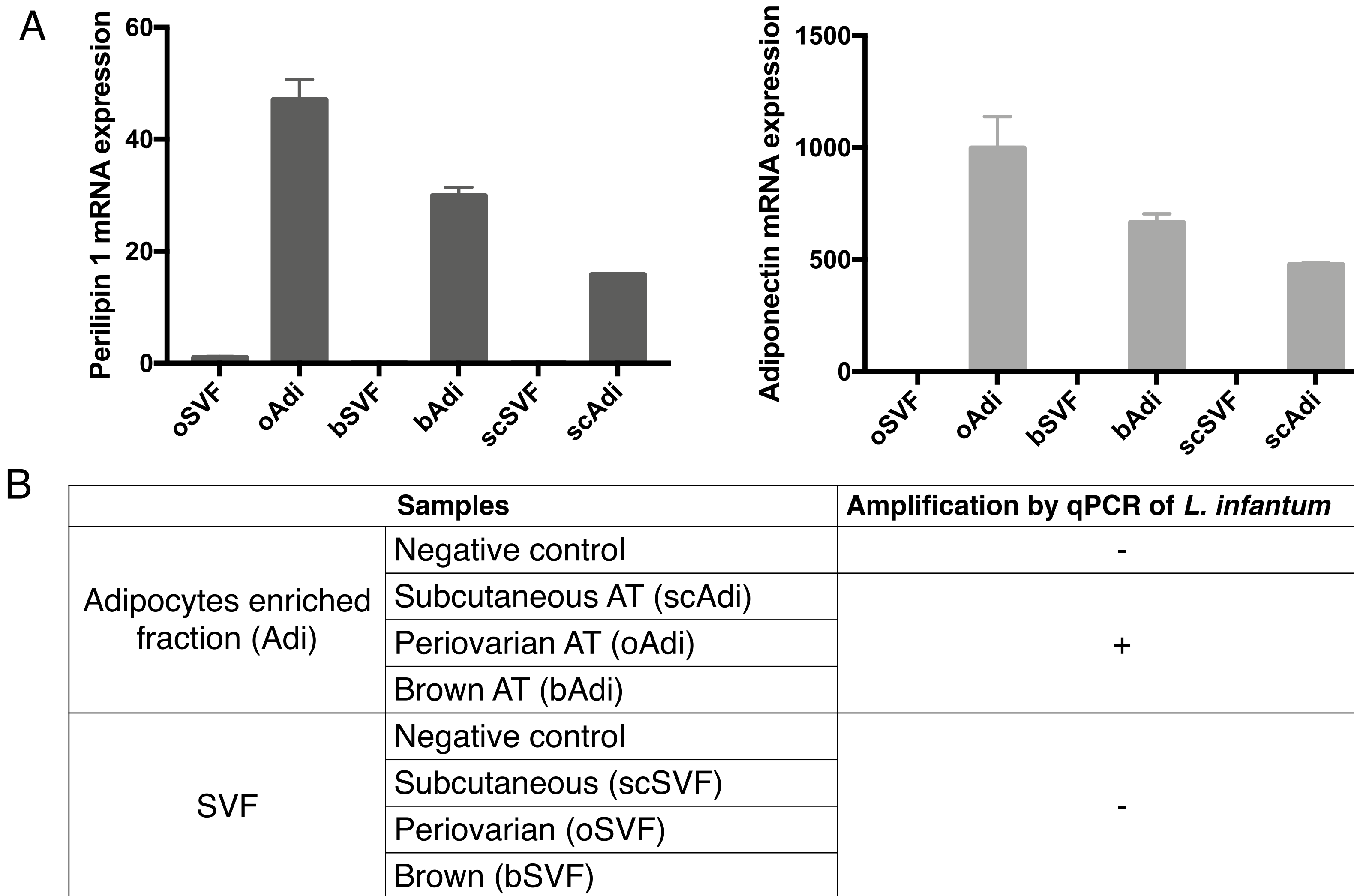
Figure 3 A. detection by qPCR of *Leishmania infantum* in adipose tissue fractions. Adipose tissues were separated into adipocytes enriched floating fraction (adi) and stromal vascular fraction (SFV). B. mRNA expression of Perilipin 1 and Adiponectin markers.
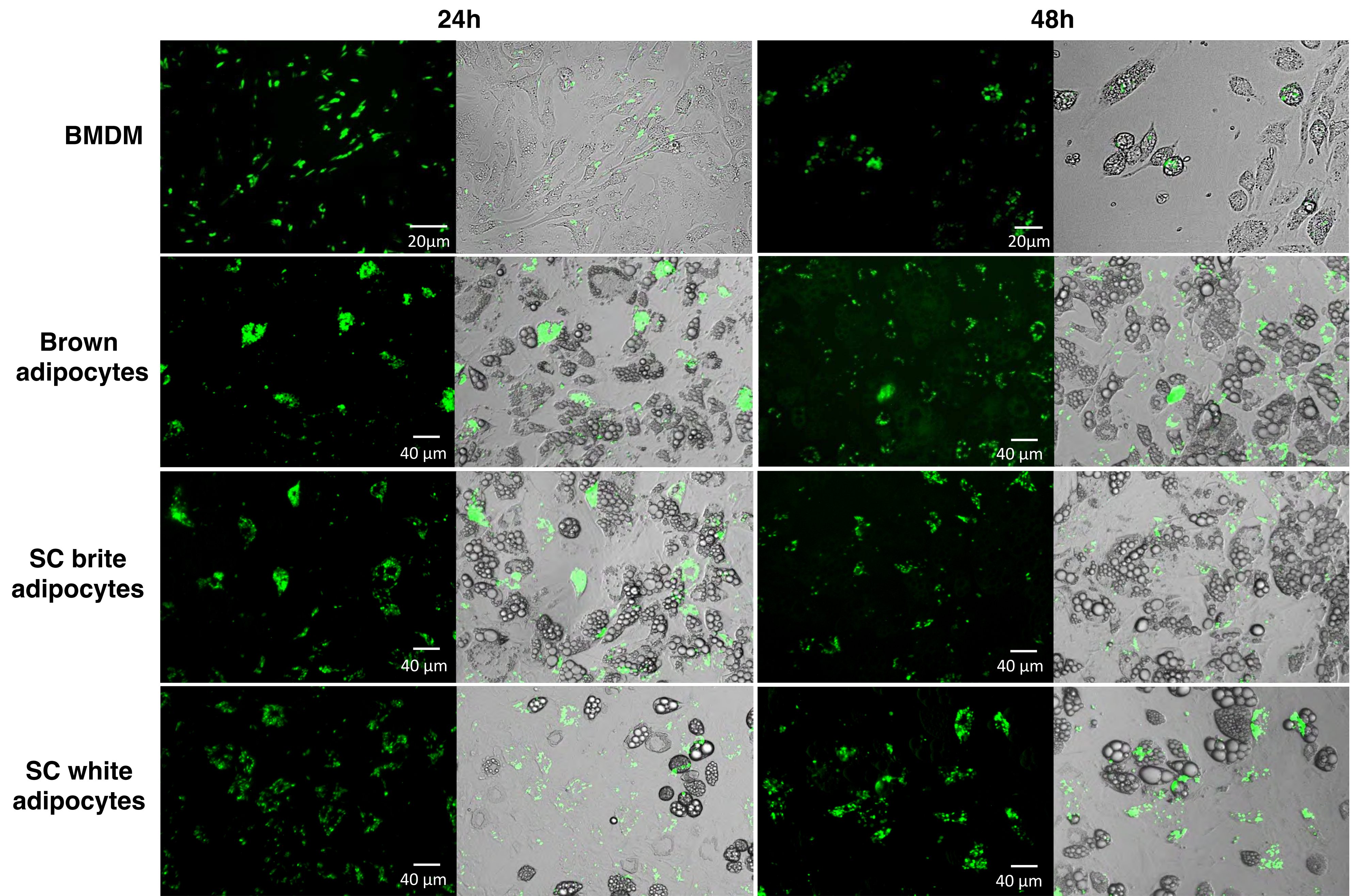
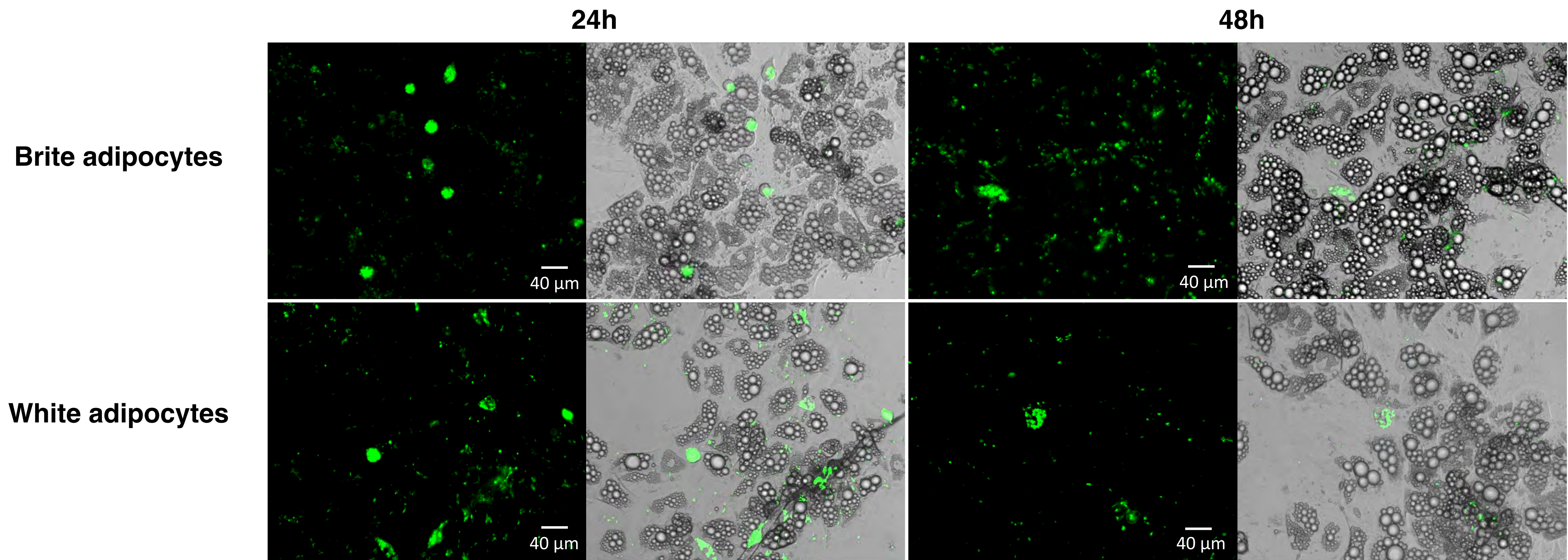**Figure 4.** *In vitro* GFP-*L. infantum* infection of BALB/C adipocytes

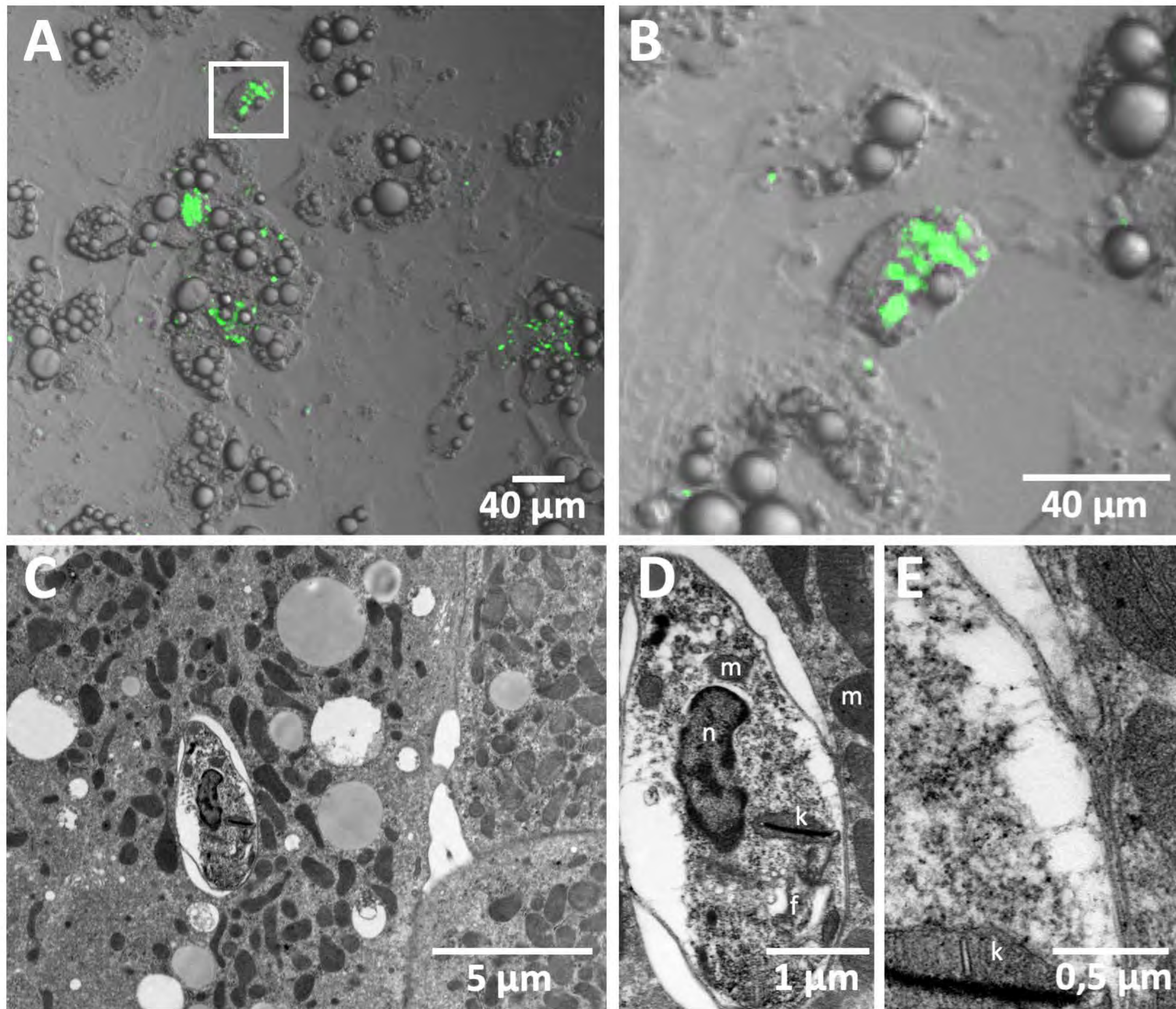**Figure 5.** *In vitro* GFP-*L. infantum* infection of different human adipocytes

Figure 5. *In vitro* infection of mouse brown adipocytes by GFP-*L. infantum.*
A, B – Epifluorescence microscopy of GFP-*L. infantum* infected Brown adipocytes,
C, D, E – Electronic microscopy of infected Brown adipocytes
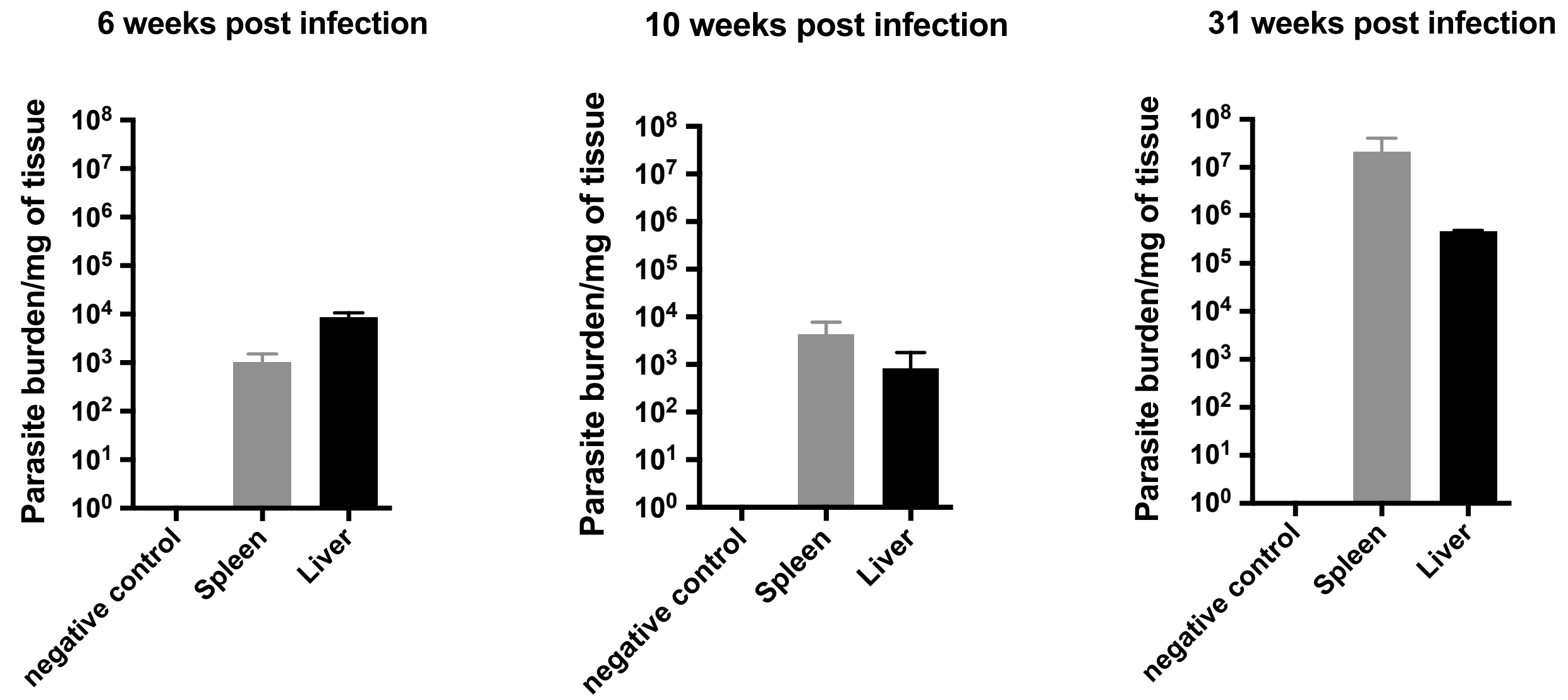(Nucleus (n), flagella (f), kinetoplast (k),mitochondrion (m))

Figure S1. Parasite burden per milligram of spleen and liver at 6, 10 and 31 weeks post infection. BALB/c mice were infected intravenously with 3.10^8 LUC-*Leishmania infantum.*
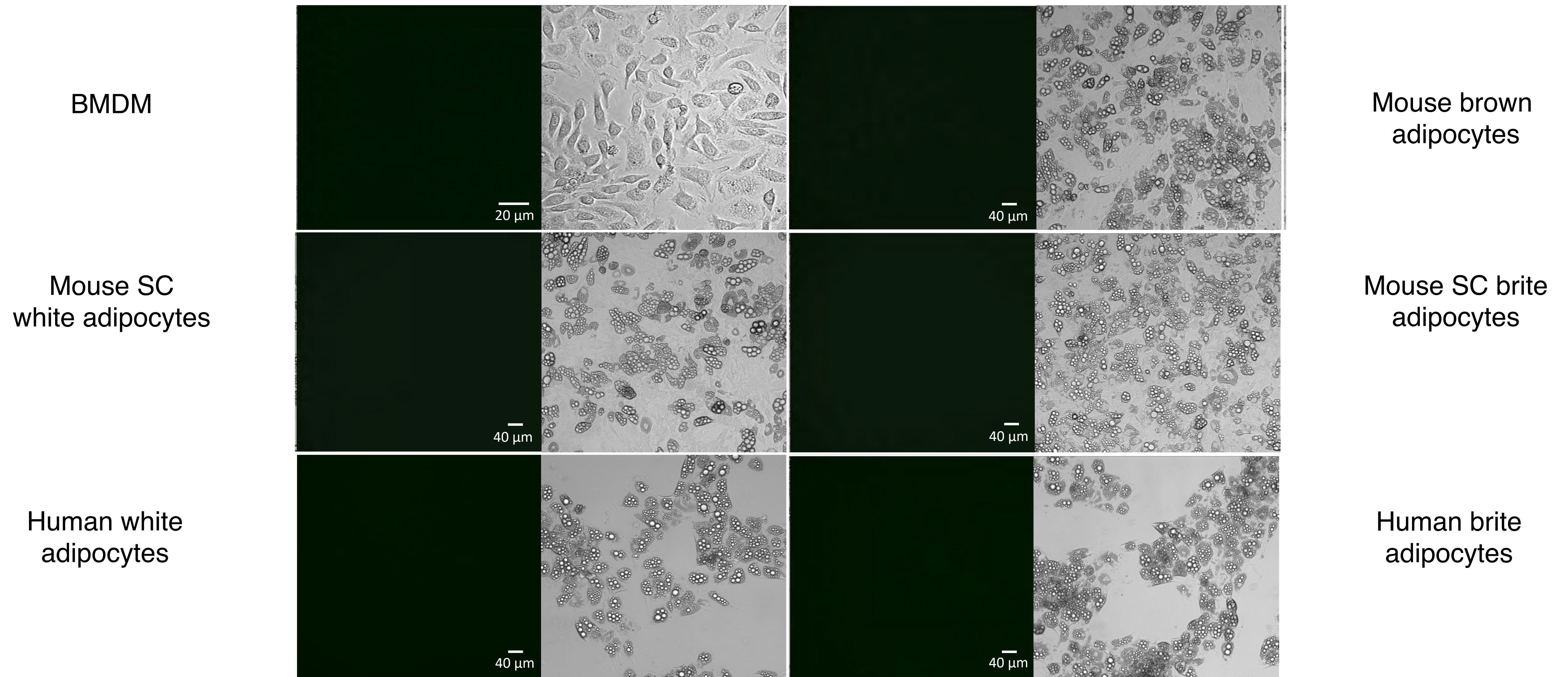
Figure S2. Microscopy controls of BMDM or Adipocytes (48h)

Samples	Parasite burden/mg of tissue	
	Mouse 1	Mouse 2
Liver	$1,2.10^{-2}$	$1,5.10^{-2}$
Spleen	Undetected	6.10^{-3}
Brown AT		$1,7.10^{-2}$
Subcutaneous AT		Undetected
Periovarian AT		

Supplemental Table 1. Parasite burden per milligram of tissue in organs of naïve mice transplanted with BALB/c-infected brown adipose tissue (AT).